Spring 2016

Mechanics of impulse force reduction for mitigating dump truck vibrations under HISLO conditions

Danish Ali

Department:

MECHANICS OF IMPULSE FORCE REDUCTION FOR MITIGATING DUMP TRUCK VIBRATIONS UNDER HISLO CONDITIONS

by

DANISH ALI

A THESIS

Presented to the Faculty of the Graduate School of the

MISSOURI UNIVERSITY OF SCIENCE AND TECHNOLOGY

In Partial Fulfillment of the Requirements for the Degree

MASTER OF SCIENCE IN MINING ENGINEERING

2016

Approved by

Dr. Samuel Frimpong, Advisor

Dr. Nassib Aouad

Dr. Greg Galecki

ABSTRACT

The deployment of large capacity shovels and dump trucks, for achieving economic bulk production capacities, has resulted in high impact shovel loading operations (HISLO). These large shovels generate high impact forces when loading dump trucks with over 100-ton passes under gravity. The impact forces also generate high frequency shock waves, which cause severe truck vibrations, and thus, expose dump truck operators to high levels of whole body vibrations (WBV). The dynamic impact force generates these vibrations, and thus, there is a need to develop efficient technologies to eliminate or reduce its impact. Existing literature and industry practice show that this problem significantly impacts the health and safety of operators. There exists no fundamental work to address this problem. Thus, the primary objective of this research study is to provide scientific solutions to this problem.

This research study develops a rigorous mathematical model to capture the dynamic impact force using all dependent underlying variables. A 3D virtual simulation model for a shovel dumping operation has also been developed using discrete element modeling (DEM) techniques in PFC3D. This model captures material dumping from a P&H 4100XPC shovel (100 tons per pass) into a CAT 793D truck. The results from the mathematical and simulation models showed good agreement. Analysis of the simulation results showed that a percent reduction of 4.88, 7.42, 11.45, 12.01, 15.08 and 17.34 % can be achieved by reducing the dumping height from 7.33 m to 6.33, 6.00, 5.50, 5.33, 5.00 and 4.9 m, respectively. The effect of the impulse force reductions on WBV exposures was examined using the model by Aouad and Frimpong (2013) in MSC ADAMS. Analysis of the results showed that for dumping height reductions to 7.33, 6.33, 6.00, 5.50, 5.33, 5.00 and 4.9 m, the RMS acceleration value of 3.56 m/s^2 from Aouad and Frimpong (2013) can be reduced by 10.42, 15.51, 15.53, 15.73, 17.22, 18.85 and 19.61 %, respectively. This is equivalent to a reduction of 3.56 m/s^2 to 2.86 m/s^2 at a dumping height of 4.90 m.

This research is a pioneering effort to address the problems associated with the operator exposures to severe WBV levels. It advances the heavy mining machinery vibrations frontier and contributes significantly to its body of knowledge. The mathematical and simulation models can be used to analyze any HISLO operation to reduce or possibly eliminate WBV exposures. This study ensures workplace safety and operator health under HISLO conditions in surface mining operations.

ACKNOWLEDGMENTS

I am thankful to my advisor, Dr. Samuel Frimpong, for his help, guidance and encouragement throughout the course of this work.

I also appreciate the guidance and encouragement of my advisory committee members – Dr. Nassib Aouad and Dr. Greg Galecki.

My gratitude also goes to Ms. Tina Alobaidan and Ms. Shirley Hall for their assistance. I will also like to mention my friends Eric Gbadam and Muhammad Wardeh for their encouragement and assistance.

I am grateful to my fiancée Annie France, for her endless support and encouragement thought this endeavor, and for being always there for me and making my stay in Rolla enjoyable.

I am thankful to my parents, my sister and my brother for their endless support during my academic pursuit.

TABLE OF CONTENTS

LIST OF FIGURES

Page

LIST OF TABLES

Page

NOMENCLATURE

Symbol	Description
Y	Young's Modulus for the Truck body (N/m^2)
A	Cross sectional area of the beam
b_m	Width of the Truck Body (m)
h	Thickness of the Truck body (m)
L	Length of Truck Body
ρ	Density for the Truck Body material (kg/m^3)
g	Acceleration due to gravity (m/s^2)
H	Heaviside Step Function
H_t	Dumping Distance (Distance b/w Truck Body & Tip of the Shovel Dipper door as it is about to open for dumping) (m)
m	Mass of the Material (kg)
ϵ	Time for which the Impulse acts (sec)
ω_n	Natural Frequency of Truck body
ω_d	Damped Natural Frequency of Truck body
ζ_n	Damping Ratio for the Truck Body
C	Damping Coefficient of the Elastic Foundation (Ns/m)
I	Area moment of Inertia for the beam/Truck body (m^4)
T	Kinetic Energy of the truck body
V	Potential Energy of the truck body due to bending
V_e	Potential Energy of the truck body due to Elastic Foundation
W_F	Virtual Work done by Distributed Force
W_D	Potential Energy due to Elastic Foundation
K	Stiffness of the Elastic foundation (N/m)

M + 1	No. of sub-passes in which a particular shovel ore-pass is divided
a	Time at which shovel starts dumping
σ	Stress in the Beam (Truck Body)
ε	Strain induced in the Beam (Truck Body)
$\eta_n(t)$	Temporal Solution for the Beam
$U_n(x)$	Spatial Solution for the Beam
$U(x,t)$	Complete response of the Beam to the Forcing (Truck Body)
$u(x,t)$	Transverse Displacement of the Beam
δu	Delta (may also be regarded as Variation in u(x,t))
t_0	Time at which Shovel Dumps the Material
∂	Partial Deferential
$\delta(t-t_0)$	Dirac Delta which turns on at t_0
v	Velocity with which the material hits the truck body
L_m	Linear momentum which the material has attained just before reaching the truck body

1. INTRODUCTION

1.1. BACKGROUND OF THE RESEARCH PROBLEM

Shovel truck system (shown in Figure 1.1) has become a more flexible, economic and productive method for surface mining operations over the years as a result of advancement in technologies. Studies have shown, for example, that one can observe a four times increase in productivity for a 380-ton dump truck, as compared with the productivity of a 120-ton truck (Frimpong, 2006). Thus one can easily achieve higher economic advantages by matching the larger shovels with larger trucks/dumpers. These large capacity shovels load large capacity dump trucks with over 100-ton passes under gravity, creating large impact forces and high frequency shock waves. The shockwaves generated, under high impact shovel loading operations (HISLO), propagate through the truck body, chassis and to the operator's cabin and the seat, thus exposing the operators' feet, legs, lower back, hands, spine and neck to these high frequency shockwaves. This experience and exposure is termed as Whole Body Vibration (WBV) phenomenon.

The WBV levels, exceeding the recommended ISO limits, can have a severe impact on the health and safety of the operators by resulting in long-term lower-back problems and various other health issues. Significant research has been done to develop solutions to the problems associated with machine vibrations, whole body vibration exposure and its impact on the operator's health and safety. The scope of existing research is limited to relatively small equipment units in industries, such as agriculture, military, aerospace, commercial transport and automotive. This research is a pioneering effort to provide solutions to the problem of high impact forces under HISLO conditions in order to provide safe and healthy environments for truck operations in surface mining operations.

1.2. STATEMENT OF THE RESEARCH PROBLEM

Haul trucks contribute significantly to injuries and accidents in surface mine operations. According of MSHA, out of 250 fatalities from 1990 to 2001 in surface mining, 40% was attributed to powered haulage. An average of 675 accidents and 21 powered haulage fatalities occur each year in surface mining and 20% of these injuries and fatalities

involve dump truck (Ruff, 2002). Based on 2000 and 2007 data, Ruff et al. (2011) showed that the third severest equipment accidents in all mines are from dump trucks and 44% of the fatal accidents in surface mines among mobile machines are caused by dump trucks. According to Adlinger et al. (1995), 46.3 % of accidents involving haul truck occur during operations and 37.7% of these accidents are due to jarring, which causes operator back injuries.

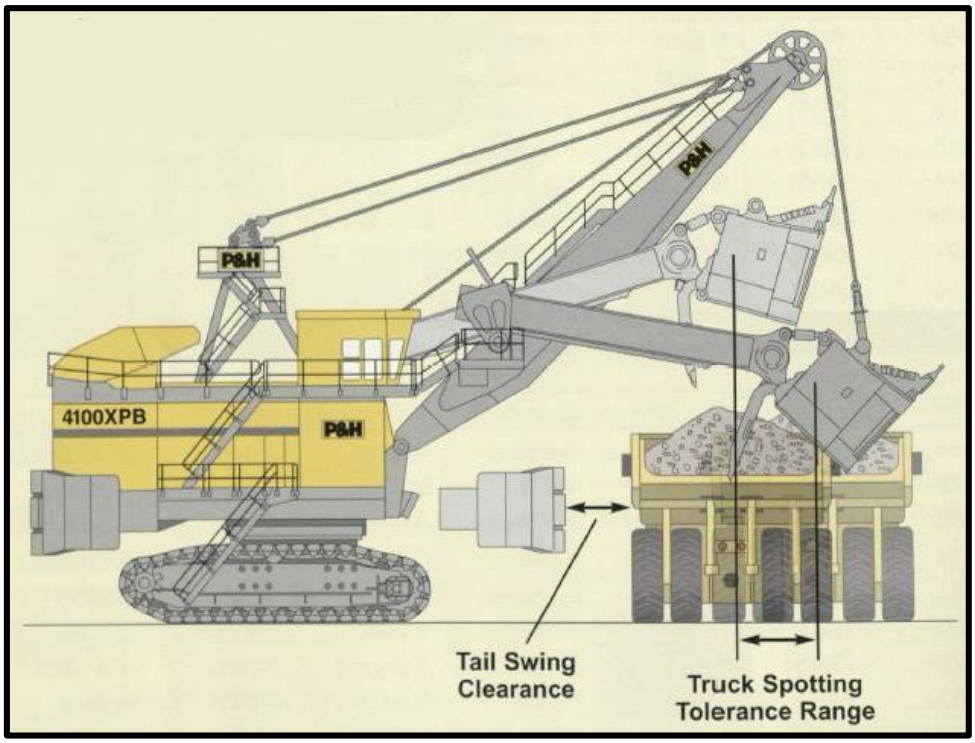

Figure 1.1. High Impact Shovel Loading Operation (HISLO) (Harnischfeger, 2003)

The International Standards Organization (ISO) has provided the recommendations on safe limits beyond which long-term exposure could cause severe lower-back, neck, and other physical disorders and disabilities. The applicable ISO standards in vehicular vibrations include Sections 1,2,4,5 of ISO 2631 (1997, 2003, 2001 and 2004). Specific threshold limits are provided within these sections in order to comply with the safe working and operating environment of vibrating equipment. Table 1.1 indicates the WBV levels and their corresponding effects on operators during an 8-hour exposure. Whenever

operators are exposed to WBV (RMS) levels equal or in excess of 1 m/sec^2, during an 8-hour duration, they become vulnerable to experiencing sacrum, lumbar and cervical problems (ISO, 2004).

Table 1.1. Expected Comfort Zones to Vibration (ISO 2631 – 1)

Acceleration Value (RMS)	Comfort Zone
Less than 0.315 m/sec^2	Not Uncomfortable
0.315 – 0.63 m/sec^2	A little Uncomfortable
0.5 – 1 m/sec^2	Fairly Uncomfortable
0.8 – 1.6 m/sec^2	Uncomfortable
1.25 – 2.5 m/sec^2	Very Uncomfortable
Greater than 2 m/sec^2	Extremely Uncomfortable

Even though a lot is known about the type of vibrations generated in mining trucks as a result of the research carried out by Aouad and Frimpong (2013), there is a lack of expertise and understanding about how to control the impact of these vibrations. Due to the fact that the dump truck is stationary and the excitation force introduced by the material being dumped into the truck body is dynamic, this phenomenon is very much different from that of military applications studied by Friedmann (1997), Wickramasinghe et al. (2004), and Moses (1997). The HISLO vibrations are forced vibrations induced by the force generated because of material impact from a dumping height. This impact force mainly depends upon the mass of the material being dumped (which further depends on factors, such as density, moisture content, angle of repose, cohesion and shovel dipper size), dumping characteristics (including height/distance of dumping, time within which the material in the dipper is dumped into the body and dumping and loading mechanism of shovel) and a few environmental conditions (including terrain conditions and space limitations).

Literature survey has been used to evaluate the contributions by researchers to the body of knowledge on impact force modeling. A number of studies has focused on

determining impact force of a single body through impact test or using virtual simulation experiments (e.g. PFC3D), such as the work by Iverson (2003) and Metz (2007). None of these researchers has focused on determining the impact force generated by flowing material under gravity. The only current mathematical model, for the soil or broken rock material flowing under gravity, was provided by Aouad and Frimpong (2013) given by Equation 1.1. This model lacks the essential parameters, over which the impact force in such a scenario should depend, including height or distance of dumping. The dumping height is the distance between the truck body and the lowest tip of the shovel dipper door as the material is being dumped into the truck. The model also does not consider the time the material remains in contact initially (impact duration) and the continuous flow of materials into the truck bowl instead of a single lump of material to reduce the overall impact force.

As a result, the impact forces generated in the model by Aouad and Frimpong (2013) are overestimated because the soil/rock material has always been considered to have been dumped at once. In reality, the material is generally well fragmented either during the direct shovel excavation or due to pre-fragmentation by blasting in hard rock materials. In such cases, the material being dumped into the truck would consist of large amount of small size particles, and thus, there will be a continuous flow of the material from the shovel dipper into the truck. Therefore, the dynamic impact force curve will be continuous over the period of shovel dumping operation. In order to execute the second pass after the first pass, the shovel swings back, digs and dumps another 100 tons of material into the dump truck. The resulting impact force is reduced compared to the first pass because of the "cushioning effect" provided by the material already in the truck from the first pass.

The resulting vibration levels within the truck body, chassis and the operator cabin are reduced correspondingly. This reduction in impact force also reduces operators' exposure to WBV levels. The impact of this cushioning effect has not been studied before. Some studies have assumed the dynamic impact force from the second pass to have a similar magnitude as that of first pass. Other studies have focused only on the first pass during the vibration analysis done for operator health risk evaluations (Yan-Hua et al., 2015). This research is therefore undertaken to formulate a more realistic dynamic impact force under HISLO conditions, with a 3D virtual simulation of the shovel dumping process,

using discrete element modeling (DEM) technique in PFC3D. The virtual DEM simulator allows the observation and consideration of the cushioning effect in subsequent passes after the first pass.

The cushioning effect and continuous material flow, which intuitively reduces the impulse force, provide a rationale for studying the effects of impulse force. The results and the findings from this work can further be used to analyze the shovel dumping process in detail. Optimum parameters (i.e. dumping height) can then be selected to design solutions that reduces the resulting impact force and minimize the shockwaves/vibrations production within the dump truck.

$$F_1(t) = \begin{cases} F_0 \int_0^{\infty} \delta(t - t_0)dt & \forall t = t_0 \\ 0 & \forall t \neq t_0 \end{cases} \tag{1.1}$$

1.3. OBJECTIVE AND SCOPE OF WORK

The primary objective of this research study is to provide a better understanding of the dynamic impulse force and using this knowledge to provide a basis for reducing this impulse force. The elements for this primary objective include: (i) developing a rigorous mathematical model for the impulse force; (ii) obtaining the optimum dumping height and sub-passes into which a single pass can be divided for reducing the impulse force; (iii) virtually simulating the whole shovel dumping process in order to obtain the actual and more realistic dynamic impulse force distribution over the dumping process; (iv) observing the cushioning effect during the subsequent passes after the first pass; (v) comparing the results from the simulation and the mathematical model in order to verify the mathematical model results and check its accuracy; (vi) obtaining the optimum dumping height, which minimizes the impulse force and maximizes the dumping process efficiencies and the overall mining system using the results from the 3D virtual simulation; and (vi) visualizing the reduction in the vertical RMS acceleration for the operator's seat using 3D virtual prototype model developed by Aouad and Frimpong (2013).

In this study, the mathematical model has been used to effectively model and analyze the impulse force for the P&H 4100XPC shovel loading a CAT 793D dump truck. However, the model can be used to obtain the optimum dumping height and the sub-ore passes for any large truck being loaded by a corresponding large shovel. The 3D virtual simulation model of the HISLO dumping process is created using the CAT 793D and P&H 4100XPC and virtually simulated in PFC3D. Using the virtual simulation results, optimum dumping heights have been obtained for the dumping process. This process can be repeated for any combination of shovels and dump trucks for determining the optimum dumping height for the corresponding dumping process.

1.4. PROPOSED RESEARCH METHODOLOGY

An analogic mathematical model of the system is developed to demonstrate the material flow under gravity. The model yields the impulse force resulting from the HISLO process. Two approaches are used to develop the mathematical model as follows: (i) developing a more rigorous mathematical model for the impulse force generated from the dumping process; and (ii) using an empirical approach to develop a mathematical model for the impulse force for the materials dumping process.

Secondly, a 3-D virtual simulation model is developed to simulate the shovel dumping process in SolidWorks and Rhino 5.0. The Rhino 5.0 meshes are then imported into PFC3D to simulate the material dumping process. The simulation model uses the P&H 4100XPC shovel to dump 100 tons of material into the CAT 793D dump truck under gravity for the first two passes. The DEM technique analyzes the behavior and the reactive forces of the complete system based on the motion of individual particles and their interactions. The impulse force from the dumping process is monitored and recorded over the complete duration of the shovel operation. The results obtained from the mathematical model and the virtual simulation processes are compared for verification. Real-world data is used to validate the 3-D simulation model of the dumping process to ensure that it can capture realistic scenarios. Finally, the optimum dumping height is obtained for the shovel dumping process from the 3-D virtual simulation process.

A detailed experimentation is carried out for the validated simulation model. Detailed analysis of the results is carried out to show the effectiveness of the models for

predicting a more realistic dynamic impulse force for the shovel dumping process. The results will also be used to demonstrate the impact of the cushioning effect by the first pass for subsequent passes and the corresponding dynamic impulse force, the resulting dump truck vibrations and the exposure of operators to WBV levels. A series of optimal dumping heights are generated for the HISLO scenarios for further design and analysis of the shovel dumping process.

Finally, the models developed in this study are coupled with the 3D virtual prototype model by Aouad and Frimpong (2013) to obtain the RMS accelerations using the reduced impact forces from this study. The model by Aouad and Frimpong (2013) is a 38-DOF virtual prototype model for the CAT 793D in MSC ADAMDS to simulate an operator's exposure to WBV levels in which the impulse force is defined by a point load. Here in this study, the virtual prototype is only used to compute the RMS acceleration for the operator's seat in z – direction (vertical motion) only for all the different dumping distances.

1.5. EXPECTED RESEARCH CONTRIBUTIONS

This research will advance the research frontiers in HISLO and WBV exposures and their impact on human operators. In particular, the expected contributions from this research include:

- Practical understanding of the dynamic impulse force shovel dumping process;
- A basis for characterizing and optimizing the shovel dumping process;
- Minimizing and possibly eliminating the impact of WBV exposures on dump truck operators under HISLO conditions; and
- Ability of mine planning engineer to modify the dumping process by optimizing the dumping height to minimize the dynamic impulse force and improve the health, safety and the efficiency of the operator within the ISO limits.

1.6. STRUCTURE OF THE M.S. THESIS

Section 1.0 contains an introduction to the M.S. thesis. The introduction lays the foundation by providing a brief discussion on the HISLO vibration problems in large scale

surface mining operations, objectives and scope of the research study, the proposed methodology and its contributions to industry and to the body of knowledge. Section 2.0 provides a critical review and analysis of the relevant literature. Section 3.0 contains a full step by step development of the mathematical models for the dynamic impact force formulated by using two different approaches. Section 4.0 provides a detail explanation of the experimental setup and the procedures for the experiments for predicting the impact force. Section 5.0 presents the 3D virtual prototype models of CAT 793D dump truck and the bucket of P&H 4100XPC cable shovel and the complete simulation procedure carried out in PFC3D. Section 6.0 presents the details about the set up and the procedure for the 3D virtual simulation using the models by Aouad and Frimpong (2013) in MSC ADAMS. Section 7.0 presents the experimental and virtual prototype simulation results with detailed discussions. Section 8.0 summarizes the findings and presents the conclusions, and contributions of this M.S. research, as well as, the recommendations for future work. All the references that have been used during the study and the development of this impulse force reduction research to mitigate the vibrations in dump trucks for HISLO conditions are listed at the end of this thesis.

2. LITERATURE REVIEW

A comprehensive review of the relevant literature has been carried out to examine the current body of knowledge, contributions from researchers and the outstanding problems in this research frontier. It covers the significant work done in the field of machine vibration, whole body vibration (WBV), impact force modelling, material dynamic simulation and discrete element analysis.

2.1. WHOLE BODY VIBRATION (WBV) – EFFECTS, MEASUREMENT AND CONTROL

In earth moving operations, whole body vibration (WBV) has a significant impact on human health. Aldinger et al. (1995) conducted a study on surface coal mining accidents and found out that equipment operation was the most common category of accident for haulage truck (46.3%) and jarring came out to be the most common type of equipment operation accidents comprising almost to 37.7%, which results in operator back injuries. In view of this vibration and its effects on human operators, research must provide solutions to control and minimize the impact of vibrations towards improving the health & safety of the heavy earthmoving equipment operator.

A truck operator can experience vibrations through jolting and jarring while being loaded by a shovel, driving truck over an obstacle in the haul road or unintentionally striking a berm on the haul road. Miller et al. (2000) devised a method for installing “black boxes” called Shox Boxes onboard equipment that already have a GPS system onboard for the assessing jolting and their root causes. That Shox Box system reviews data in real time and sends pertinent information via radio to a central database. The Shox Box prototype was developed in a surface mining environment and it is a useful tool for assessing and recommending proactive actions towards maintaining jolting within an acceptable range.

Kittusamy (2002) investigated the vibration exposure at the seat/operator interface, transmissibility of vibration in z-axis, and the psychological ratings of vibration discomfort level and evaluated the postural requirements of the job. A triaxial piezo-resistive seat pad accelerometer (Model VT-3) and a single axis piezo-resistive accelerometer (Model 7265A-HS) were used to assess the whole-body vibrations at the seat/operator interface

and at the floor level, respectively. The results from that study revealed that the operators were exposed to WBV levels significantly higher more than the allowable limits established by the European Commission. It was recommended that the design of the seats should be such that the vibrations at the lower frequencies (1 – 8 Hz) are attenuated appropriately. Kittusamy (2002 and 2004) extended his previous research and formulated a check list to evaluate the cab design of heavy construction equipment. He evaluated different loaders and excavators using his list and found out that a majority of the vibration could be felt through the floor and at the seats. Therefore, these heavy equipment do contribute to a high prevalence of musco-skeletal symptoms and injuries among the operators.

Kittusamy et al. (2003) conducted a study to compare the NIOSH seat design with a design that is already being used on underground haulage vehicles. Accelerometers were used to gather the objective data and subjective data was gathered with a visual analog scale (VAS) and a questionnaire. Based on the results, it was concluded that the NIOSH seat design is quite better in providing comfort and reducing vibration as compared to the seat design that already in place.

Kittusamy (2003) also conducted a study using a questionnaire to assess demographics, work information, job history, and musculoskeletal symptoms in operators of heavy earthmoving equipment. The study focused on the neck, middle/upper back, low-back, shoulder/upper-arm, elbow/forearm, wrist/hand, hip, knee, and ankle/foot areas. The results indicated that the workers were at risk for developing musculoskeletal disorders.

Furthermore, Kittusamy et al. (2005) conducted a study to determine the effectiveness of a continuous passive lumbar motion system in reducing low back discomfort among operators of heavy earthmoving equipment. The results indicated that the use of a continuous passive lumbar motion system can effectively reduce the low back discomfort which is experienced by the operators of heavy earthmoving equipment.

Eger et al. (2005), during the small and large load haul dump (LHD) vehicles operation, measured the whole body vibration (WBV) exposures at the vehicle and operator seat interfaces. A tri-axial seat-pad accelerometer and a tri-axial accelerometer mounted with a large magnet were used, respectively, to measure WBV exposures at the seat pad/operator interface and vehicle floor/seat base interface. The results from those tests

were compared to the ISO 2631-1 health caution zones in order to determine safe exposure durations. Those results indicated that LHD operators were exposed to WBV levels, which exceeded the ISO 2631-1 exposure guidelines, putting them at risk for injuries. In larger LHDs, the highest magnitudes of vibrations were observed within a range between 0.89 and 1.18 m/s^2 in the z-axis. For smaller LHDs, the highest magnitude of vibration was observed within 0.55 and 0.64 m/s^2 in the x-axis.

Hoy et al. (2005) investigated the risk from WB V exposure and posture demands for low back pain (LBP) among forklift truck (forklift) drivers. Vibrations at the seat were measured in all the three axes (x, y and z) under actual working conditions and compared with ISO 2631-1 limits. The results indicated that the lower back pain is more prevalent among the forklift truck drivers as compared to the non-drivers and that WB V exposure contribute, among other factors, to cause lower back pain. It was also shown that the WBV exposures in x & y directions are well within the acceptable limits (below 0.5 m/s^2) based on the ISO 2631-1 limits. However, the vibration levels in the z-axis direction (0.73 m/s^2), with a peak ranging between 1.24 and 24.46 m/s^2, exceeded the ISO 2631-1 limits.

Wenzhang et al. (2000) used MSC. ADAMS software to build a vehicle dynamic simulation model and studied the non-linear dynamic characteristic of its rubber component. It showed that one can consider the effect of linear and non-linear dynamic characteristics of the rubber component in a vehicle during a process of vehicle dynamic analysis. The dynamic stiffness of the rubber component was found to be 14 kN/mm based on exciting frequency, component mass and damping ratio of 11 Hz, 245 kg and 0.2, respectively. The results showed that the corresponding single DOF system vibrates with the natural frequency of 11 Hz. For non-linear stiffness characteristics of rubber component, it showed that the peak response frequency was at 12 Hz with a displacement of 0.1mm.

Kim et al. (2001) modeled a vehicle with flexible body frame and active height control (AHC) system using MSC. ADAMS with 86-DOF. The proposed AHC system consisted of an automatic air leveling and semi-active suspension system for sport utility vehicles. The virtual prototype model was simulated to analyze the vehicle control and handling performances for various driving conditions. A total of 8 mode shapes were observed ranging from 26.9 HZ for the 1^{st} mode to 54.4 Hz for the 8^{th} mode. The simulation

results indicated that the AHC system automatically responded to the additional 200 kg on the rear side of the SUV and the spring was compressed by 25 mm due to this extra load. The spring was leveled back by the AHC system to its normal position after 19.62 sec by the compressed air that was supplied for 4.03 sec. The leveling speed was 1.6 mm/sec and did not cause passenger discomfort.

Chang et al. (2011) investigated ten dump trucks driven by domestic truck driver at the sandstone field for the preliminary vibration determination. Tolerable exposure time per day for drivers was evaluated using the ISO 2631-1 (1997) and article 301 in Taiwan's regulation "Rules of Equipment and measures for Protecting Laborers' Safety and health". The health risk was also assessed using ISO 2631-5 (2004) for dump truck drivers. Using ISO 2631-1 (1997), it was found out that the tolerable exposure time of these dump trucks were all being exceeded in the study. Based on ISO 2631-5 (2004), the study showed that the dump truck drivers had a high probability of experiencing an adverse health effect.

The most fundamental research in terms of whole body vibration (WBV) and its impact on dump truck's operator was carried out by Frimpong et al. (2011). They developed mathematical models to capture the vibration response of an integrated operator–machine–material system under high-impact shovel loading operations (HISLO). MSC.ADAMS was used to develop the virtual prototype models to simulate the response of the integrated system suspension to vibrations. The results showed that the shock waves, during dumping, which are being propagated into the operator's cabin are not being effectively attenuated, or reduced to a satisfactory level, by the current suspension mechanisms resulting in an adverse impact on operator's safety and health.

Aouad and Frimpong (2013) also developed comprehensive mathematical models and a 3D virtual prototype simulator for truck vibrations under HISLO conditions.

Aouad and Frimpong (2014) carried a fundamental research to model the HISLO during the shovel dumping process. Equations of motions, governing the concerned HISLO problem, were formulated by using the Lagrangian formulation. The Fehberg fourth–fifth order Runge–Kutta (RKF45) numerical method was used to solve the equations of motion in the MAPLE environment. The results showed that the vertical root mean square (RMS) accelerations were 3.56, 1.12, and 0.87 m/s^2, respectively, for the operator's seat, lower back and cervical regions. Comparing these vibration levels to the ISO 2631-1 limits (less

than 0.315 m/s^2), it was concluded that these levels fall within the extremely uncomfortable zone. This exposure poses severe health threats including severe long term lower-back, neck and other disorders to truck operators over long period of time.

2.2. IMPACT FORCE MODELLING AND DISCRETE ELEMENT ANALYSIS

Doktan (2001) studied the blast fragmentation effects on shovel-truck fleet performance. He utilized 3D particle flow code (PFC3D) package and linear-mixture packing model to study the optimum size distribution for densely packed load. He found out that with a better fragmentation, truck's loading time can be decreased by 22% resulting in an increase in loading productivity from 3261 to 4213 tonnes per hour which in turn makes it possible to achieve a 9% saving in loading and haulage costs.

Iverson et al. (2003) used the MSC software's 2-D working model (WM2D) and Itasca's particle flow code in 2-D (PFC2D) to investigate the dynamic loading at the bottom end of the chute with different ore pass angles. The results showed that there could be a considerable reduction in impact loads with increasing ore pass inclination. There is even further reduction in dynamic loads with dogleg transition. Comparison between the results from WM2D and PFC2D, showed that with PFC2D, cohesion can be modeled using bonds, which is impossible with WM2D. The PFC2D code, during relaxation and compression of each particle collision, required time-stepping, which is not a requirement in WM2D.

Metz (2007) presented a guide to compute the impact energy using the impact force which is measured during an impact test. It was shown that a simple test method for measuring impact force versus displacement and then integrating the area under the force-displacement curve can be used to obtain the energy units. Expected impact force needs to be evaluated in order to select the sensor with adequate range. Newton's 2nd law was used to select the proper force sensor measuring range. Quartz piezoelectric force sensors have the stiffness required to measure high-impact forces with fast rise times and the durability required to perform and survive in difficult test conditions. The results indicated that the impact force obtained through an impact test was comparable to the impact force calculated using Newton's 2nd law of motion.

Moriguchi et al. (2009), conducted a laboratory scale physical modelling of sand flow at different slopes. They allowed the sand particles to impact the fixed rigid wall on

their path and measured the resulting impact force. Numerical simulation using computational fluid dynamics algorithms was used to simulate and analyze the laboratory test results. The simulation models took into consideration the overtopping of the wall with sand and captured accurately the change of the impact force with slope angle. Finally, they used models to study the estimation of quasi-static force generated as the sediments comes to rest after impacting the wall.

Bobaru et al. (2009) analyzed the behavior of granular layers under bending deformation using coupled 2-D discrete element method-finite element method (DEM-FEM) simulations. Quasi-Static bending of granular layer was simulated and the coupled 2-D DEM-FEM model was validated using an FEM only model. Mixing can be enhanced as a result of the behavior of force chains generated during bending. In free vibration, the behavior of the granular layer is independent of the layer thickness and rolling resistance due to the absence of the force chain reversal as compared to the quasi static case.

Teufelsbauer et al. (2011) demonstrated the effectiveness of DEM as an appropriate tool for modeling granular flows and their interaction with the various obstructions when they presented a model for simulating dry granular avalanche down an incline. They studied the flow pattern along with the impact forces and compared the results with the experimental data for granular particles flowing along an inclined channel. The flow model was made more realistic with the inclusion of rotational constraints. Agreement between the simulations and the experimental results for impact forces and the flow patterns indicated that the DEM model can be used for a different experimental setups.

Hosseininia (2012) investigated the effect of inherent anisotropy on macroscopic mechanical behavior of the granular materials, through numerical simulation of biaxial compression tests using DEM. Irregular convex-polygonal and regular oval shaped particles were used. The results showed that the initial anisotropic condition has a much greater influence over the strength and deformational behavior of the assembled granular particles. It was also observed that the angularity of the particles also influence the shear strength and the volume change. Simulation results were compared with the experimental results and they showed good agreement.

Law et al. (2013) used DEM to investigate the impact process and the whole dynamic interaction between the granular surge flow and baffles. The granular flow

medium was modeled as frictional spherical discrete elements. They recorded and analyzed the respective location, velocities and forces acting on those discrete elements during the impact and the interaction. They found out that a single row of baffles can effectively reduce the kinetic energy and the discharge of the granular surge flow.

Albaba et al. (2014) developed a model for simulating the impact behavior of dry granular flow against a rigid wall using DEM. Poly-dispersed clumps consisting of two overlapping spherical particles were used which resembles the gravels. The particles were made to flow in an inclined flume at different inclination angles and impact force was recorded on every occasion. The final test gave a peak impact force of 735 N/m and the final residual force of 576 N/m. The model was then validated for the peak impact force (i.e., the time at which peak force occurs) and for the final residual force for each test.

Leonardi et al. (2014) developed a computational framework for a coupled DEM-FEM model of a cable-net barrier with an idealized debris flow. DEM is coupled with Lattice-Boltzman Method (LBM) in order to obtain the debris flow through simultaneous simulations of a flow of a fluid-grain mixture. The DEM governs the motions of the grain and Non-Newtonian fluid phase is solved using LBM. It has been shown in their work that a flexible barrier reduces the peak impact force and distributes the dynamic load over a longer time more efficiently.

2.3. SUMMARY

Literature survey been used to evaluate the contributions to the body of knowledge in machine vibration, impact force modeling, material dynamic simulation and discrete element analysis. A number of studies has focused on the determination of the impact force of a single body through impact test. None of these previous studies has focused on determining the impact force generated by flowing material under gravity.

Aouad and Frimpong (2013) developed the only model for dump truck vibrations under high-impact shovel loading operations (HISLO) conditions. In the field of WBV exposures, previous research studies have either focused on vibration control in military equipment or modification of the seat ergonomics and seat design of the underground haulage equipment. No research has been carried out to reduce or possibly eliminate the

impact of vibrations from the dynamic impact force generated by material flow under gravity in shovel dumping process.

This research is thus a pioneering effort to providing the basis for modeling the dynamic impact force in the shovel loading process using comprehensive mathematical, numerical and virtual simulation techniques. A 3D virtual simulation of the shovel dumping process, using discrete element modeling (DEM) technique is carried out to model and simulate the shovel dumping process. The virtual DEM simulator allows the accurate estimation of the dynamic impact force. The model also provides a basis for understanding the cushioning effect for subsequent passes after the first pass. Using these results and the findings, shovel dumping process can be analyzed in detail to select optimum parameters (i.e. dumping height). This dumping height can be used to reduce the resulting impact force, minimize the generation of vibrations and operators' exposures to high WBV levels.

3. IMPULSE FORCE MATHEMATICAL MODELLING

A detailed mathematical model is formulated for the dynamic impulse force under HISLO conditions. Every component of the mathematical model and the detailed steps are discussed in this section. The complete setup and parameters used for the numerical experiments for the particular case of shovel dumping operations have been presented in the model.

3.1. MATHEMATICAL MODEL USING THE RESPONSE OF THE TRUCK BODY

The mathematical model is developed using the following assumptions for the shovel dumping process:

- Truck body is assumed to behave like a beam over a visco-elastic foundation;
- Truck body (beam) material properties are linear;
- Truck body (beam) is slender;
- The damping and the stiffness of the foundation are linear and constant;
- Impulse force is uniform along the length of the truck body (beam); and
- Impulse force is dynamic with changing magnitude with time.

Figure 3.1 illustrates the layout of the impact force generation during a shovel dumping process along with some of the important parameters which play a key role in impulse force generation process. At time t = 0 sec, all the material is contained inside the shovel bucket so there is no impact force generated on the truck body. Z – axis in Figure 3.1 is in accordance with x – axis in the mathematical model. The shovel dipper door opens and the material begins to fall under gravity. The material strikes the truck body at 0.1 sec. Figure 3.2 illustrates the layout of the impact force generation during a shovel dumping process just as the material hits the truck body. Impact force begin to increase, resulting in high frequency shockwave production which travels though the truck body, chassis and reaches the operator's cabin. The reaction forces generated by the truck body, chassis and the tires are also shown in Figure 3.2. Figure 3.3 shows the layout of the impact force generation during a shovel dumping process as the majority of the material fall off, resulting in the maximum magnitude of the impact force at time t = ε/2 sec. The reaction

forces from truck body, chassis and the tires increases as well. Finally, Figure 3.4 shows the layout of the impact force generation during the final step of shovel dumping process as all the material now rests on the truck body as the shovel bucket begin to swing back to excavate another 100 tons of material at time t = ε sec. As the material is at rest, the impact force magnitude is now equal to the static gravitational load of the material and remains constant until the next batch of material is dumped by the shovel. Shockwaves are not produced and the reaction forces remains constant as there is no dumping of material taking place. Following this detailed description of impact force generation during the complete the shovel dumping process, rigorous mathematical model will be developed in order to capture the generation of dynamic impact force, onto the truck body, during the shovel dumping operation.

Considering the force function (from the dumping process), with similar behavior as a unit triangular impulse force with a maximum magnitude of 'F_o' and given by equation (3.1). This means that the dipper payload is dumped into the truck body in a continuous profile within the dumping time. As the dumping process continues, the impulse force increases to a maximum and then reduces gradually from this maximum until it reaches zero upon completion of the dumping process.

$$F(x,t) = \frac{F_o}{\epsilon}[2(t-a)H(t-a) - 4(t-b)H(t-b) + 2(t-c)H(t-c)] \tag{3.1}$$

Where,

$$b = a + \frac{1}{2}\epsilon$$

$$c = a + \epsilon$$

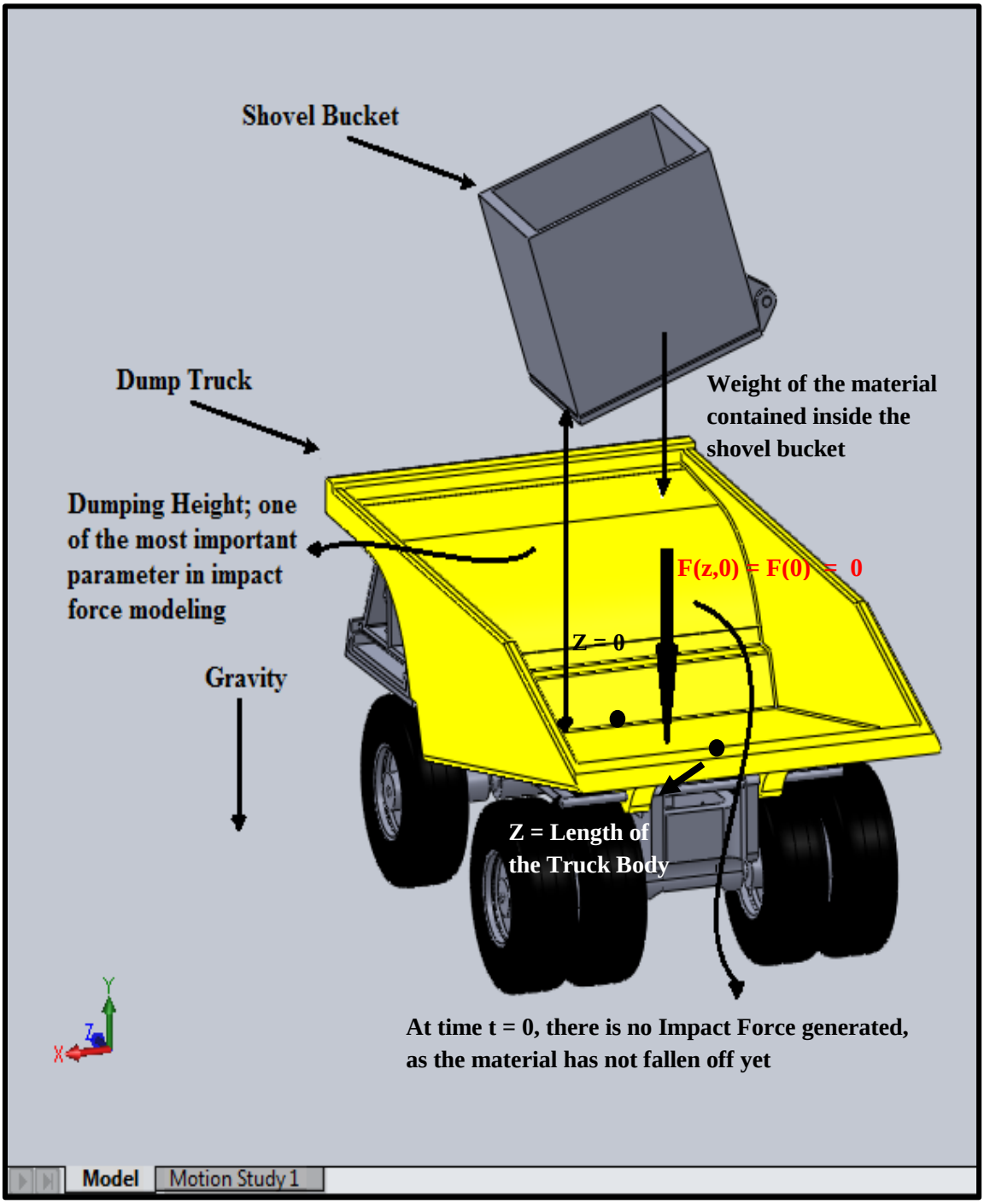

Figure 3.1. Shovel Dumping Process showing the Impact Force generation at Time t = 0 sec, with notable parameters

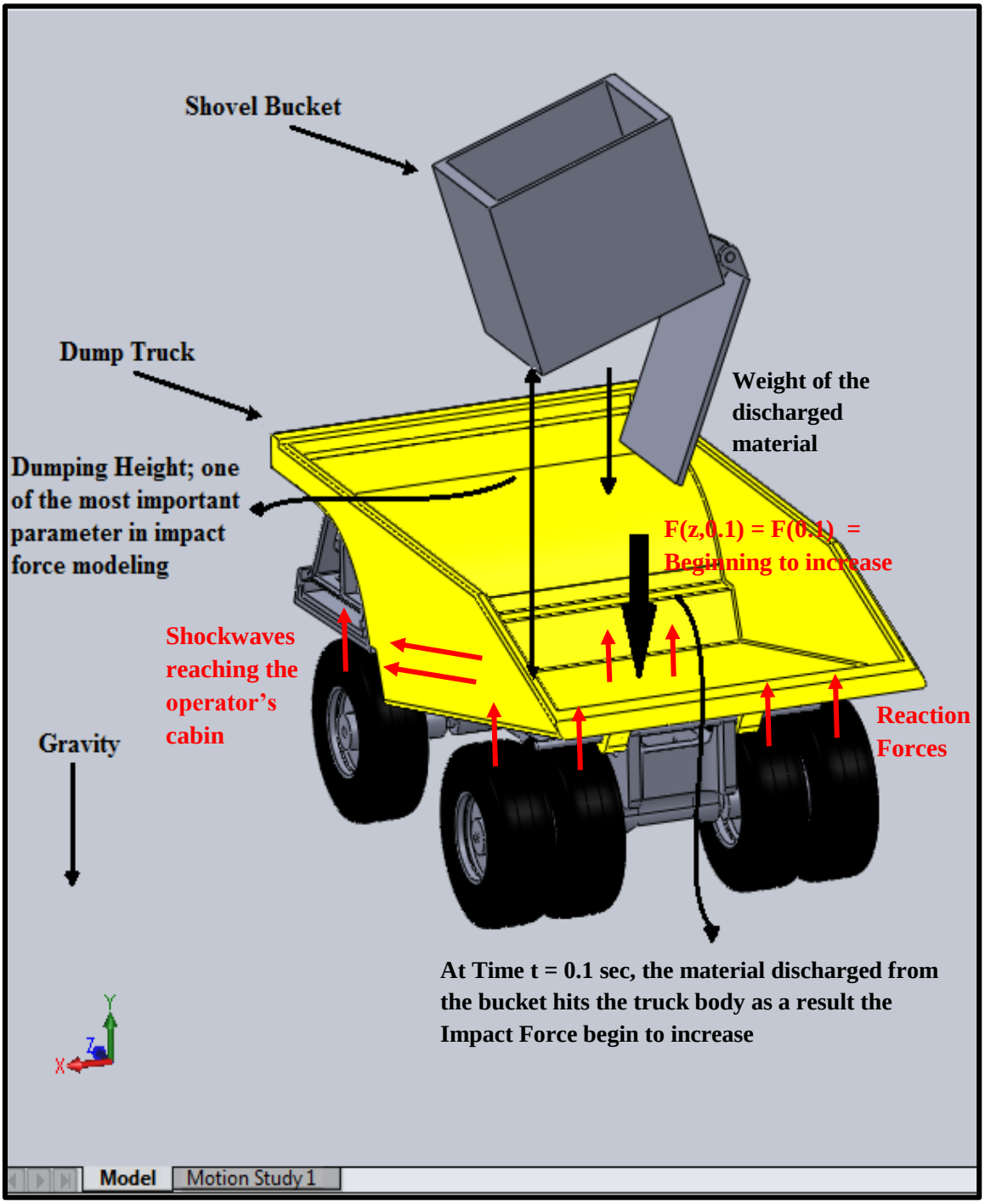

Figure 3.2. Shovel Dumping Process showing the Impact Force generation at Time t = 0.1 sec, with notable parameters

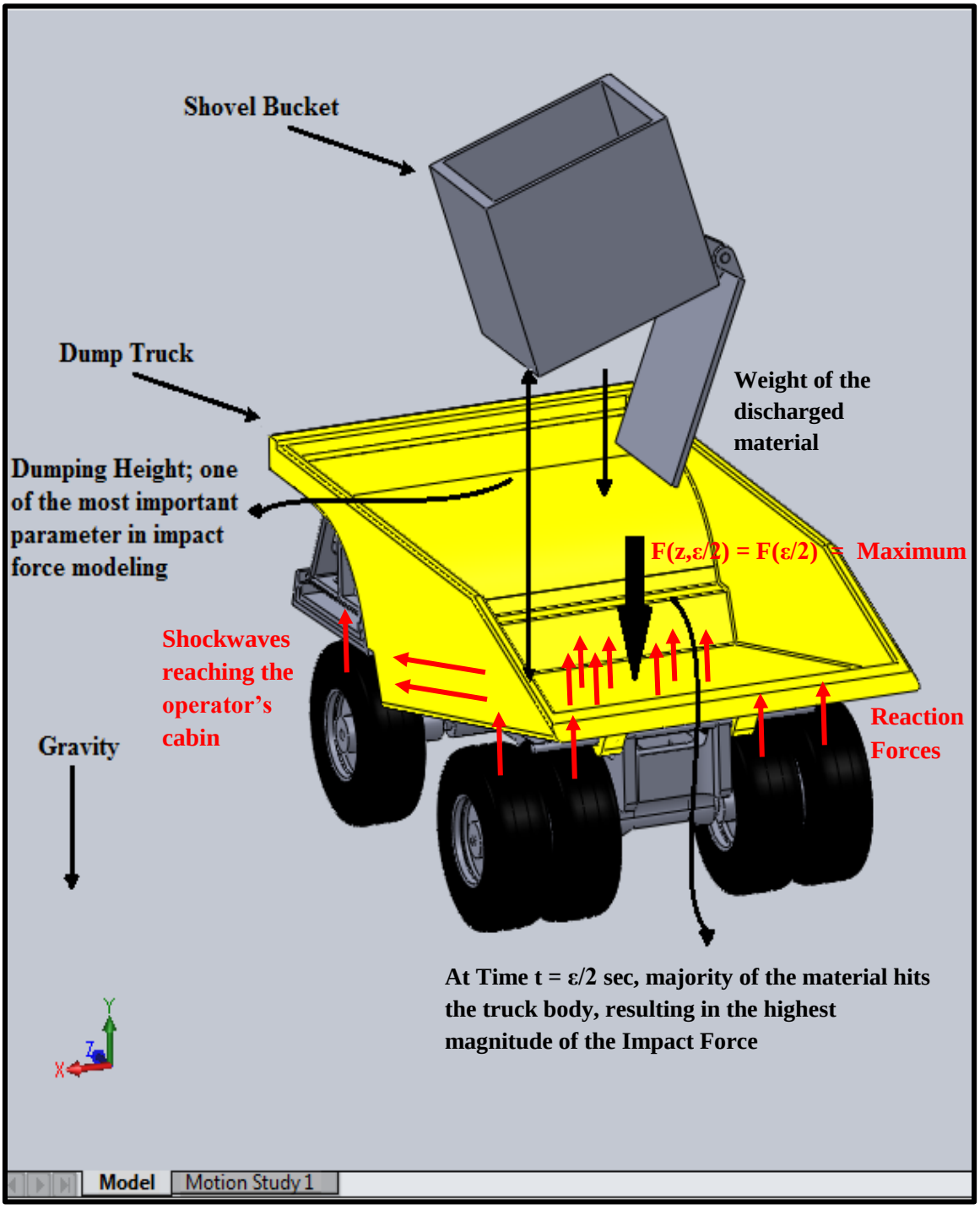

Figure 3.3. Shovel Dumping Process showing the Impact Force, Reaction forces and Shockwaves generation at Time t = ε/2 sec, with notable parameters

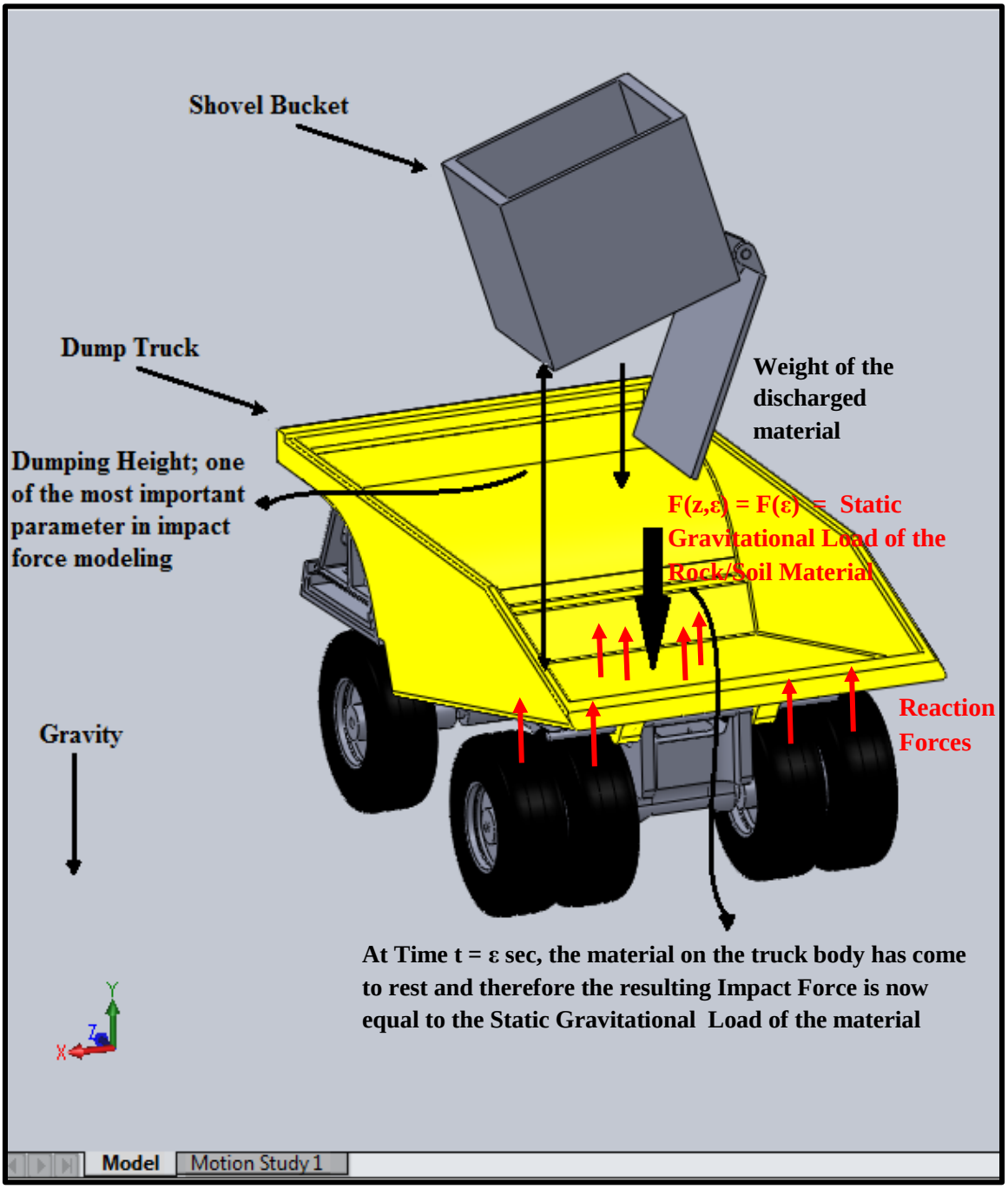

Figure 3.4. Shovel Dumping Process showing the Impact Force and Reaction forces generation at Time t = ε sec, with notable parameters

The kinetic energy of the whole system can is written as shown in equation (3.2) (Soedel, 2005). Rotary inertia of the beam is neglected since the beam is assumed to be slender.

$$\mathrm{T} = \frac{1}{2}\rho bh\int_o^L \left(\frac{\partial u}{\partial t}\right)^2 dx \tag{3.2}$$

The potential energy due to bending can also be written as equation (3.3) (Soedel, 2005). “Y” and “I” are not included within the integral, given the assumption that the beam material properties are linear and constant.

$$\mathrm{V} = \frac{1}{2}YI\int_o^L \left(\frac{\partial^2 u}{\partial x^2}\right)^2 dx \tag{3.3}$$

The potential energy due to elastic foundation can be written as equation (3.4). “K” is not included within the integral given the assumption that the spring modulus of the foundation is linear and constant.

$$\mathrm{Ve} = \frac{1}{2}K\int_o^L u^2(x,t)dx \tag{3.4}$$

The virtual work done by the distributed force is given by equation (3.5). The force is integrated over the length given the assumption that the load is uniform along the beam length. The –ve sign in equation (3.5) shows that the load (Impulse force) adds energy to the overall system by forcing the truck body (beam) in the direction of displacement.

$$\delta W_F = -\int_o^L F(x,t)\delta u dx \tag{3.5}$$

The virtual work done against damping of foundation is given by equation (3.6) (Basu and Rao, 2012). “C” is not included within the integral, given the assumption that the damping of the foundation is linear and constant.

$$\delta W_F = C\int_o^L \frac{\partial u}{\partial t}\delta u dx \tag{3.6}$$

The use of Hamilton's Principle yields equation (3.7).

$$\delta \int_{t_1}^{t_2} [T - V] dt = \int_{t_1}^{t_2} \delta W dt \quad [19] \tag{3.7}$$

Inserting equations (3.2) through (3.6) into equation (3.7) and carrying out the necessary integration and the algebra, yields equation (3.8).

$$\begin{aligned} \int_{t_1}^{t_2} \Bigg\{ \int_{o}^{L} \left[-\rho bh \left(\frac{\partial^2 u}{\partial t^2} \right) - YI \left(\frac{\partial^4 u}{\partial x^4} \right) - C \frac{\partial u}{\partial t} - Ku(x,t) + F(x,t) \right] \delta u dx \\ - YI \left(\frac{\partial^2 u(L,t)}{\partial x^2} \right) \delta \frac{\partial u(L,t)}{\partial x} + YI \left(\frac{\partial^2 u(0,t)}{\partial x^2} \right) \delta \frac{\partial u(0,t)}{\partial x} \\ + YI \left(\frac{\partial^3 u(L,t)}{\partial x^3} \right) \delta u(L,t) - YI \left(\frac{\partial^3 u(0,t)}{\partial x^3} \right) \delta u(0,t) \Bigg\} dt \\ = 0 \end{aligned} \tag{3.8}$$

Since all of the variations are arbitrary and independent, the equation of motion and the boundary conditions for the system can be obtained from equation (3.8). The governing equation of motion for the complete system, as given by equation (3.9), is developed by setting the 1st expression within the square brackets in equation (3.8) to zero.

$$YI \left(\frac{\partial^4 u}{\partial x^4} \right) + \rho bh \left(\frac{\partial^2 u}{\partial t^2} \right) + C \frac{\partial u}{\partial t} + Ku(x,t) = F(x,t) \tag{3.9}$$

The boundary conditions are obtained from the remaining terms in equation (3.8). Considering that the transverse displacement is not zero at the ends of the beam, the shear terms can be set to zero at the ends (x = 0, x = L) for equation (3.8) to be consistent. And, due to lack of bending, the slope terms can also set to be zero at the ends (x = 0, x = L) in order to obtain the necessary boundary conditions for the system. These steps yield the following boundary conditions.

$$\frac{\partial u(L,t)}{\partial x} = 0 \tag{3.10}$$

$$YI\left(\frac{\partial^3 u(L,t)}{\partial x^3}\right) = 0 \tag{3.11}$$

$$\frac{\partial u(0,t)}{\partial x} = 0 \tag{3.12}$$

$$YI\left(\frac{\partial^3 u(0,t)}{\partial x^3}\right) = 0 \tag{3.13}$$

3.1.1. Solving the Homogenous Problem (Eigen Value Problem). Using the separation of variable method and assuming a solution of the form: U(x,t) = U(x)T(t), and plugging it back into the E.O.M (equation (3.9)) and disregarding the damping and the forcing, result in equations (3.14) and (3.15).

$$U(x) = D_1\cos(\beta x) + D_2\sin(\beta x) + D_3\cos\mathrm{h}(\beta x) + D_4\sinh(\beta x) \tag{3.14}$$

$$T(t) = C_1\cos(\alpha t) + C_2\sin(\alpha t) \tag{3.15}$$

3.1.2. Applying the Boundary Conditions. At X = 0 (putting equation (3.14) in equations (3.10) and (3.12)), the systems yields we will obtain equation (3.16) as a boundary condition.

$$D_2 = D_4 = 0 \tag{3.16}$$

At X = L (putting equations (3.14) and (3.16) in equations (3.11) and (3.13)), the system yields equation (3.17) as a boundary condition. $D_3 \sin h(\beta L) = 0 \; and \; \sin h(\beta L) \neq 0$. Assuming $D_3 = 0$, which is also true as the solution cannot be unbounded and 'sinh' gives unbounded solution, the system yields equations (3.17) and (3.18).

$$\sin(\beta L) = 0 \tag{3.17}$$

$$\beta_n = \frac{n\pi}{L} \tag{3.18}$$

Inserting equations (3.16) and (3.18) into equation (3.14), the general mode equation can be obtained as equation (3.19).

$$U_n(x) = \cos\frac{n\pi}{L}X \tag{3.19}$$

3.1.3. Applying Modal Expansion to Solve for the Forced & Damped Problem.

In order to obtain the complete response of the truck body (beam) to the impulse force, modal expansion can be applied as follows**:**

$$U(x,t) = \sum_{n=1}^{\infty} \eta_n(t)\, U_n(x) = \sum_{n=1}^{\infty} \eta_n(t) \cos\frac{n\pi}{L}X \tag{3.20}$$

Inserting equation (3.20) back into the equation of motion (equation (3.9)), results in equation (3.21).

$$\ddot{\eta_n}(t) + 2\zeta_n\omega_n\dot{\eta_n}(t) + \omega_n^2\eta_n(t) = \frac{2}{\rho bhL}\int_0^L F(x,t)\cos\frac{n\pi}{L}Xdx \tag{3.21}$$

Equation (3.21) is the equation of motion in canonical form for '$\eta_n(t)$', which yields the temporal solution of the system.

3.1.4. Response Due to Initial Conditions.

$$\eta_0(t) = 0 \text{ As } \eta(0) = \dot{\eta}(0) = 0 \tag{3.22}$$

(The Truck body is at rest initially; the initial displacement and the initial velocity of the system are zero.)

3.1.5. Response Due to F(x,t). Inserting equation (3.1) into equation (3.21) yields equation (3.23).

$$\begin{aligned}\ddot{\eta_n}(t) + 2\zeta_n\omega_n\dot{\eta_n}(t) + \omega_n^2\eta_n(t) \\ = |F_n(t)|[2(t-a)H(t-a) - 4(t-b)H(t-b) \\ + 2(t-c)H(t-c)]\end{aligned} \tag{3.23}$$

Where,

$$|F_n(t)| = \frac{2}{\rho bhL}\frac{F_o}{\epsilon}\int_0^L \cos\frac{n\pi}{L}Xdx$$

Solving equation (3.23) using Laplace transformation, the temporal solution of the system can be obtained as equation (3.24) and the complete solution can be obtained as equation (3.25).

$$\eta_n(t) = \frac{|F_n(t)|}{\omega_n^3}\Bigg\{2\Bigg[-2\zeta_n + \omega_n(t-a) + e^{-\zeta_n\omega(t-a)}\Bigg(2\zeta_n \operatorname{Cos}\big(\omega_d(t-a)\big) + \frac{2\zeta_n^2}{\sqrt{1-\zeta_n^2}}Sin\big(\omega_d(t-a)\big) - \frac{1}{\sqrt{1-\zeta_n^2}}Sin\big(\omega_d(t-a)\big)\Bigg)\Bigg]H(t-a) - 4\Bigg[-2\zeta_n + \omega(t-b) + e^{-\zeta_n\omega(t-b)}\Bigg(2\zeta_n \operatorname{Cos}\big(\omega_d(t-b)\big) + \frac{2\zeta_n^2}{\sqrt{1-\zeta_n^2}}Sin\big(\omega_d(t-b)\big) - \frac{1}{\sqrt{1-\zeta_n^2}}Sin\big(\omega_d(t-b)\big)\Bigg)\Bigg]H(t-b) + 2\Bigg[-2\zeta_n + \omega(t-c) + e^{-\zeta_n\omega(t-c)}\Bigg(2\zeta_n \operatorname{Cos}\big(\omega_d(t-c)\big) + \frac{2\zeta_n^2}{\sqrt{1-\zeta_n^2}}Sin\big(\omega_d(t-c)\big) - \frac{1}{\sqrt{1-\zeta_n^2}}Sin\big(\omega_d(t-c)\big)\Bigg)\Bigg]H(t-c)\Bigg\} \tag{3.24}$$

$$U(x,t) = \sum_{n=1}^{\infty}\eta_n(t)\cos\frac{n\pi}{L}X \qquad \forall\, n \in N \tag{3.25}$$

By inserting equation (3.24) into equation (3.25), the complete response of the truck body (beam) due to the applied impulse force can be obtained. This response of the truck body (beam) can be used to obtain a more rigorous mathematical model for the applied impulse force.

3.1.6. Finally Predicting the Impact Force using the Response of the System.

The general concept of stress is defined by equation (3.26):

$$\sigma = \frac{F}{A} \tag{3.26}$$

$$F = \sigma A = Y\varepsilon A = Y\frac{\partial u(x,t)}{\partial x}A \tag{3.27}$$

Inserting the complete response of the truck body (beam), due to the applied impulse force (obtained from equation (3.25)), into equation (3.27), a more rigorous mathematical model for the applied impulse force can be obtained as equation (3.28).

3.2. EMPIRICAL MODEL FOR THE DYNAMIC IMPACT FORCE

The mathematical model in equation (3.28) contains a number of parameters. These parameters include dimensional parameters of truck body, material properties of the truck, damping and stiffness properties of the truck body and the visco-elastic foundation upon which it rest (primarily the chassis and front and the rear wheel/tire assembly). If it can be assumed that these truck parameters will not significantly affect the impulse force, they can be eliminated from the process for developing the empirical model for the impulse force. Such an empirical model requires the definition of the magnitude of the impulse force, which varies with time throughout the dumping process.

The underlying assumptions for the empirical model include the following.

- Similar to the mathematical model, the impulse force is dynamic and it is modeled as a unit triangular impulse force. Based on these assumptions, the impulse force can be modeled using the Heaviside step function ‘H’ in equation (3.32).
- The magnitude of the impulse force is developed using the law of conservation of energy and the law of conservation of linear momentum.

$$F = YA\frac{2}{\rho bhL}\frac{\sqrt{2gH_t}\,m}{\omega_n^3\epsilon^2}\sum_{n=1}^{\infty}\Bigg\{2\Bigg[-2\zeta_n + \omega(t-a) + e^{-\zeta_n\omega(t-a)}\Bigg(2\zeta_n\,\mathrm{Cos}\big(\omega_d(t-a)\big) + \frac{2\zeta_n^2}{\sqrt{1-\zeta_n^2}}Sin\big(\omega_d(t-a)\big) - \frac{1}{\sqrt{1-\zeta_n^2}}Sin\big(\omega_d(t-a)\big)\Bigg)\Bigg]H(t-a) - 4\Bigg[-2\zeta_n + \omega(t-b) + e^{-\zeta_n\omega(t-b)}\Bigg(2\zeta_n\,\mathrm{Cos}\big(\omega_d(t-b)\big) + \frac{2\zeta_n^2}{\sqrt{1-\zeta_n^2}}Sin\big(\omega_d(t-b)\big) - \frac{1}{\sqrt{1-\zeta_n^2}}Sin\big(\omega_d(t-b)\big)\Bigg)\Bigg]H(t-b) + 2\Bigg[-2\zeta_n + \omega(t-c) + e^{-\zeta_n\omega(t-c)}\Bigg(2\zeta_n\,\mathrm{Cos}\big(\omega_d(t-c)\big) + \frac{2\zeta_n^2}{\sqrt{1-\zeta_n^2}}Sin\big(\omega_d(t-c)\big) - \frac{1}{\sqrt{1-\zeta_n^2}}Sin\big(\omega_d(t-c)\big)\Bigg)\Bigg]H(t - c)\Bigg\}\frac{\partial}{\partial x}\Bigg(\int_0^L \cos\frac{n\pi}{L}X dx\cos\frac{n\pi}{L}X\Bigg) \tag{3.28}$$

Using the law of conservation of energy, the velocity for the free falling material, just before reaching the truck body (impact velocity), is given by equation (3.29). Using equation (3.29), and law of conservation of linear momentum, the linear momentum of the

material just before reaching the truck body, is given by equation (3.30). Finally, the magnitude of the impact force can be obtained using the equation (3.30) and the definition of the impulse, given by equation (3.31). From these equations and equation (3.31), the definition of the unit triangular impulse (defining the impact force) with a provision for multi sub-passes can be obtained using equation (3.32).

$$v = \sqrt{2gH_t} \tag{3.29}$$

$$L_m = \sqrt{2gH_t}\, m \tag{3.30}$$

$$Magnitude\ of\ Imapct\ Force = \frac{\sqrt{2gH_t}\, m}{\epsilon} \tag{3.31}$$

$$\begin{aligned} F(t) = \frac{\sqrt{2gH_t}\, m}{\epsilon^2 (M+1)} \sum_{j=0}^{M} \Bigg[& 2\left(t - \left(j\left(\frac{\epsilon}{a}\right)a\right)\right) H\left(t - \left(j\left(\frac{\epsilon}{a}\right)a\right)\right) \\ & - 4\left(t - \left(j\left(\frac{\epsilon}{a}\right)a\right) - \frac{\epsilon}{2}\right) H\left(t - \left(j\left(\frac{\epsilon}{a}\right)a\right) - \frac{\epsilon}{2}\right) \\ & + 2\left(t - \left(j\left(\frac{\epsilon}{a}\right)a\right) - \epsilon\right) H\left(t - \left(j\left(\frac{\epsilon}{a}\right)a\right) - \epsilon\right) \Bigg] \end{aligned} \tag{3.32}$$

3.3. SUMMARY

Detailed mathematical model for the dynamic impact force under HISLO conditions has been presented in this section. Initially, the response of the truck body has been used to come up the mathematical model for the impact force. Afterwards, in order to make it more applicable, an empirical approach has been use to formulate the mathematical model for the dynamic impact force using the fundamental laws. Using the mathematical model, we can find the impact force resulting at the truck body due to the gravity dumping of the material during the shovel dumping process. The forces obtained through the

mathematical model can then be used to find the vibrations at each component, especially the operator's seat, under the HISLO conditions. And then it can determined whether these vibration levels are harmful for the operator. The modelling framework formulated, was based on the necessary assumptions and limitations. This framework provide us with the cause of the dump truck vibrations under HISLO conditions which is dynamic impact force. The variables, such as dumping height, time the material takes in dumping and then coming to rest after dumping and the provision to divide the shovel ore-pass into more than one sub-pass are included in the rigorous mathematical model for dynamic impact force. The finding will serve as a guideline for the complete impulse force reduction technology research.

4. EXPERIMENTAL DESIGN AND EXPERIMENTATION

Detail explanation of the experimental setup and the procedures for the experiments for predicting the impact force have been illustrated in this section. Experiments were conducted to analyze the effectiveness of the mathematical model for predicting a more realistic dynamic impulse force for the shovel dumping process. A series of optimal dumping heights are generated for the HISLO scenarios for the analysis of the shovel dumping process.

4.1. EXPERIMENTAL DESIGN

Numerical experiments are conducted in order to predict the dynamic impact force for a shovel dumping operation. The final equation presented in the previous section as part of the mathematical model given by equation (3.32) is used to model the impact force. MAPLE© is chosen as a platform to obtain the required solution. MAPLE© offers a vast library of computational algorithms and can handle symbolic analysis in the development of the solution. Mathematical model given by equation (3.32) is embedded into the MAPLE©. All the required input variables for the mathematical model are obtained from the real world shovel dumping operation and are input directly into the system. The arguments of the mathematical model are evaluated numerically using the default floating – point environment in MAPLE©.

A total of seven experiments are conducted in order to predict the dynamic impact force for the shovel dumping operation. The objective was to analyze the effectiveness of the mathematical model for predicting a the dynamic impulse force for the shovel dumping process; investigate the reduction in the impact force magnitude associated the decrease in the dumping height; and then finally to obtain the series of optimal dumping heights for the HISLO scenarios keeping in view the minimum clearance required.

These dumping height reduction experiments provided a basis for examining the safe distance with clearance that minimizes the impact of the impulse force on the truck body, which impacts the magnitudes of WBV exposures, and hence the health and safety of dump truck operators.

4.2. DETAILED EXPERIMENTATION

In order to obtain the impact force representation, numerical experiments were conducted with P&H 4100 XPC cable shovel dumping 100-ton material into the CAT 793D for varying dump distances. Material was dumping from a maximum distance of 'H_t = 7.33 m' to a minimum of 4.9 m, under similar conditions. The minimum dumping distance of 4.9 m is the minimum height that ensures a safe clearance without any jolting of the dipper door with dump truck edges based on equation (3.32). Note that the maximum and the optimal dumping heights in this study apply only to the case used, i.e., the P&H 4100 XPC cable shovel and the CAT 793D dump truck. For any other shovel-truck combination, these heights may change. All the required input parameters i.e. mass of the dumped material, time which the material takes to settle down, time at which the shovel starts dumping and dumping distances were taken from the real world shovel dumping operation of P&H 4100 XPC cable shovel dumping 100-ton material into the CAT 793D and were input into the mathematical model embedded in MAPLE© to predict the dynamic impact force. The value for the parameter 'ϵ' has been initially approximated from the 3D virtual simulation, which will be explained in the latter section, conducted under the similar conditions set for the experimentation. The value has to be taken as the time between which the material hits the truck body up to the time at which it completely falls off. The value of the parameter has been verified later against the real world shovel dumping operation. The general range is between 1.1 sec and 1.5 sec. Table 4.1 contains all the values for constant parameters used for the experiments.

Table 4.1. Values for constant parameters

Parameter	Value
ϵ	1.28 sec
m	90,718.5 kg
g	9.81 m/s^2
a	0.1sec

Furthermore, for every particular dumping distance, a single shovel pass was divided into more than one sub-pass and again the impulse force for each case was modeled taking into account such sub-divisions. These sub-divisions included zero sub-division, 2, 3 and 4 sub-divisions to study the effect of the divisions on the impact force. It should be noted that all these different dumping parameters used in these seven experiments are particular to the case of P&H 4100 XPC shovel and CAT 793D dump truck operation. For any other shovel truck combination, these parameters have to be re-determined from that corresponding real time shovel dumping operation.

4.3. EXPERIMENT #1

Dumping distance is set at 7.33 m to examine the impact force for the HISLO process (Table 4.2).

Table 4.2. Dumping parameters for Experiment #1

Shovel Dumping Height (A)	**Truck Loading Height (B)**	**Truck Inside Body Depth (C)**	**Clearance (D = A – B)**	**H_t (Clearance + C)**
10.87 m	5.87 m	2.33 m	5 m	7.33 m

4.4. EXPERIMENT #2

Dumping distance is set at 6.33 m to examine the impact force for the HISLO process (Table 4.3).

4.5. EXPERIMENT #3

Dumping distance is set at 6.00 m to examine the impact force for the HISLO process (Table 4.4).

Table 4.3. Dumping parameters for Experiment #2

Shovel Dumping Height (A)	**Truck Loading Height (B)**	**Truck Inside Body Depth (C)**	**Clearance (D = A – B)**	**H_t (Clearance + C)**
9.87 m	5.87 m	2.33 m	4 m	6.33 m

Table 4.4. Dumping parameters for Experiment #3

Shovel Dumping Height (A)	**Truck Loading Height (B)**	**Truck Inside Body Depth (C)**	**Clearance (D = A – B)**	**H_t (Clearance + C)**
9.54 m	5.87 m	2.33 m	3.67 m	6.0 m

4.6. EXPERIMENT #4

Dumping distance is set at 5.50 m to examine the impact force for the HISLO process (Table 4.5).

Table 4.5. Dumping parameters for Experiment #4

Shovel Dumping Height (A)	**Truck Loading Height (B)**	**Truck Inside Body Depth (C)**	**Clearance (D = A – B)**	**H_t (Clearance + C)**
9.04 m	5.87 m	2.33 m	3.17 m	5.5 m

4.7. EXPERIMENT #5

Dumping distance is set at 5.33 m to examine the impact force for the HISLO process (Table 4.6).

Table 4.6. Dumping parameters for Experiment #5

Shovel Dumping Height (A)	**Truck Loading Height (B)**	**Truck Inside Body Depth (C)**	**Clearance (D = A – B)**	**H_t (Clearance + C)**
8.87 m	5.87 m	2.33 m	3 m	5.33 m

4.8. EXPERIMENT #6

Dumping distance is set at 5.00 m to examine the impact force for the HISLO process (Table 4.7).

4.9. EXPERIMENT #7

Dumping distance is set at 4.90 m to examine the impact force for the HISLO process (Table 4.8).

Table 4.7. Dumping parameters for Experiment #6

Shovel Dumping Height (A)	**Truck Loading Height (B)**	**Truck Inside Body Depth (C)**	**Clearance (D = A – B)**	**H_t (Clearance + C)**
8.54 m	5.87 m	2.33 m	2.67 m	5.0 m

Table 4.8. Dumping parameters for Experiment #7

Shovel Dumping Height (A)	**Truck Loading Height (B)**	**Truck Inside Body Depth (C)**	**Clearance (D = A – B)**	**H_t (Clearance + C)**
8.44 m	5.87 m	2.33 m	2.57 m	4.9 m

4.10. SUMMARY

Numerical experiments are conducted for the case where P&H 4100 XPC cable shovel is dumping 100-ton material into the CAT 793D. The developed mathematical model as given by equation (3.32) is embedded into MAPLE to predict the dynamic impact force for the shovel dumping operation. By varying the dumping height, reduction in the impact force magnitude is investigated and a series of optimal dumping heights are generated for the HISLO scenarios keeping in view the minimum clearance required.

5. VIRTUAL SIMULATION OF SHOVEL DUMPING PROCESS

This section presents the 3-D virtual simulation of the shovel dumping process. The methodology and procedures have been developed for building the 3-D virtual model of the CAT 793D dump truck and the P&H 4100XPC shovel dipper using SolidWorks. Also discussed are the detailed steps and methodologies for meshing and the complete simulation of the virtual models for various dumping heights using Rhino 5.0 and PFC3D with model dimensions and constraints. This section also discusses the DEM method used by PFC3D software for the shovel dumping virtual simulation. Then virtual model developed by Aouad and Frimpong (2013) has been used to carry out the vibration analysis in MSC ADAMS. The virtual simulation is carried for CAT 793D to obtain the vertical RMS acceleration of the operator's seat for the corresponding impact force results. Virtual simulation results from MSC ADAMS by Aouad and Frimpong (2013) have been presented and discussed in detail. Mathematical model and virtual simulator have been verified and validated by comparing the results with that of Aouad and Frimpong (2013).

5.1. DISCRETE/DISTINCT ELEMENT METHOD (DEM) IN PFC3D (PFC, 2014)

Particle Flow Code (PFC) has been used successfully by researchers and companies around the world (Itasca, 2011). It has been used for problems ranging from fundamental research on soil and rock behavior at the laboratory scale to slope stability and rockfall hazard mitigation, hydraulic fracturing, rock-tool interactions, bulk flow, mixing, conveying and compaction of aggregates and powders, and blast furnace modeling (Itasca, 2011).

The PFC models the movement and interaction of stressed assemblies of rigid (circular in 2D; spherical in 3D) particles using the discrete/distinct element method (DEM). The DEM technique was introduced by Cundall (1971) for analyzing rock-mechanics problems. Then it was applied for analyzing soil-mechanics problems by Cundall (1979). A thorough description of the method is given in the two-part paper by Cundall (1988) and Hart (1988), and in the UDEC manual (Itasca, 2011). PFC is classified as a discrete element code based on the definition by Cundall (1992). It allows finite

displacements and rotations of discrete bodies (including complete detachment) and recognizes new contacts automatically as the calculation progresses. PFC can be viewed as a simplified implementation of DEM because of the restriction to rigid (circular in 2D; spherical in 3D) particles. The general DEM can handle deformable polygonal-shaped particles.

The PFC model simulates the movements and interactions of many finite-sized particles. The particles are rigid bodies with finite mass that move independently of one another and can both translate and rotate. Particles interact at pair-wise contacts by means of an internal force and moment. Contact mechanics is embodied in particle-interaction laws that update the internal forces and moments. The time evolution of this system is computed via the discrete -element method, which provides an explicit dynamic solution to Newton's laws of motion.

PFC provides a particle-flow model containing the following assumptions.

- The particles are treated as rigid bodies.
- The fundamental particle shape is denoted as a ball (considered as disks with unit thickness in 2D; spheres in 3D).
- The clump logic supports the creation of rigidly attached bodies denoted as pebbles (considered as disks with unit thickness in 2D; spheres in 3D). Each clump consists of a set of overlapping pebbles that acts as a rigid body with a deformable boundary. Clumps may be of arbitrary shape.
- Particles interact at pair-wise contacts by means of an internal force and moment. Contact mechanics is embodied in particle-interaction laws that update the internal forces and moments.
- Behavior at physical contacts uses a soft-contact approach where the rigid particles are allowed to overlap with one another at contact points. The contacts occur over a vanishingly small area (i.e., at a point), and the magnitude of the overlap and/or the relative displacement at the contact point are related to the contact force via the force-displacement law.
- Bonds can exist at contacts between particles.
- Long range interactions can also be derived from energy potential functions.

In DEM, particle-particle interaction is treated as a dynamic process reaching equilibrium whenever the internal forces balance. Contact forces and displacements of a stressed assembly of particles are found by tracing the movements of individual particles. Movements result from the propagation through the particle system of disturbances caused by specified wall and particle motion and/or body forces. This is a dynamic process in which the propagation speed depends on physical properties of the discrete system. The dynamic behavior is defined numerically by a time-step algorithm with an assumption that velocities and accelerations are constant within each time step. The solution scheme is identical to the explicit finite-difference method for continuum analysis. DEM is based on the idea that the time step chosen may be so small that, during a single time step, disturbances cannot propagate further from any particle than its immediate neighbors. At all times, the forces acting on any particle are determined exclusively by its interactions with contact particles.

The DEM calculations alternate between the application of Newton's second law to the particles and a force-displacement law at the contacts. Newton's second law is used to determine the motion of each particle from the contact and body forces acting on it, while the force-displacement law is used to update the contact forces arising from the relative motion at each contact. The presence of walls in PFC requires only that the force-displacement law accounts for contacts with wall facets. Newton's second law is not applied to walls because the wall motion is specified by the user.

5.2. CAD GEOMETRY AND MESHING IN SOLIDWORKS AND RHINO 5.0

The first step in setting up the virtual simulation consists of creating a detailed CAD geometry of the truck and shovel dipper that reflects the actual process using SolidWorks. A detailed CAD geometry of the dumping process is created and assembled with the proper dumping height. The CAD models maintain the shape and dimensions of components, as well as the relative location of components with respect to each other.

Figure 5.1 shows a 2D schematic diagram of the side, front and rear views of the CAT 793D dump truck. Table 5.1 lists the dimensions for the corresponding side, front and the rear views of CAT 793D in Figure 5.1. Figure 5.2 shows a sketch of the P&H 4100XPC

shovel, with the required dimensions for the CAD model in SolidWorks. Using the data in Figures 5.1 and 5.2 and Table 5.1, the dumping process was created to capture the actual CAT 793D truck and P&H 4100XPC shovel dipper. Figure 5.3 shows the isometric, front and side views of the CAT 793D truck in SolidWorks. Figure 5.4 shows the isometric, front and side views of the P&H 4100XPC shovel dipper in SolidWorks. The shovel dipper in the CAD models is positioned at a proper dumping height to mimic the dumping process. Different dumping heights have been used (from 7.33 m to 4.9 m) for the dumping process. This minimum distance ensures that a good clearance between the dipper door and the truck edges to prevent jolting and to maintain the effectiveness and the efficiency of the dumping process.

These different dumping heights have also been used to examine the gradual reduction in impact force with varying heights. Complex geometries of the dumping process require very fine meshes, which consumes large CPU times in DEM. The simplification of the shovel dipper model prevents problems during the meshing of the parts with corresponding ease in the DEM analysis. Figure 5.5 and Figure 5.6 represents the isometric and the front views of the truck body assembly and the simplified shovel dipper in SolidWorks for the dumping heights of 7.33 m and 6.33 m, respectively.

Figure 5.7 and Figure 5.8 shows the isometric and the front views of the truck and the shovel dipper in SolidWorks for dumping heights of 6.00 m and 5.50 m, respectively. Figure 5.9 and Figure 5.10 shows the isometric and the front views of the truck and shovel dipper in SolidWorks for heights of 5.33 m and 5.00 m, respectively. Figure 5.11 shows the isometric and the front views of the truck and shovel dipper in SolidWorks for the minimum height of 4.9 m. The assemblies are imported into Rhino 5.0 for meshing. The truck model uses fine polygonal mesh due to the forces developed in truck body. The shovel dipper uses simple polygonal meshing because of the concern for any of the forces in the dipper. The simplified mesh for shovel dipper saves a lot of computational time during DEM analysis in PFC3D. Figure 5.12 shows the mesh for the dump truck and the shovel dipper assemblies in Rhino 5.0.

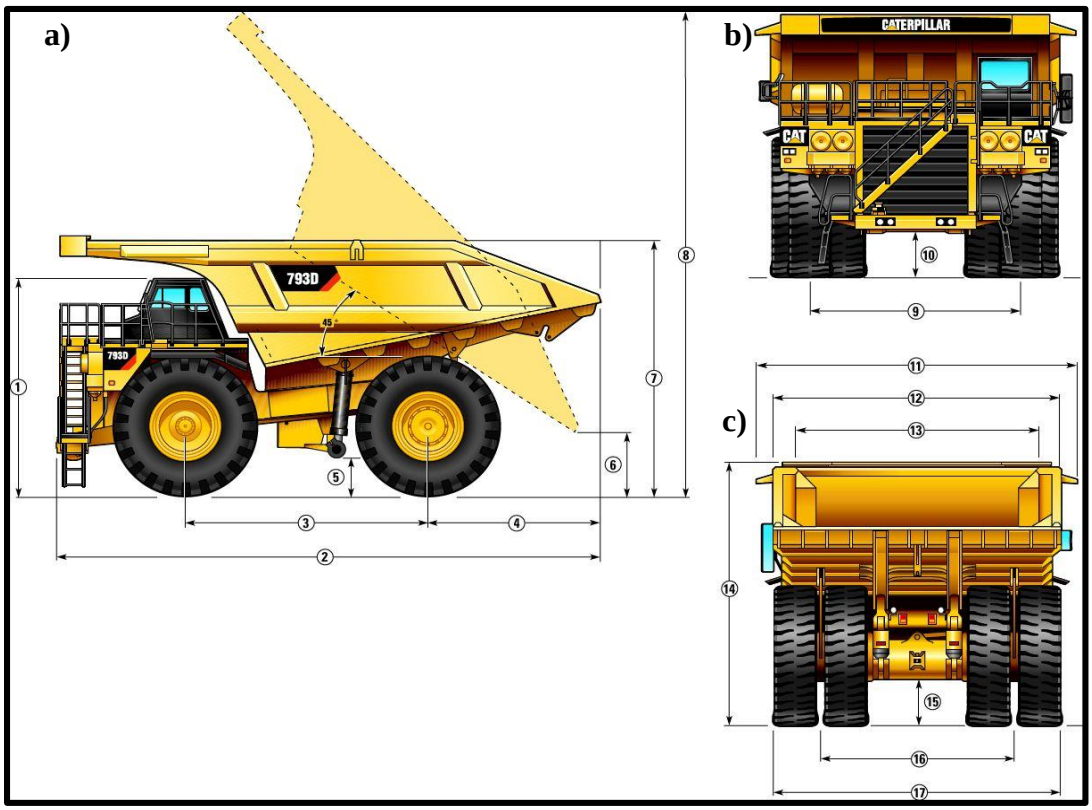

Figure 5.1. CAT 793D a) Side View, b) Front View, c) Rear View

Figure 5.2. Engineering Sketch for P&H 4100XPC Shovel

Table 5.1. CAT 793D Dimensions

	Descriptions	Dimensions (mm)
1	Height to Top of ROPS – Empty	5584 mm
2	Overall length	12862 mm
3	Wheelbase	5905 mm
4	Rear axle to tail	3772 mm
5	Ground clearance – Empty	1005 mm
6	Dump Clearance	1364 mm
7	Loading height – Empty	5871 mm
8	Overall Height – Body Raised	13113 mm
9	Centerline front tire width	5610 mm
10	Engine guard clearance – empty	1294 mm
11	Overall canopy width	7680 mm
12	Outside body width	6940 mm
13	Inside body width	6500 mm
14	Front canopy height	6494 mm
15	Rear Axle Clearance	1128 mm
16	Centerline Rear dual tire width	4963 mm

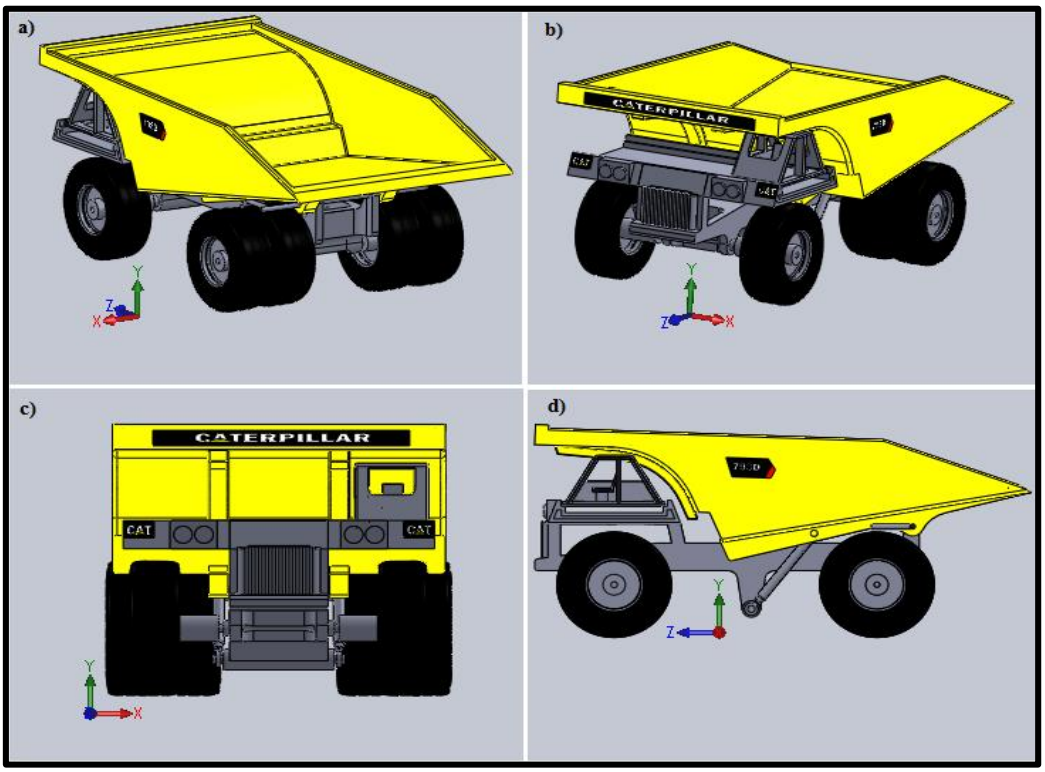

Figure 5.3. CAT793D Model: a) Back Isometric, b) Front Isometric, c) Front, d) Side Views

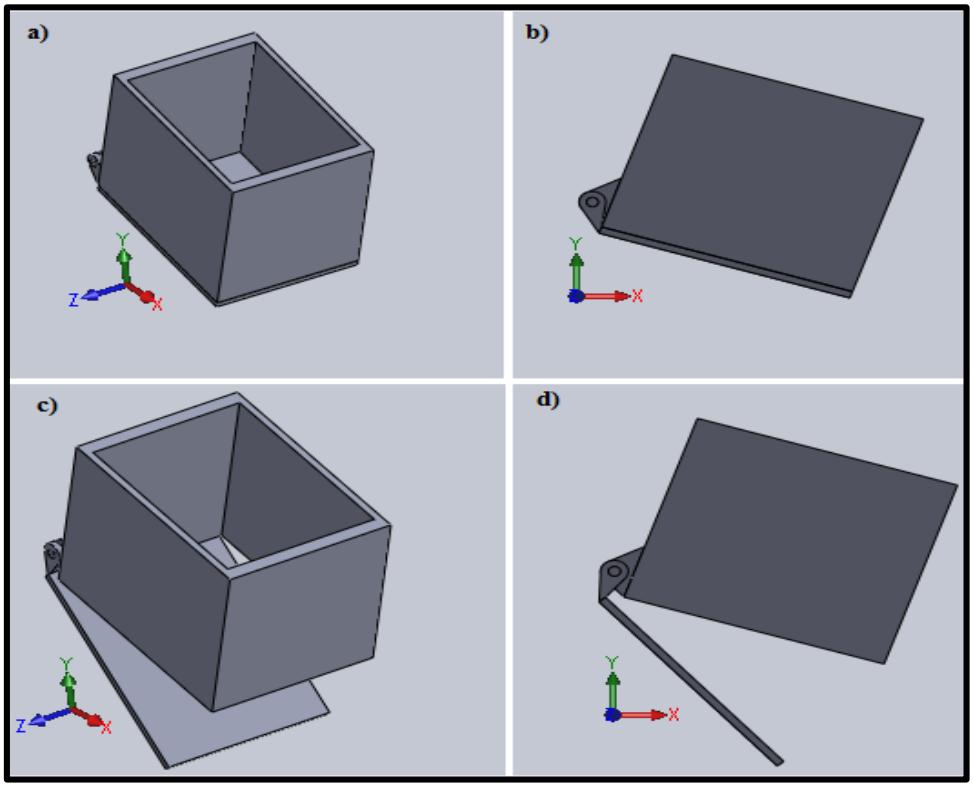

Figure 5.4. P&H 4100XPC Shovel Dipper Model: a) Isometric, b) Side, c) Isometric with Door Rotated, and d) Side Views with Door Rotated

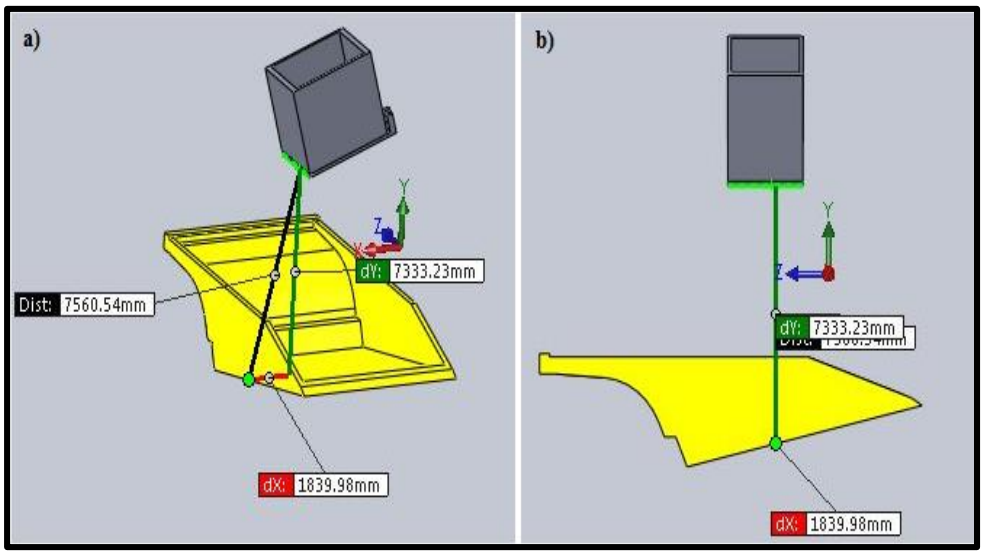

Figure 5.5. Truck Body and Shovel Dipper CAD Assembly for H_t = 7.33 m (7333 mm): a) Isometric View b) Side View

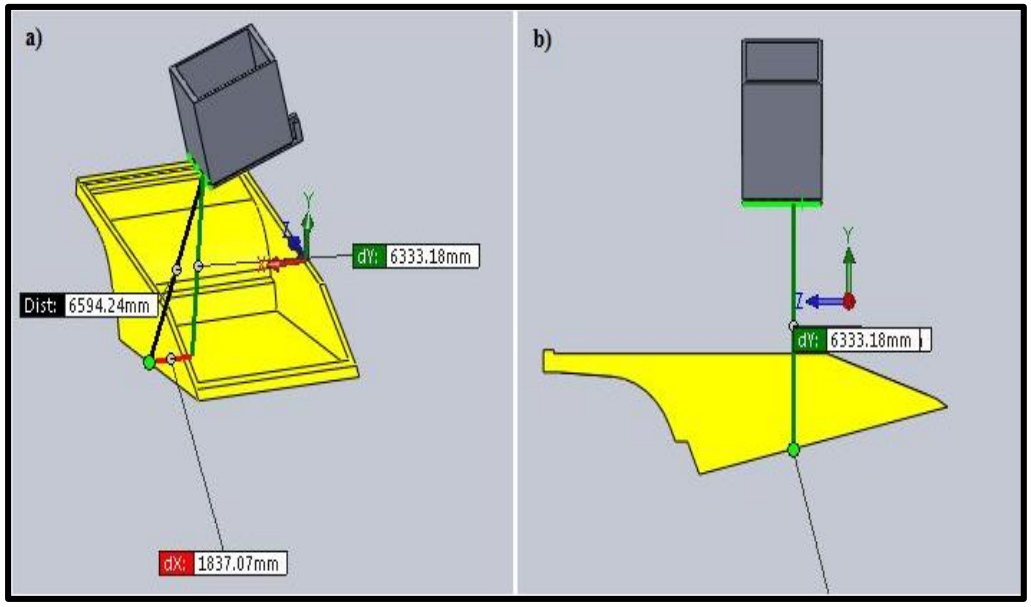

Figure 5.6. Truck Body and Shovel Dipper CAD Assembly for H_t = 6.33 m (6333 mm): a) Isometric View b) Side View

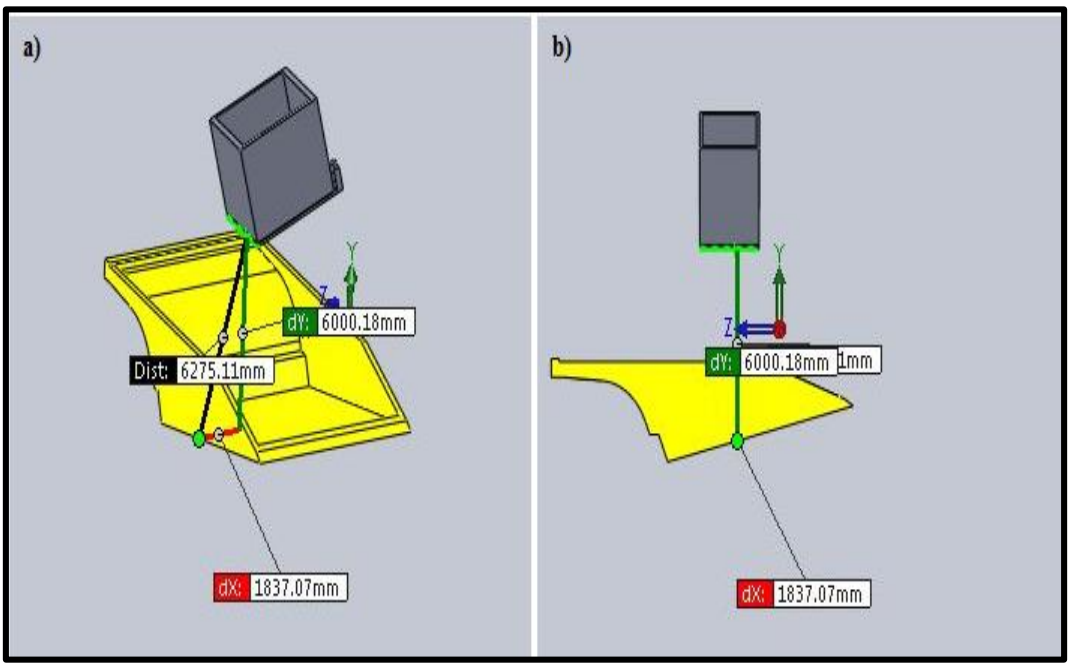

Figure 5.7. Truck Body and Shovel Dipper CAD Assembly for H_t = 6.00 m (6000 mm): a) Isometric View b) Side View

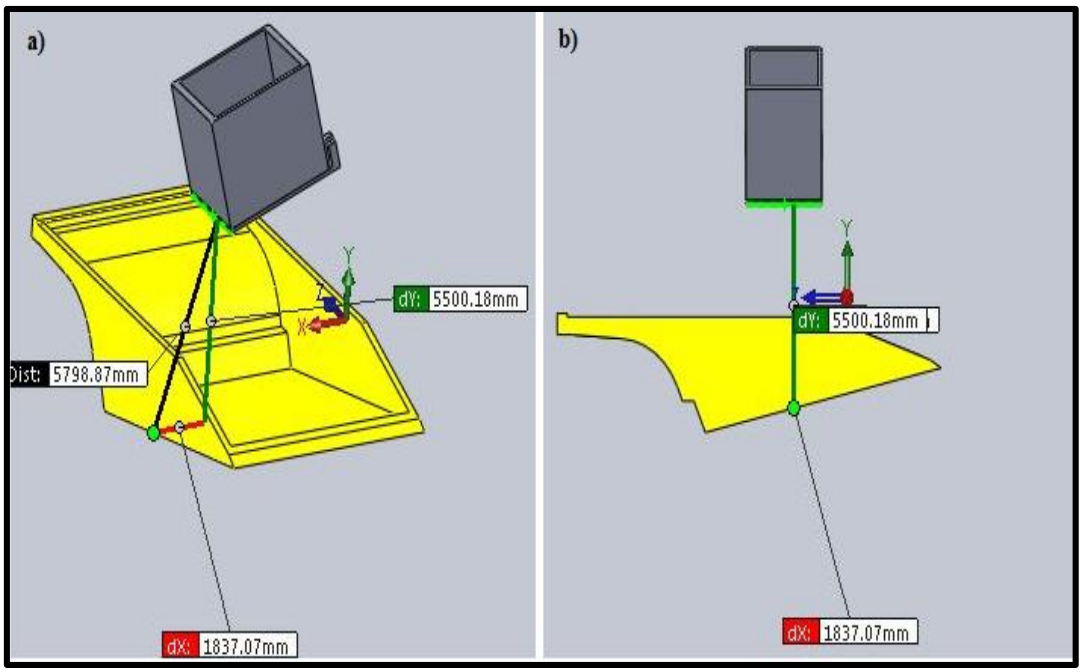

Figure 5.8. Truck Body and Shovel Dipper CAD Assembly for H_t = 5.5 m (5500 mm): a) Isometric View b) Side View

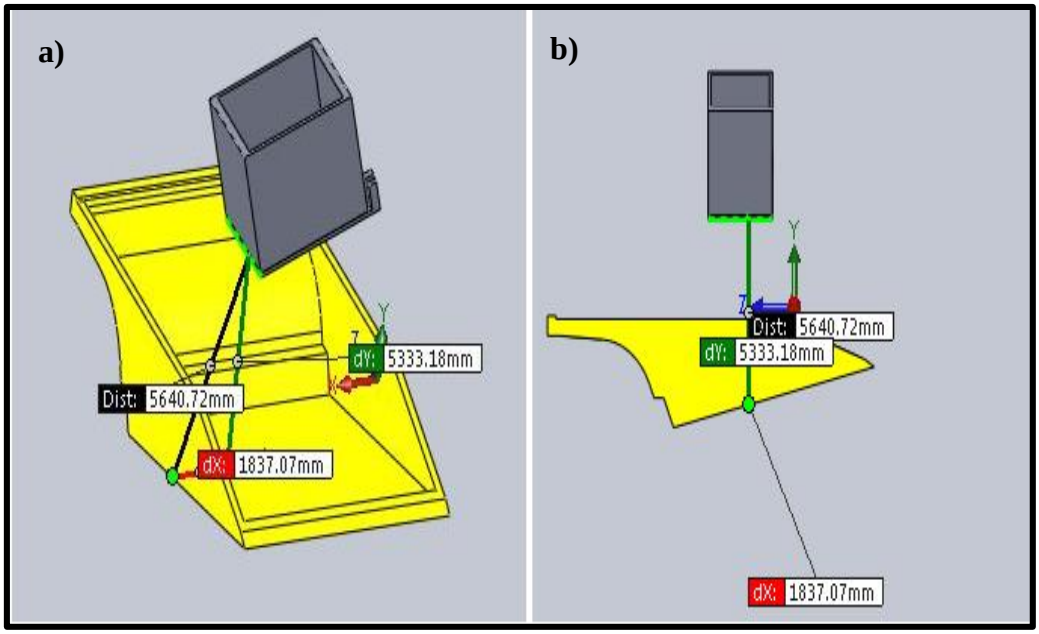

Figure 5.9. Truck Body and Shovel Dipper CAD Assembly for H_t = 5.33 m (5333 mm): a) Isometric View b) Side View

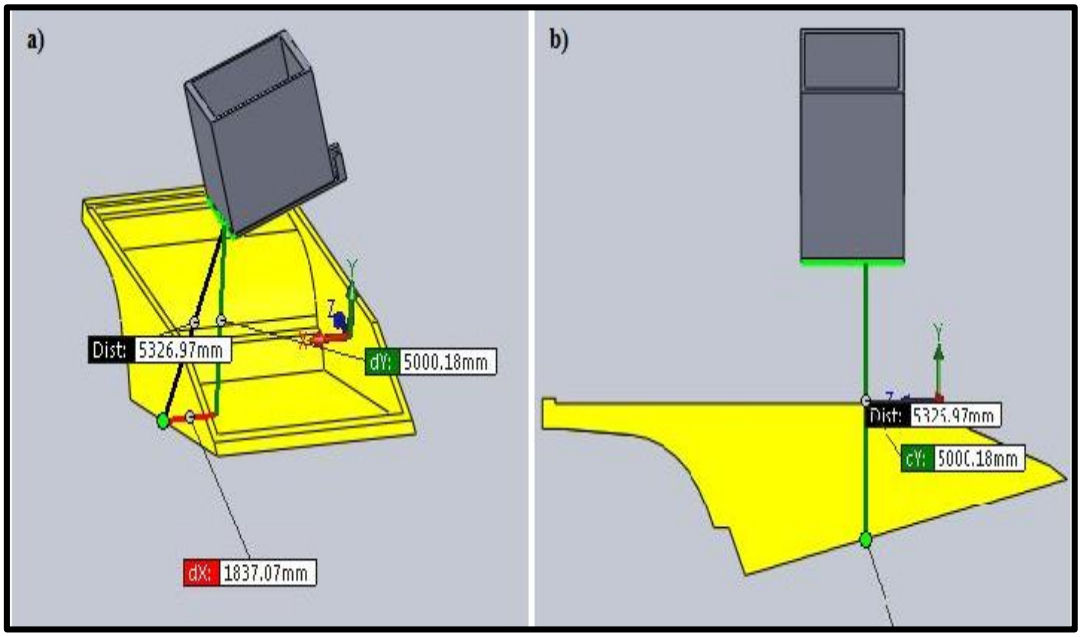

Figure 5.10. Truck Body and Shovel Dipper CAD Assembly for H_t = 5.00 m (5000 mm): a) Isometric View b) Side View

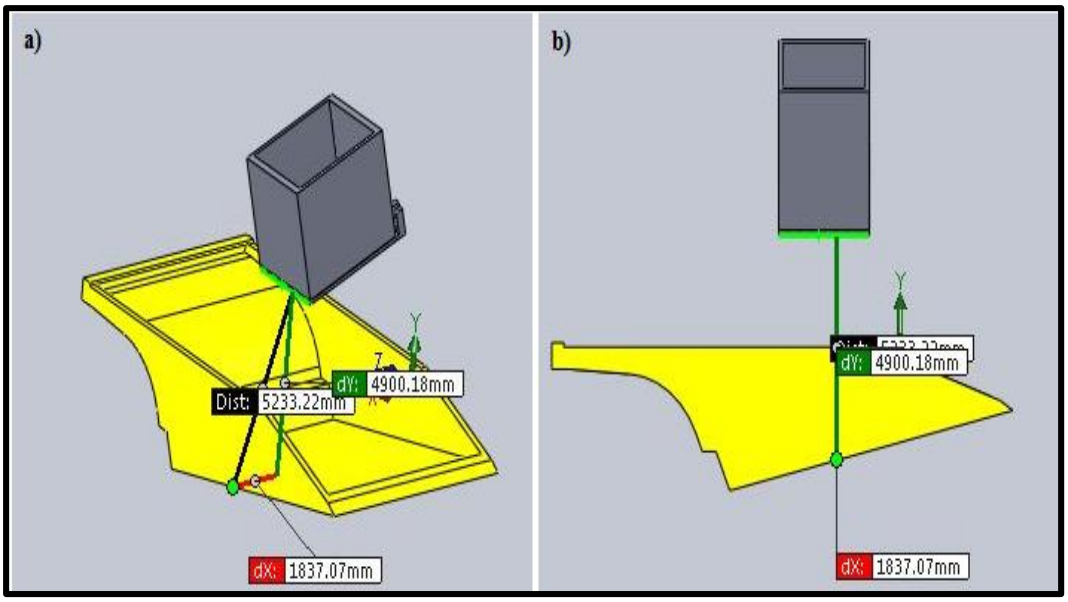

Figure 5.11. Truck Body and Shovel Dipper CAD Assembly for H_t = 4.90 m (4900 mm): a) Isometric View b) Side View

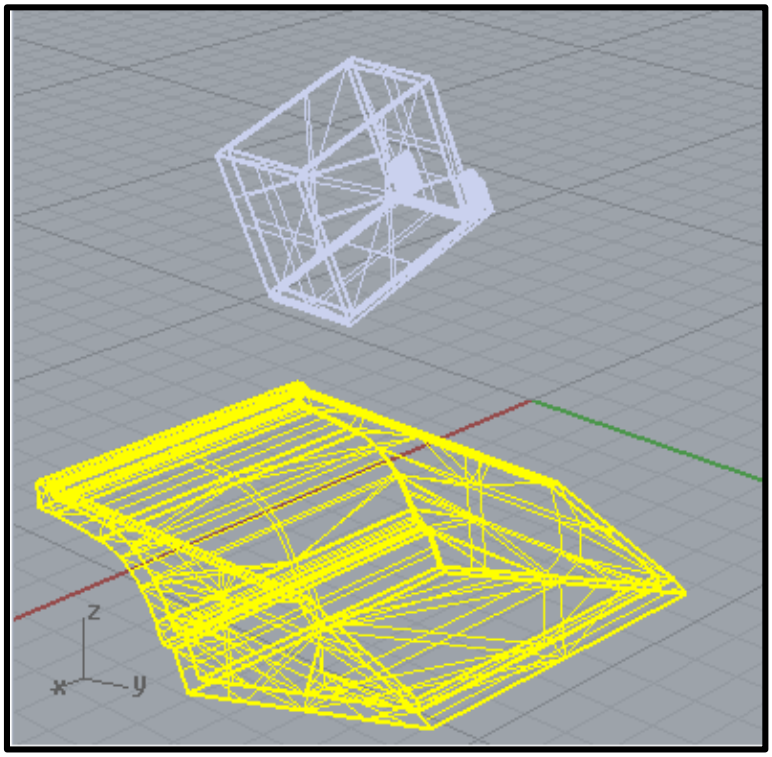

Figure 5.12. Mesh for Truck and Shovel Dipper CAD Models in Rhino 5.0

5.3. 3D VIRTUAL SIMULATION IN PFC3D

The dipper payload is either fragmented or soft material. In either case, the dipper payload normally consists of large amount of small particles of varying sizes and shapes. The DEM technique is the best analytical technique for such cases in which the materials are considered as a large collection of small particles interacting with each other and with other surfaces. The DEM technique is used to analyze the behavior and reactive forces of the combined system by computing and analyzing the motion of individual particles. Thus, the DEM technique simulates the dipper payload to mimic reality as it allows the creation of individual particles with specific properties and with interactions with each other and with other surfaces.

The impact force, which is exerted on the truck body is due to the gravity dumping of the dipper payload into the dump truck. PFC3D 5.0 is used to virtually simulate the shovel dumping process and observe, record and analyze the impact force exerted on the truck body during the process. The 3D virtual simulation of the dumping process allows

the correct representation of the impact force. It also provides insight into the scientific observation of the cushioning effect due to previously dumped materials in the truck body. By reducing the dumping height, with subsequent virtual simulation, the reduction in the resulting impact force can be observed to attain an optimum dumping height. The optimum height is the threshold height with minimum impact force and with a good clearance between the dipper door and truck edges that prevent jolting to compromise the system.

For virtual simulation, the truck body and shovel dipper meshes are first imported into PFC3D. The geometries of the mesh surfaces are then converted into "walls" so that material particles can interact with those walls. The material particles in the form of small spherical balls are then generated into the shovel dipper. The radius of the material is distributed between 0.1 and 0.15 m. PFC3D distributes the particles using a uniform size distribution. The distribution process ceases as soon as the target density and porosity are achieved within the specified volume. The positions and the radii of the particles are drawn from the uniform distributions throughout the provided model domain, which is P&H4100 XPC shovel dipper in this case. There may be overlaps between the particles during the particle generation process. Once the command is executed and particles are generated with the modal constraint, to achieve the specified porosity and density, overlaps can be reduced by letting the balls re-arrange.

Once the particles have been created in the shovel dipper, time cushion is allowed for them to get settled. This time cushion will allow the overlaps to get reduced and the particles will also lose their energies and will come to rest before the shovel dipper door is opened. The particles can also be distributed using the Gaussian distribution. Figure 5.13 illustrates the complete particle radius distribution in PFC3D for the input radius range. The appropriate number of material particles are generated into the shovel dipper to achieve a combined weight of 100 tons. The material properties assigned in PFC3D to those generated material particles are given in Table 5.2. Normal and shear stiffness are input as 0.5×10^8 N/m and 0.3×10^8 N/m, respectively. Coefficient of friction is kept at 0.65 for the material. Damping provided is typical for the impact tests (Itasca, 2011). Density of 2739 kg/m^3 is used which is typical for rock material. Porosity is kept around 0.32 – 0.33. Radius for the material particles is kept within 0.1 – 0.15 m. After generating the 100 tons of material particles, contacts are established so that the particles can interact with one

another and with the other surfaces (‘walls’ in PFC3D). Thus, the particles can be contained inside the dipper first and then, after the dumping process, in the truck. The contacts include particle–particle, particles– dipper, particles–door and particles–truck body.

In PFC3D, the contact can only be established between the particles or the particles with the walls. No contact can be established between the walls. Linear contact model is used for establishing the contact. Linear contact model, developed by Cundall (1979), has been mostly used for the cases where the impact of the particles on any particular surface is to be studied. After establishing the contacts, gravity is activated and the system is allowed to run for a few seconds for the material to get settled into the dipper. As the particles get settled, rotation is activated on the dipper door. As the door rotates, the equation of motion is solved for each particle and the particles begin to drop from the dipper under gravity into the truck body to produce the impact force. After the first pass is dumped and the dipper door rotates back to close, the shovel swings back after 30 seconds to load a second 100 tons of material to repeat the process until the truck and filled within the simulation. Figure 5.14 illustrates the dynamics of the first pass within the simulation. Figure 5.14 a) shows the point where the particles are contained within the shovel dipper and they are allowed to settle into the dipper. Figure 5.14 b) shows the point where the dipper door is rotated and the particles are allowed to fall under gravity. Figure 5.14 c) shows the point when the particles strike the surface of the truck bottom, and thus, exerting impact force on the truck body. Figure 5.14 d) shows the point where all the particles from the first pass have been dumped completely into the truck.

Figure 5.15 illustrates the dynamics of the second pass within the simulation. Figure 5.15 a) shows the point where the particles reappear and are allowed to settle in the shovel dipper for the second pass. Note that the particles from the first pass are already present into the truck body. Figure 5.15 b) shows the point where the dipper door is rotated again and the particles are allowed to fall under gravity. Figure 5.15 c) shows the point when the particles from the second pass strike the particles which are already in the truck from the first pass. In this way, the particles in the second pass are cushioned by the materials from the first pass, and therefore will exert lesser impact force. Figure 5.15 d)

shows the point where all the particles from the second pass are dumped over the first pass materials in the truck.

Table 5.2. Material Properties in PFC3D

Rock/Soil Properties/Parameters	Values
Normal Stiffness	0.5 x 10^8 N/m
Shear Stiffness	0.3 x 10^8 N/m
Coefficient of Friction	0.65
Damping	0.04%
Porosity	0.32 – 0.33
Density	2739 kg/m^3
Radius	0.1 – 0.15 m

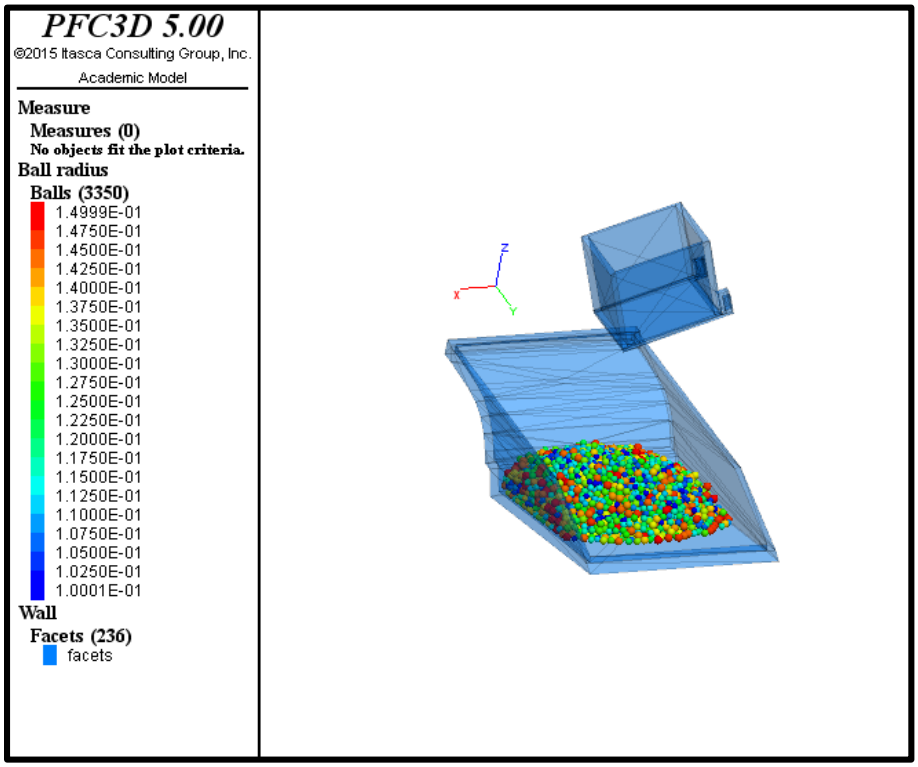

Figure 5.13. Particles Radius Distribution

5.4. MSC ADAMS VIRTUAL SIMULATION SETUP

The 3D virtual prototype model (Figure 5.16) developed by Aouad and Frimpong (2013) is used to obtain the RMS accelerations for the corresponding impact force results, obtained for different dumping distances, as outlined in the previous section. Aouad and Frimpong, 2013 had developed a virtual prototype simulator for CAT 793D in MSC ADAMS. The 38-DOF ADAMS model was developed to generate the complete vibration solution including the dynamics of the different truck components under the same ground characteristics and the physical environment to virtually simulate the actual HISLO conditions (Aouad and Frimpong, 2013). It should be noted that x – direction (front – back motion), y – direction (right – left motion) and z – direction (up – down motion) in the 3-D virtual model provided by Aouad and Frimpong (2013) have been changed to x – direction (front – back motion), y – direction (up – down motion) and z – direction (right – left motion) in the current setup up. The focus of this study was to compute the RMS acceleration for the operator's seat in y – direction (up – down) only. Rather than using the approximate magnitude of impact force of 1 x 10^6 N, more realistic impact force values, as obtained by the 3D virtual simulation in PFC3D and provided in the Table 6.4, are used to obtain the required RMS acceleration of the seat.

To carry out the simulation, the following necessary assumptions and modifications have been made:

- The operator's body is fixed to the seat.
- The springs connecting the seat with the cabin are kept in pre-loaded state as an initial condition to incorporate the weight of the operator.
- The seat is only allowed to have 3 DOFs i.e. movement along y – axis (vertically up – down), movement along x – axis (longitudinally right – left) and yawing (rotation) about z – axis.

5.5. VERIFICATION

3D virtual simulation results obtained from PFC3D were compared with that of the experimental results. Table 5.3 shows a comparison among the results obtained from the

experiments, using the mathematical model, and the 3D virtual simulation for the maximum dynamic impact force.

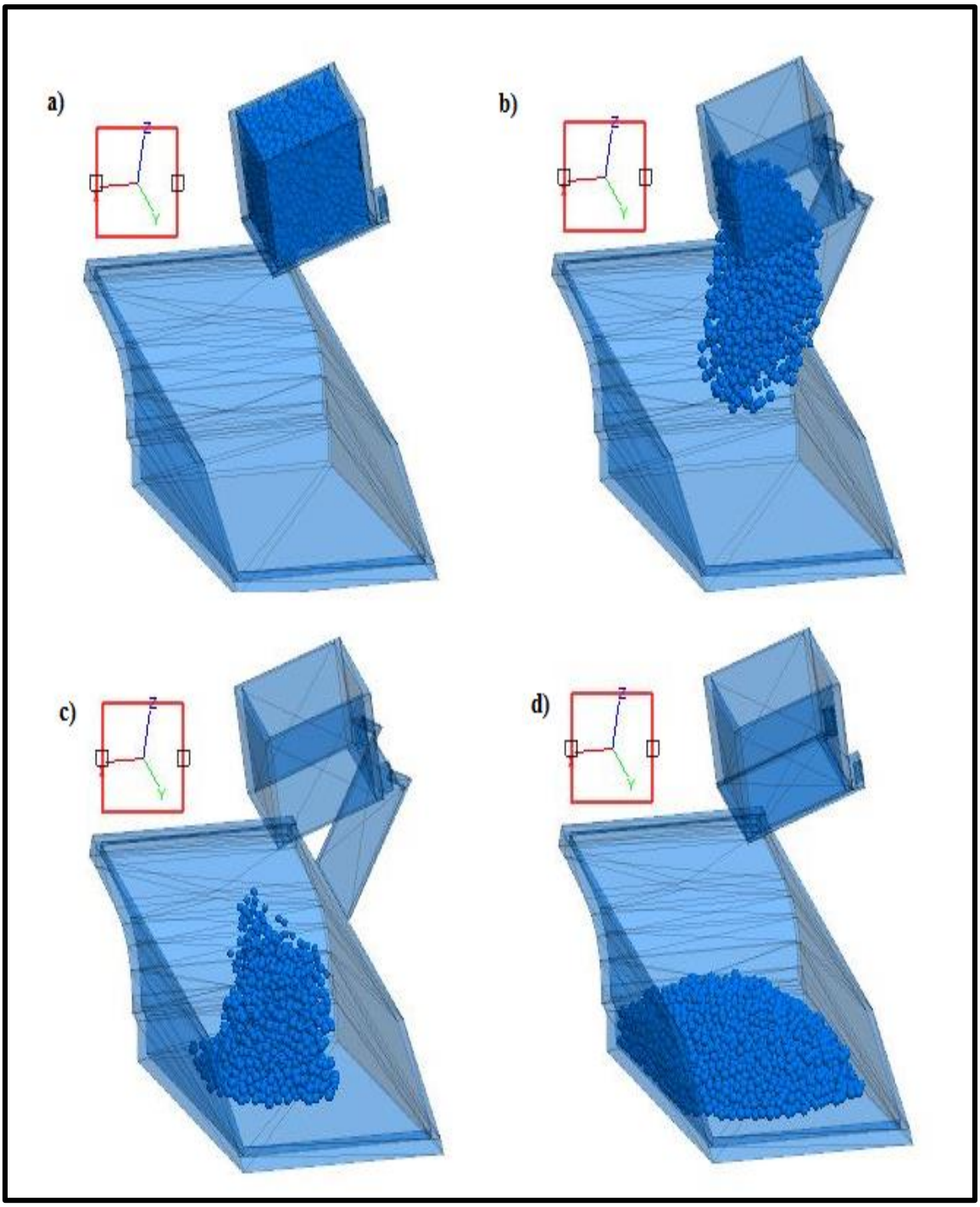

Figure 5.14. Dynamics of 1st Shovel Pass

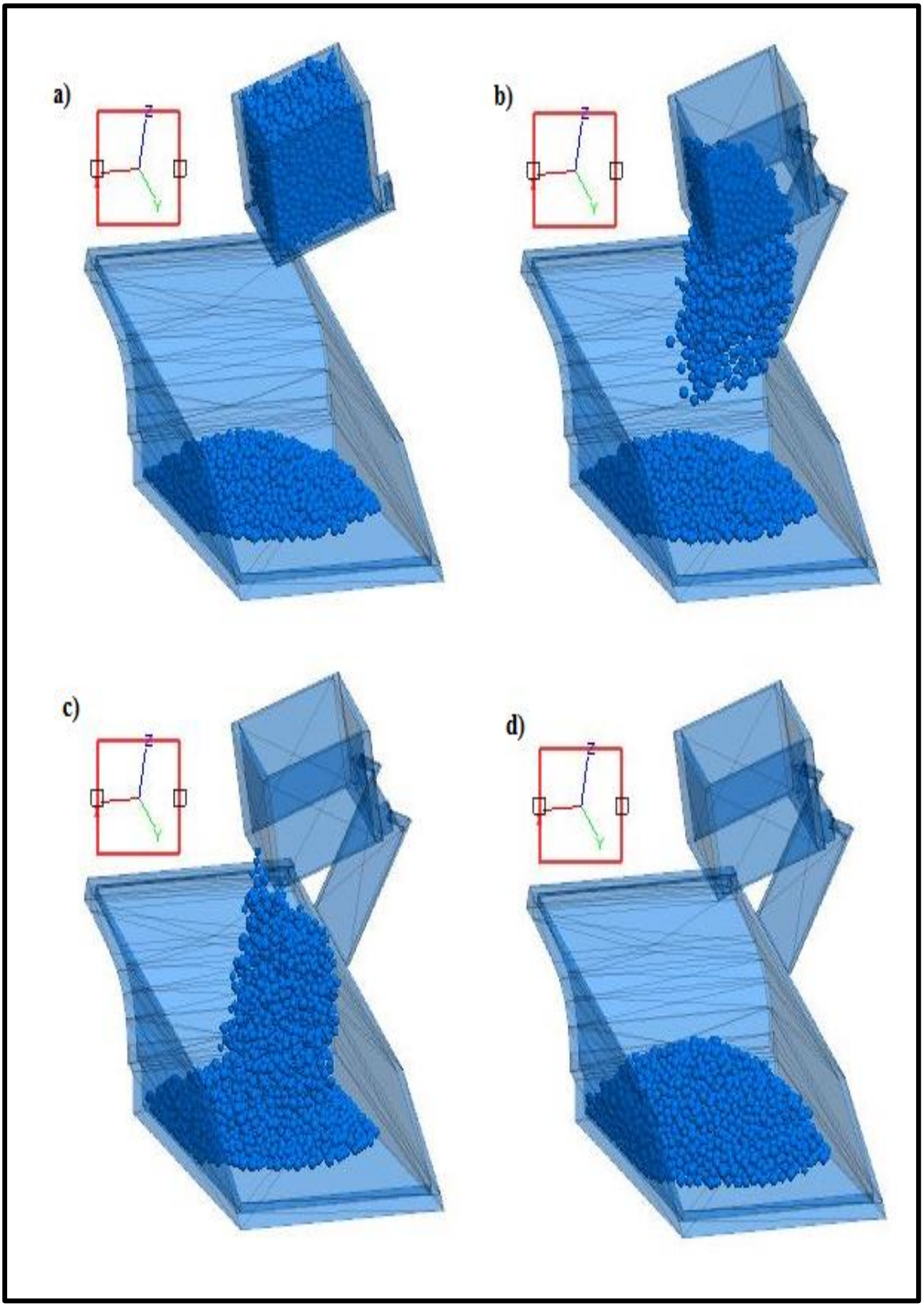

Figure 5.15. Dynamics of 2nd Shovel Pass

Table 5.3 also shows the percent difference between the results. Only the impact force from the first shovel pass is considered for the comparison because of its predominance in the overall truck vibration problem. The results from the 3-D virtual simulation show strong agreement with those obtained through mathematical model. The percent difference ranged between 0.03% and 1.48%. This shows that the mathematical modeling technique can be used for predicting the maximum dynamic impact force with confidence in place of the virtual simulation process.

5.6. VALIDATION

Validation is the process of checking the developed model against the real world data. In this study, the mathematical model of the impulse force function was validated using the published RMS acceleration results from the model developed by Aouad and Frimpong (2013) under the same constraints and environment. The impulse force function in equation (3.32) is used to obtain the input impact force in the 38-DOF CAT 793D model in the MSC ADAMS virtual platform for generating the RMS acceleration. The results from the new impulse force model in this work were compared with the impulse force model developed by Aouad and Frimpong (2013). The significance of this validation process is to ensure that: (i) the model is reliable for explaining a real world phenomenon; (ii) the model is robust enough to provide solutions in prescribed parametric domains; and (iii) the impact force results can be reproduced under similar conditions in different paradigms.

The input parameters for the mathematical model are contained in Table 4.1. The dumping height, H_t, is 10 m for the work by Aouad and Frimpong (2013). Figure 5.17 shows the impact force for the 1^{st} shovel pass in the 38-DOF CAT 793D virtual model in MSC ADAMS using equation (3.32). This impact force serves as the input force for generating the RMS acceleration value under similar conditions for the work carried out by Aouad and Frimpong (2013).

5.6.1. Virtual Simulation Results from Aouad and Frimpong (2013). Aouad and Frimpong (2013) carried out the virtual simulations in MSC ADAMS. The purpose of that simulation was to study the effect of vibrations and their impact on dump truck operators during shovel dumping operation. The test was performed using the CAT 793D truck by

exerting the impact force from dumping the 100-ton payload into the empty truck from a 10-m dump height. Vibrations at chassis, cabin, seat and operator's cervical and lumbar region were measured in front – back (x-axis), right – left (y-axis) and up – down (z-axis) axes. RMS accelerations were calculated for all truck components and operator's body. Data was gathered for the first and second shovel passes. Table 5.4 contains the RMS acceleration values resulting from the first and shovel passes in the x, y and z components of the acceleration of the cervical, lumbar, and operator seat regions.

Table 5.3. Maximum Impact Force for Mathematical Model and Virtual Simulation Results

Dumping Distance (H_t)	Maximum Impact Force Magnitude		Percent Difference
	Mathematical Model Results	Virtual Simulation Results	
(m)	(N)	(N)	(%)
7.33	846	838	0.98
6.33	785	797	1.49
6.00	766	775	1.19
5.50	734	742	1.10
5.33	721	720	0.08
5.00	700	705	0.71
4.90	693	692	0.03

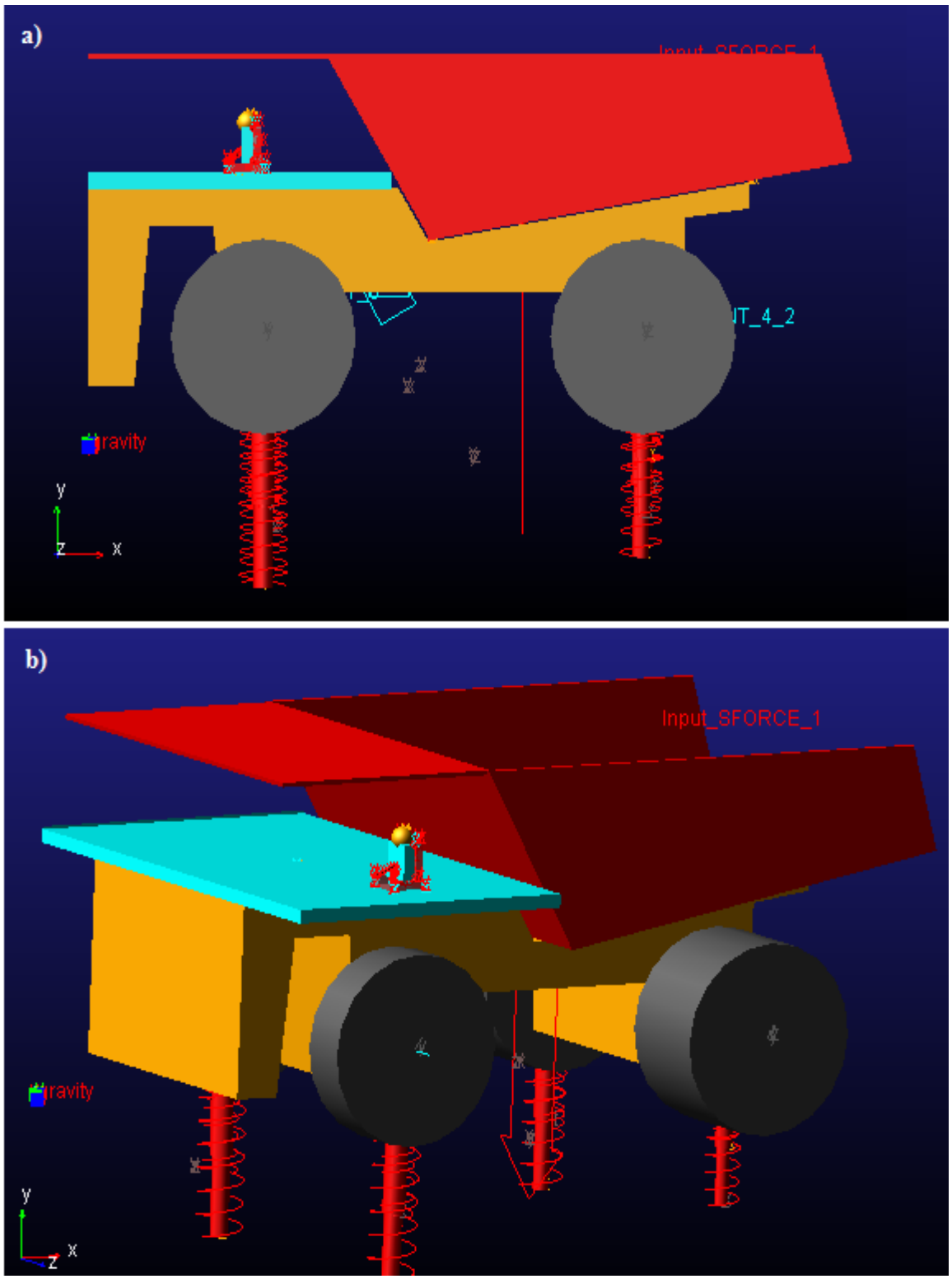

Figure 5.16. 38 - DOF Virtual Prototype Model for CAT 793D in MSC ADAMS Environment a) Wireframe Side View b) Solidframe Isometric View

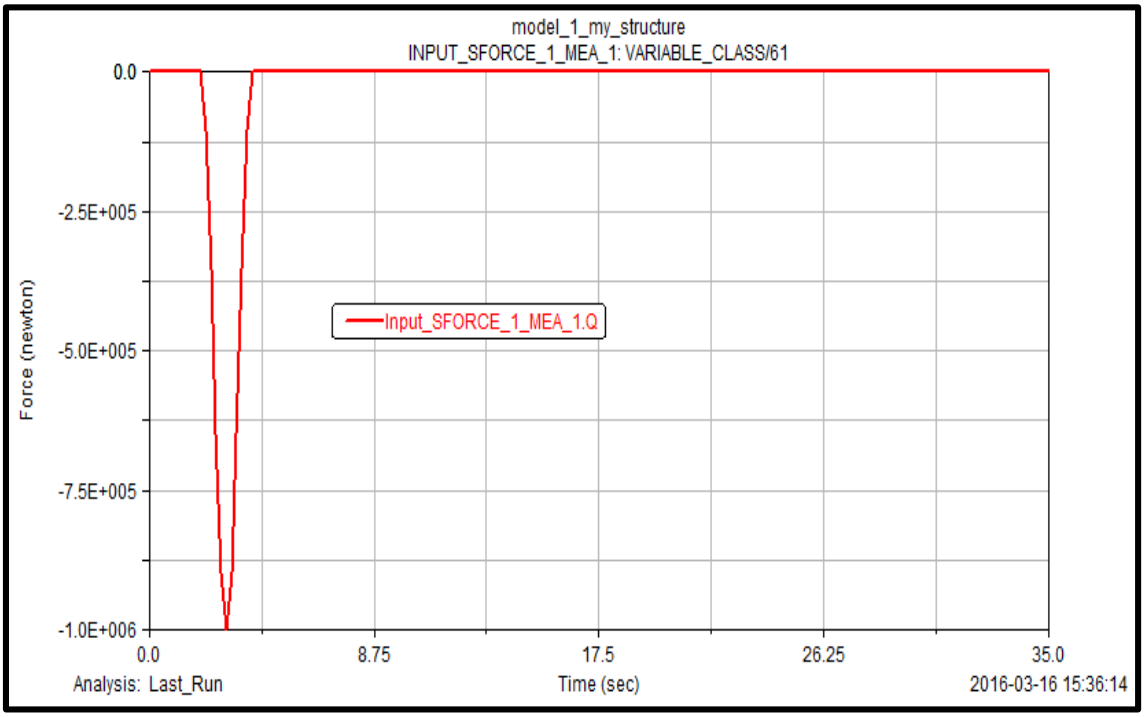

Figure 5.17. Input force obtained through Mathematical Model in MSC ADAMS

Table 5.4. RMS Accelerations from Aouad and Frimpong (2013)

	X (front – back)	Y (right – left)	Z (up – down)
Passes	RMS Acceleration at Cervical Region (m/s^2)		
1st	0.36	0.53	0.90
2nd	0.23	0.36	0.39
	RMS Acceleration at Lumbar Region (m/s^2)		
1st	0.40	0.42	1.12
2nd	0.23	0.38	0.56
	RMS Acceleration at Operator's Seat (m/s^2)		
1st	1.49	1.08	3.56
2nd	0.71	0.82	1.32

5.6.1. Comparison of Simulation Results. The simulation results from the virtual prototype model based on the mathematical model in equation (3.32) are compared with that obtained by Aouad and Frimpong (2013). The virtual model generates the complete vibration solution for the 38-DOF system. The three major components including operator's lumbar and cervical region and his seat are compared by using the RMS acceleration in x, y and z axes. Table 5.5 contains the comparison of the virtual simulation results from this research study and that from Aouad and Frimpong (2013). The results from this study show good agreement with that from Aouad and Frimpong (2013). The percent difference ranged between 0.56% and 7.02%. This shows that the mathematical model accurately predicts the RMS acceleration values.

Table 5.5. RMS Acceleration: New Model vs. Aouad and Frimpong (2013)

RMS Acceleration (m/s^2)	New Virtual Model Results	Aouad and Frimpong (2013) Results	Percent Difference (%)
Cervical Region			
a_x	0.33	0.36	5.56
a_y	0.58	0.53	7.02
a_z	0.92	0.90	2.17
Lumbar Region			
a_x	0.38	0.40	5.00
a_y	0.40	0.42	4.76
a_z	1.15	1.12	2.61
Operator's Seat			
a_x	1.51	1.49	1.32
a_y	1.15	1.08	6.09
a_z	3.58	3.56	0.56

5.7. SUMMARY

A mathematical model is developed to define the impulse force under HISLO conditions. A 3D virtual simulation of the shovel dumping process and truck vibration is carried out in this section. SolidWorks is used for building the 3D virtual model of the P&H 4100XPC shovel and the CAT 793D dump truck. The meshed CAD models and the virtual simulation are carried out in Rhino 5.0 and PFC3D, respectively. Detailed steps and methodologies for meshing and the complete simulation of the virtual models for various dumping heights, with model dimensions and constraints, have been presented in this section. The DEM method used by PFC3D for the virtual shovel dumping simulation has also been discussed in detail. The mathematical model is verified by comparing its results with that from the virtual simulation experiments.

The virtual model by Aouad and Frimpong (2013), with the impulse force developed in this research study, has been used to carry out the vibration experiments for the CAT 793D truck. These experiments are carried out in MSC ADAMS to obtain the vertical RMS acceleration at the seat. The virtual simulation results, with the new mathematical model, are validated with the virtual simulation results from Aouad and Frimpong (2013). The results show that the mathematical model accurately simulates the actual dumping process. The range of variation between the results from the two virtual simulation categories is between 0.56% and 7.02%. Therefore, the mathematical model can be used for predicting the maximum dynamic impact force with confidence in place of the virtual simulation process for HISLO conditions.

6. ANALYSIS AND DISCUSSION OF RESULTS

This section presents the experimental and virtual simulation results for shovel dumping process and truck vibration. Impact force results for various dumping height, from both the experiments and virtual simulation, have been discussed in detail. Simulation results of 38-DOF truck model in MSC ADAMS have also been presented and discussed in detail. The purpose and the significance of this section to the overall work is to show how effectively the impact force can be reduced by optimizing the dumping height under the HISLO conditions; and show the effectiveness of impulse force reduction by displaying the reduction in vertical RMS acceleration at operator's seat due to the decrease in the dumping height.

6.1. EXPERIMENTAL RESULTS AND DISCUSSION

The impulse force is mathematically modeled using two different approaches in Equations (3.28) and (3.32). Virtual simulation models are developed, verified and validated with real-world data to check accuracy and their performance based on real-world data. Analysis and discussions of the results have been carried out to understand the behavior of the virtual models under real-world constraints.

Figure 6.1 shows the impact force for all the seven experiments conducted when the material is dumped in a single pass (no divisions into sub-passes) with different dumping distances. It can be seen that this mathematical model provides a much better representation of the dynamic impulse force. The impact force increases as the material is being dumped, reaching its maximum value with most of the bulk material in the truck body. From this maximum value, the impact force decreases with further material dumping, gradually reaching zero value upon complete dumping. Moreover, as the dumping height increases, the behavior of the resulting impact force remains the same but it can be clearly seen that there is a decrease in the maximum magnitude of the impact force. Table 6.1 provides the exact values for the maximum magnitude for every particular dumping distance.

Figure 6.2 illustrates the reduction in the maximum magnitude of the impact force when the single shovel ore-pass is divided into more than one sub-pass at a dumping distance of 7.33 m. The subdivision of the one pass into sub-passes does not change the behavior of the impulse force. In the subdivision scenario, there is a considerable reduction in the maximum magnitude of the impulse force resulting from individual sub-passes. Comparing Figure 6.1(a) and Figure 6.2, it can be observed that the maximum impulse forces are 846 kN, 421 kN, 282 kN, 212 kN for M = 0, 1, 2 and 3, respectively (M is the number of sub-passes in a single pass). Thus, there is a percentage reduction of 50.28%, 66.63% and 74.97% for M = 1, 2 and 3, respectively as compared to M = 0. This clearly indicates that the impulse force reduces considerably as the single shovel pass is divided into sub-passes.

Similarly, Figures 6.3, 6.4, 6.5, 6.6, 6.7 and 6.8 demonstrate similar reductions in the dynamic impulse force for dumping heights of 6.33 m, 6.0 m, 5.5 m, 5.33 m, 5.0 m and 4.9 m, respectively. Comparing Figure 6.1(b) and Figure 6.3 for a dumping height of 6.33 m, it can be observed that the maximum impulse forces are 785 kN, 394 kN, 262 kN, 196 kN for M = 0, 1, 2, and 3, respectively. Thus, there are percentage reductions of 7.19%, 53.47%, 68.99% and 76.83% for M = 0, 1, 2 and 3, respectively, as compared to M = 0 with a dumping height of 7.33 m. Comparing Figure 6.1(c) and Figure 6.4 for dumping height of 6.00 m, it can be observed that the maximum impulse forces are 766 kN, 383 kN, 255 kN, 191 kN for M = 0, 1, 2 and 3 respectively. Thus, there are percentage reductions of 9.40%, 54.70%, 69.81% and 77.44% for M = 0, 1, 2 and 3, respectively, as compared to M = 0 with a dumping height of 7.33 m.

Comparing Figure 6.1(d) and Figure 6.5 for dumping height of 5.5 m, it can be observed that the maximum impulse forces are 734 kN, 367 kN, 245 kN, 183 kN for M = 0, 1, 2 and 3, respectively. Thus, there are percentage reductions of 13.27%, 56.62%, 71.09% and 78.40% for M = 0, 1, 2 and 3, respectively, as compared to M = 0 with a dumping height of 7.33 m. Similarly, by comparing Figure 6.1(e) and Figure 6.6 for a dumping height of 5.33 m, it can be observed that the maximum impulse forces are 721 kN, 361 kN, 241 kN, 180 kN for M = 0, 1, 2 and 3, respectively. Thus, there are percentage reductions of 14.8%, 57.30%, 71.54% and 78.73% for M = 0, 1, 2 and 3, respectively, as compared to M = 0 with a dumping height of 7.33 m. Similar comparisons can be made

using Figure 6.1(f) and Figure 6.1(g) with Figure 6.7 and Figure 6.8 to examine the reductions in the maximum impulse forces for sub-divided passes for dumping heights of 5.0 m and 4.9 m respectively.

Table 6.1 and Table 6.2 contain the results from Figures 6.1, 6.2, 6.3, 6.4, 6.5, 6.6, 6.7 and 6.8. Table 6.1 shows the maximum dynamic impulse forces for all the experiments. Table 6.2 shows the percentage reductions in the maximum dynamic impulse forces for all the experiments compared with M = 0 with a dumping height of 7.33 m. From these tables, considerable reductions in the impulse force can be achieved by either reducing the dumping height or by dividing the single shovel ore-pass into multiple sub-passes. If the material is dumped in multiple sub-passes, percentage reductions of 7.19%, 9.40%, 13.27%, 14.80%, 17.30% and 18.13% can be achieved by reducing the dumping height to 6.33 m, 6.0 m, 5.5 m, 5.33 m, 5.0 m and 4.9 m, respectively, as compared to the dumping distance of 7.33 m. If the shovel pass is divided into two sub-passes, for the same reductions in dumping height, percentage reductions of 53.47%, 54.7%, 56.62%, 57.3%, 58.64% and 59.06%, respectively, can be achieved as compared to a single pass with a dumping distance of 7.33 m. Figure 6.9 and Figure 6.10 provide the graphical illustrations of Table 6.1 and Table 6.2, respectively.

6.2. PFC3D VIRTUAL SIMULATION RESULTS AND DISCUSSION

The virtual simulation allowed the examination of the different scenarios in place of physical experiments, which are not only expensive but very time consuming. The virtual simulation results include the impact force exerted on the dump truck due to gravity dumping of the dipper payload. The dumping process is virtually visualized to better understand the different components of the operation and the evaluation of the impact force. The purpose of the simulation was (i) to capture the dynamic impact force exerted on the dump truck; (ii) investigate the cushioning effect, which is achieved during the subsequent passes after the first pass, resulting in the impact force reduction; (iii) visualize and analyze the impact force; and (iv) obtain the optimum dumping height while maintaining the minimum clearance between the dipper door and the truck edges during material dumping.

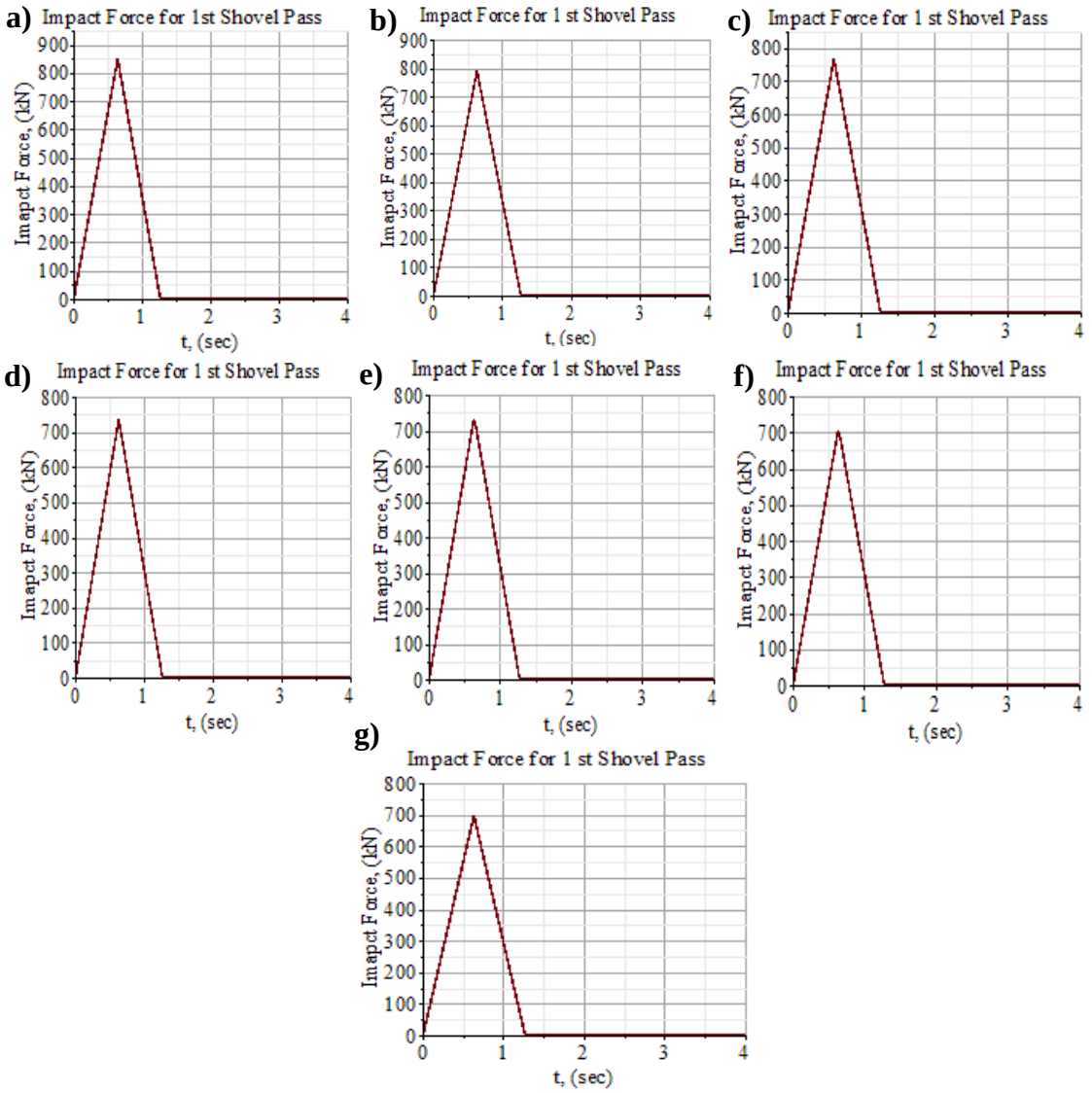

Figure 6.1. Impact Force Plotting for M = 0 (No sub-divisions of shovel pass) a) H_t = 7.33 m b) H_t = 6.33 m c) H_t = 6.0 m d) H_t = 5.5m e) H_t = 5.33m f) H_t = 5.0m g) H_t = 4.9m

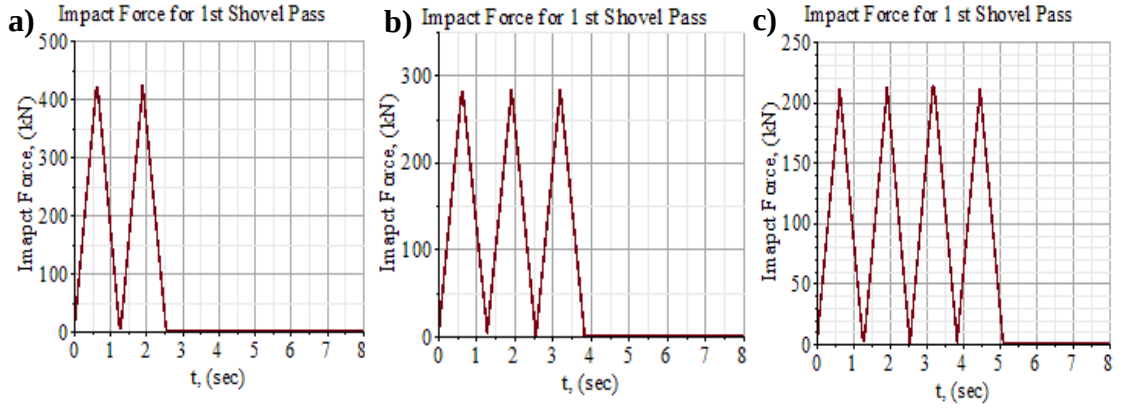

Figure 6.2. Impact Force Plotting for Experiment No. 1 with H_t = 7.33 m a) M = 1 b) M = 2 c) M = 3

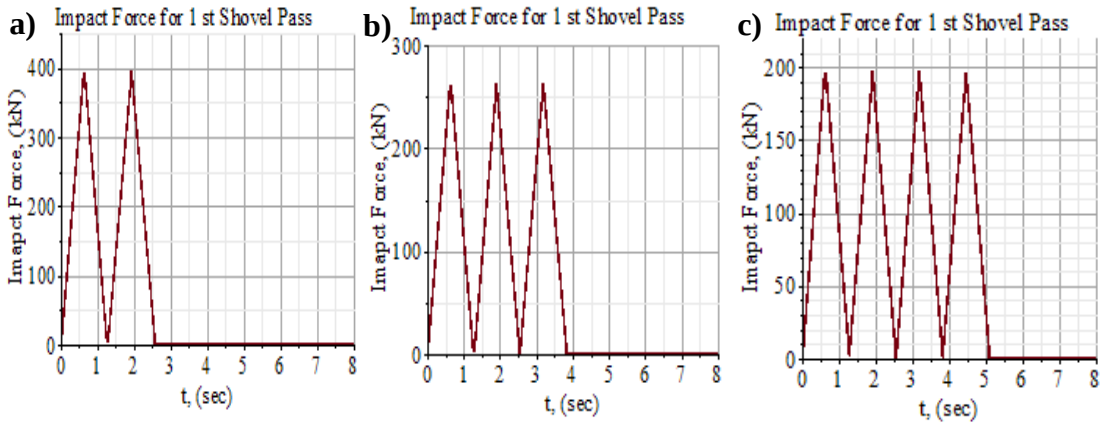

Figure 6.3. Impact Force Plotting for Experiment No. 2 with H_t = 6.33 m a) M = 1 b) M = 2 c) M = 3

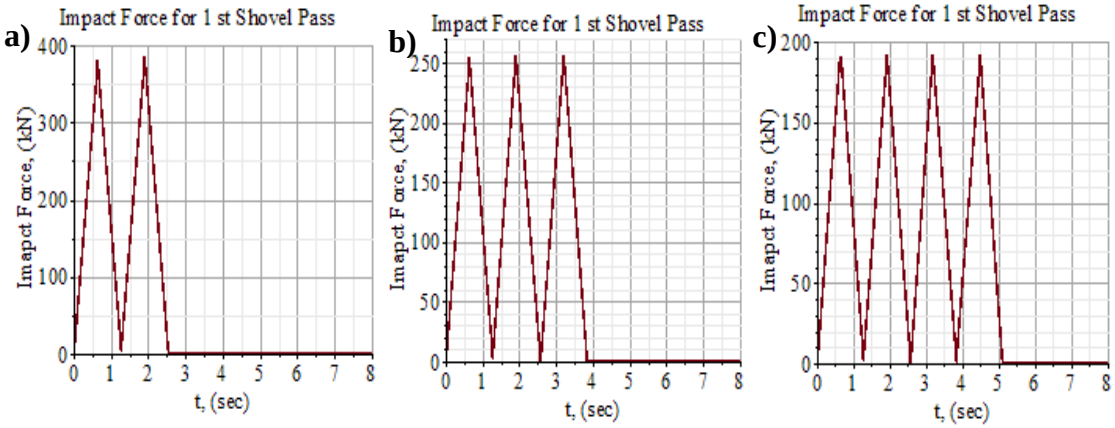

Figure 6.4. Impact Force Plotting for Experiment No. 3 with H_t = 6.0 m a) M = 1 b) M = 2 c) M = 3

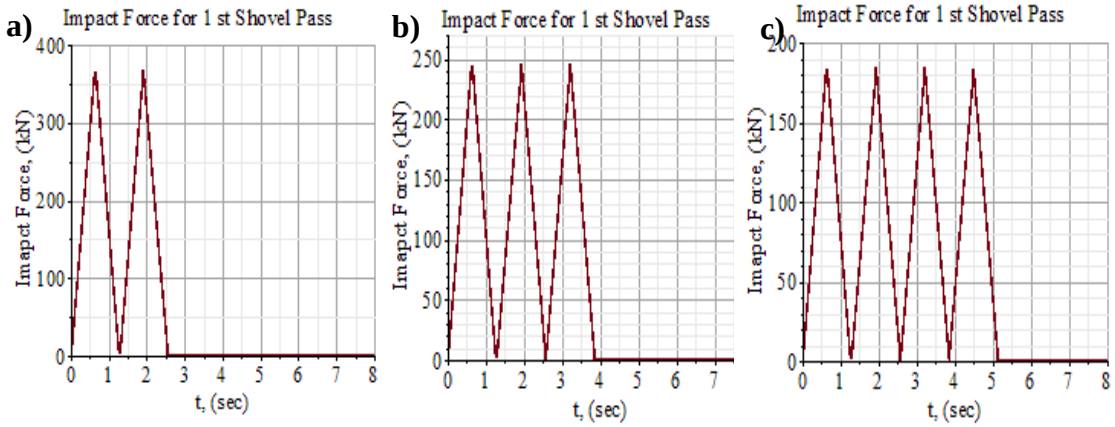

Figure 6.5. Impact Force Plotting for Experiment No. 4 with H_t = 5.5 m a) M = 1 b) M = 2 c) M = 3

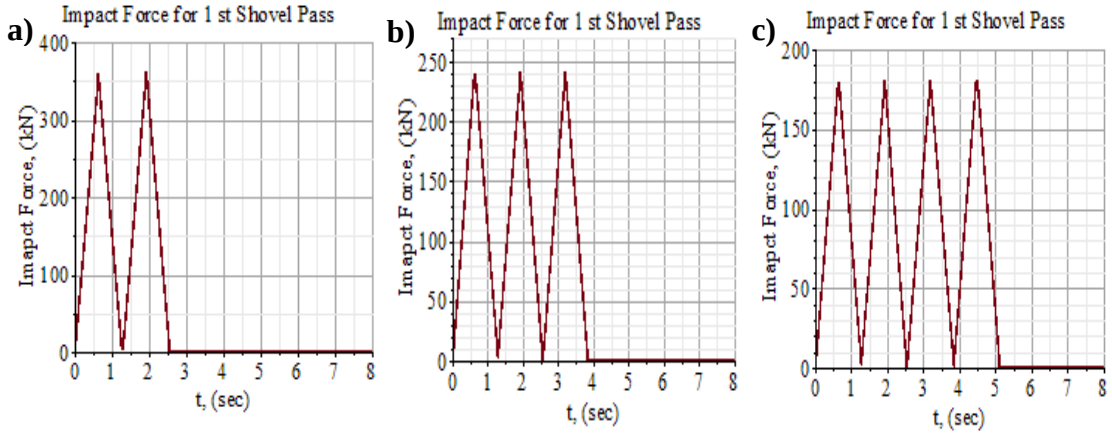

Figure 6.6. Impact Force Plotting for Experiment No. 5 with H_t = 5.33 m a) M = 1 b) M = 2 c) M = 3

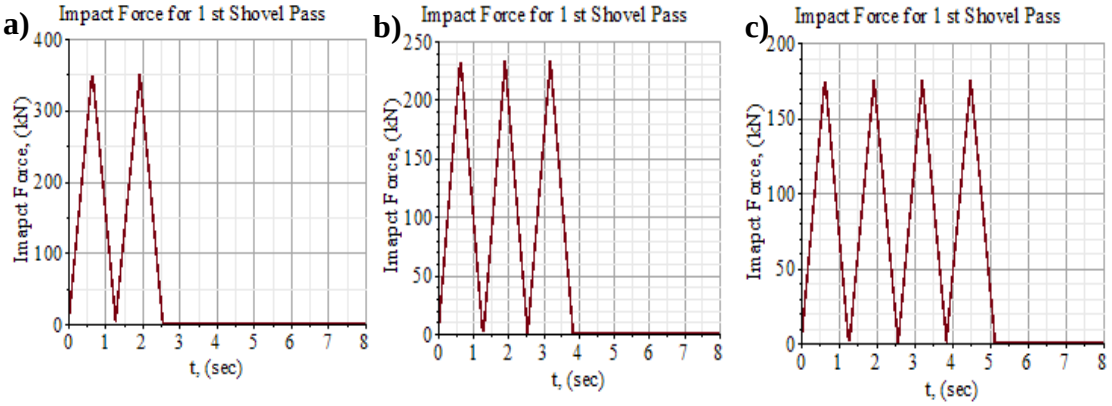

Figure 6.7. Impact Force Plotting for Experiment No. 6 with H_t = 5.0 m a) M = 1 b) M = 2 c) M = 3

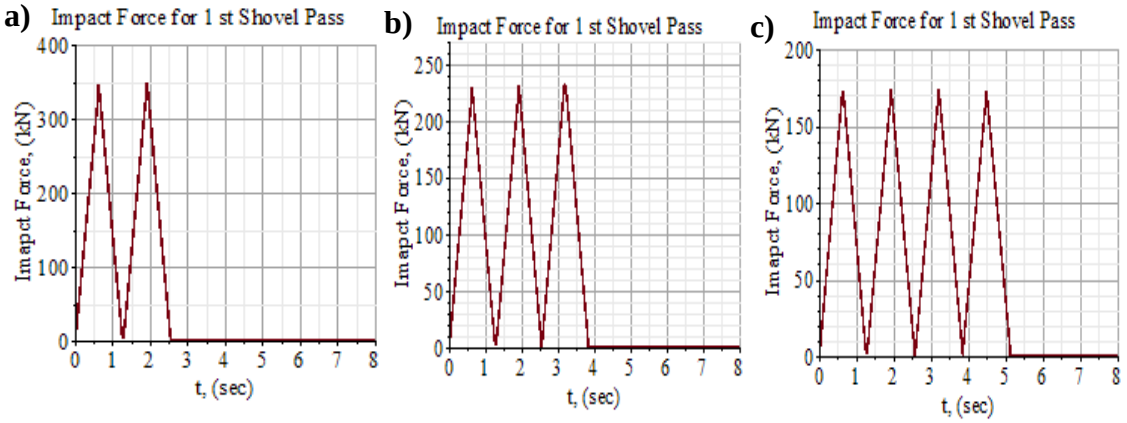

Figure 6.8. Impact Force Plotting for Experiment No. 7 with H_t = 4.9 m a) M = 1 b) M = 2 c) M = 3

Table 6.1. Maximum Impact Force (kN) for Dumping Heights and Sub-Passes

Sub-Passes (M)	**Dumping Height, H_t (m)**						
	7.33	**6.33**	**6.0**	**5.5**	**5.33**	**5.0**	**4.9**
0	846	785	766	734	721	700	693
1	421	394	383	367	361	350	346
2	282	262	255	245	241	233	231
3	212	196	191	183	180	174	172

Table 6.2. % difference between Maximum Impact Force for all cases and First Case (H_t =7.33 m & M=0)

Sub-Passes (M)	**Dumping Height, H_t (m)**						
	7.33	**6.33**	**6.0**	**5.5**	**5.33**	**5.0**	**4.9**
0	0	7.19	9.4	13.27	14.8	17.30	18.13
1	50.28	53.47	54.7	56.62	57.3	58.64	59.06
2	66.63	68.99	69.81	71.09	71.54	72.43	72.72
3	74.97	76.83	77.44	78.40	78.73	79.4	79.61

Two shovel passes are simulated in the 3D virtual simulation in PFC3D. The maximum dumping height of 7.33 m is used as the starting point in the simulation experiments, and gradually reduced to 4.90 m, the optimum dumping height in this study. It must be noted that the maximum and the optimal dumping heights in this study apply only to the case used, i.e., the P&H 4100 XPC cable shovel and the CAT 793D dump truck. For any other shovel-truck combinations, these dumping heights may be different. The discussions also focus on the cushioning effect achieved during the second shovel pass due to the first pass material. Furthermore, the percent reduction and the percent increase compared to the maximum height of 7.33 m and the minimum height of 4.9 m, respectively, for the first shovel pass are provided in this section. Finally, a comparison of the maximum

impact force is carried out between the results from the mathematical model and the 3-D virtual simulation for the first pass.

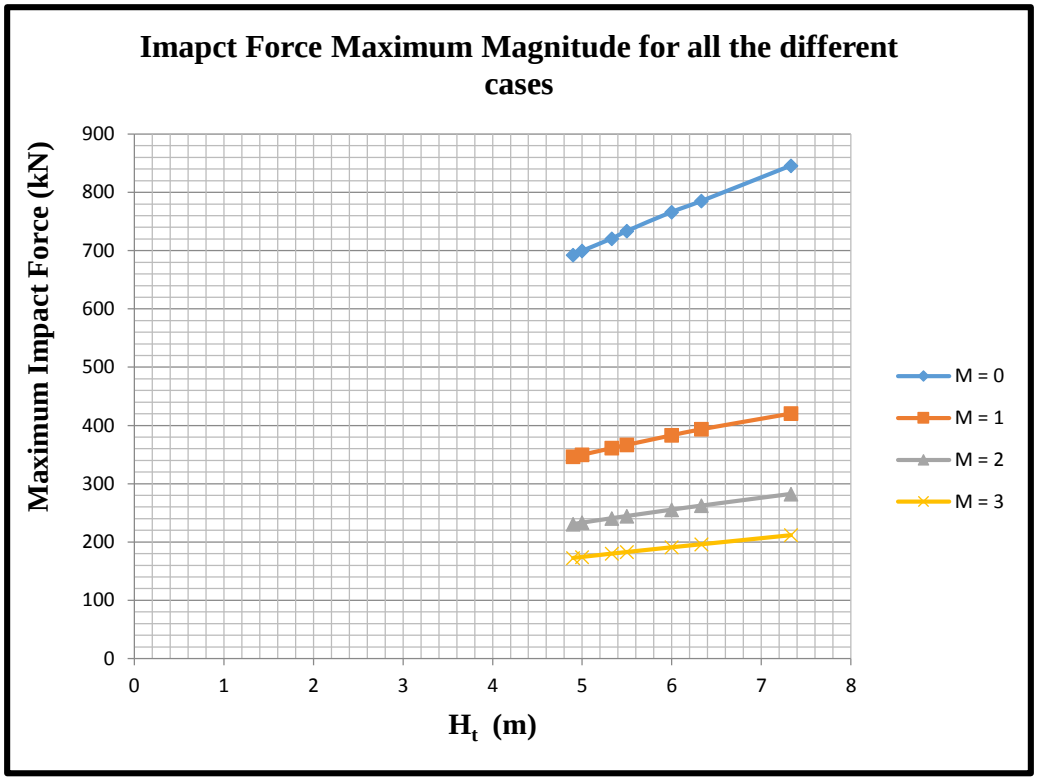

Figure 6.9. Maximum Impact Force Variation with Dumping Height

Figure 6.11 shows the impact force on the truck body due to gravity dumping of material from the shovel dipper with a dumping height of 7.33 m in the simulation experiment. Initially, the material settles within few seconds after dumping. The material makes the first contact with the truck body, in the first pass, at 7.44 seconds. The maximum impact force of 838 kN occurs during the first pass at 8.72 seconds. At 12.3 seconds, the shovel completes the first pass and returns to repeat the process.

It should be noted that the particles completely come to rest at 20 seconds, which is almost 8 seconds after the first pass. Upon completing the first pass and the particles settle, the force on the truck still exists and remains constant until after the second pass. This constant force is the total gravitational force of the material in the truck. The impact

forces recorded in the initial portion which are above this constant force are only due to the fact that the material particles bounce off a little after their first impact with the truck body. This phenomenon is due to the rigidness of the truck body. The simulation model detects the force and marks the point on the curve only when the particles come in contact with the truck body. When few particles loses their contact with the truck body, the point marked on the curve goes above the constant total gravitational force. After the first pass, the shovel swings back and take about 30 seconds to loads the next 100 tons of material and then swings back to complete the second pass. The second pass material makes the first contact with the truck body at 43.72 seconds. The maximum impact force in the second pass occurs at 45 seconds with a magnitude of 757 kN. It should be noted that the impact force from the second shovel pass is less than that of the first pass. This is due to the cushioning effect from the material already in the truck from the first pass. At 56 seconds, the particles settle and the impact force again is constant, which now includes the total material gravitational force from the passes on the truck.

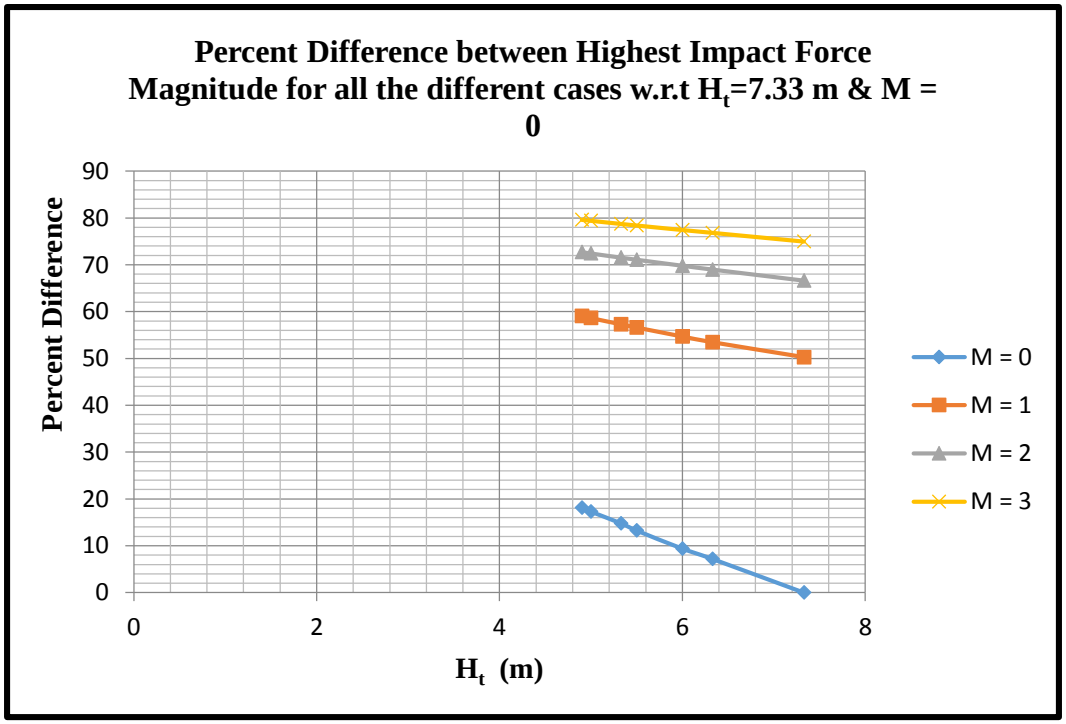

Figure 6.10. Plot for % Difference b/w Maximum Impact Force Magnitude w.r.t. ' H_t = 7.33 m' & 'M = 0'

Figure 6.12 shows the impact force on the truck due to gravity dumping of material from the shovel dipper with a dumping distance of 6.33 m. Again two shovel passes are simulated and the material takes few seconds to settle in the dipper. The material makes the first contact with the truck at 8.34 seconds in the first pass. The maximum impact force of 800 kN occurs at 11.92 seconds during the first pass. The shovel completes the first pass and returns at 13.3 seconds. It should be noted that the particles settle at 24 seconds. After the first pass is completed and the particles settle, the total gravitational force of the material in the truck still exists and it is equal to that of the gravitational force in Figure 6.11 for H_t = 7.33 m because the material has the same weight of 100 tons. The shovel swings back in 30 seconds after the first pass to load another 100 tons of material and dumped into the truck for the second pass. The materials in the second shovel pass makes the first contact with truck at 43.3 seconds. The maximum impact force of 723 kN occurs at 45.7 seconds during the second pass. Again the impact force from the second shovel pass is less than that of the first pass due to the cushioning effect. At 57 seconds, the particles settle and the impact force again is constant, and this force includes the total gravitational force of the material from two passes in the truck. Comparing Figure 6.12 and Figure 6.11, it can clearly be observed that the maximum impact forces in both shovel passes have been reduced because of a reduction in the shovel dumping height by 1 m.

Figure 6.13 shows the impact force on the truck due to gravity dumping of the material from the shovel dipper with a dumping height of 6.00 m. Again two shovel passes are simulated and few seconds are given for the material to settle in the dipper. The material makes the first contact with the truck at 7.24 seconds during the first pass. The maximum impact force of 775 kN occurs at 8.52 seconds during the first pass. The shovel completes the first pass and returns within 10.3 seconds. The particles settle within 19 seconds. After the first pass is dumped and the particles settle, the total gravitational force of the material on the truck still exists. It is similar to the previous cases because the dipper dumps the same amount of 100 tons material.

After the first pass, the shovel takes 30 seconds to swing back, load the next 100 tons of material and then swings back to dump the second pass into the truck. The second-pass material makes the first contact with the truck in 40 seconds. The maximum impact force of 708 kN occurs at 43 seconds during the second pass. Again the impact force from

the second pass is less than that of first pass due to the cushioning effect. The particles settle within 55 seconds and the impact force becomes constant. This force includes the total gravitational force of the material from two passes in the truck. Comparing Figure 6.13 with the previous two cases, it can be observed that the maximum impact forces in both passes are reduced because of the reduced dumping height.

Figure 6.14 shows the impact force on the truck due to gravity dumping of the material from the dipper with a dumping height of 5.5 m. The material makes the first contact with the truck body at 8.1 seconds during the first pass. The maximum impact force of 742 kN occurs at 10.1 seconds during the first pass. The shovel completes the first pass at 13.5 seconds and returns. The particles settles at 18 seconds. After completing the first pass and the particles settle, the total gravitational force of the material in the truck still exists because the dipper dumps the same 100 tons material. After the first pass, the shovel takes 30 seconds to swing back, load the next 100 tons of material and then swings back to complete the second pass. The material makes the first contact with the truck at 44.5 seconds in the second pass. The maximum impact force of 680 kN occurs at 46.6 seconds during the second pass. The impact force from the second pass is less than that of first pass due to the cushioning effect. The particles settle at 56 seconds and the impact force again is constant. This force includes the total gravitational force of the material from two passes in the truck. Comparing Figure 6.14 with the previous cases, it can be observed that the maximum impact forces in both passes are reduced because of further reductions in dumping height.

Figure 6.15 shows the impact force on the truck due to gravity dumping of the dipper material with a dumping height of 5.33 m. The first pass material makes a first contact with the truck at 7.11 seconds. The maximum impact force of 720 kN occurs at 8.26 seconds during the first shovel pass. The shovel completes the first pass at 12.2 seconds and returns to repeat the process. The particles completely settle at 21 seconds. After completing the first pass and the particles settle, the total gravitational force of the material in the truck exists and is similar to the previous cases. After the first pass, the shovel swings back in 30 seconds, loads 100 tons of material and swings back to complete the second pass. The second pass material makes the first contact with the truck at 42.9 seconds. The maximum impact force of 661 kN occurs at 46 seconds during the second

pass. The impact force from the second pass is less than that of first pass due to the cushioning effect. The particles settle at 56 seconds and the impact force again is constant and it includes the total gravitational force of the material from the two passes in the truck. Comparing Figure 6.15 with previous cases, it can be observed that the maximum impact forces from the two passes are reduced because of reductions in shovel dumping height.

Figure 6.16 shows the impact force on the truck due to gravity dumping of the dipper payload with a dumping height of 5.00 m. The first pass material makes contact with the truck at 7.11 seconds. The maximum impact force of 705 kN occurs at 9.6 seconds during the first pass. The shovel completes the first pass at 12.2 seconds and returns to repeat the process. The particles completely settle at 19.5 seconds. After completing the first pass and the particles settle, the total gravitational force of the material in the truck exists and is similar to the previous cases.

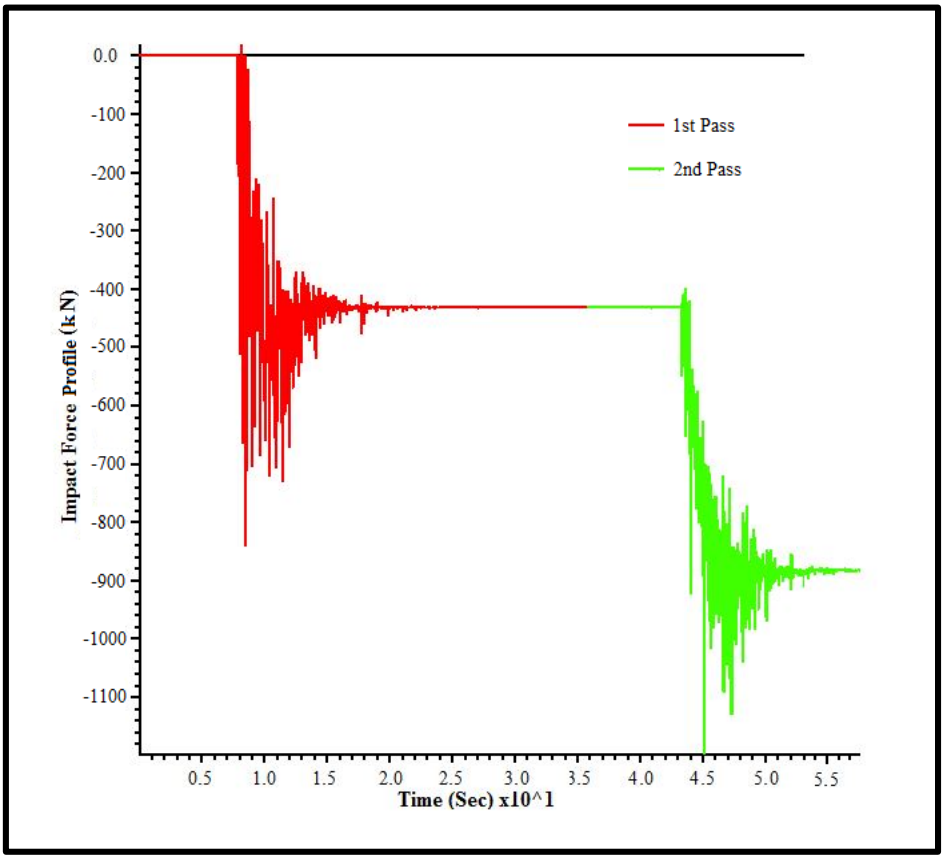

Figure 6.11. DEM Impact Profile on Truck Body due to Shovel Dumping at H_t = 7.33 m

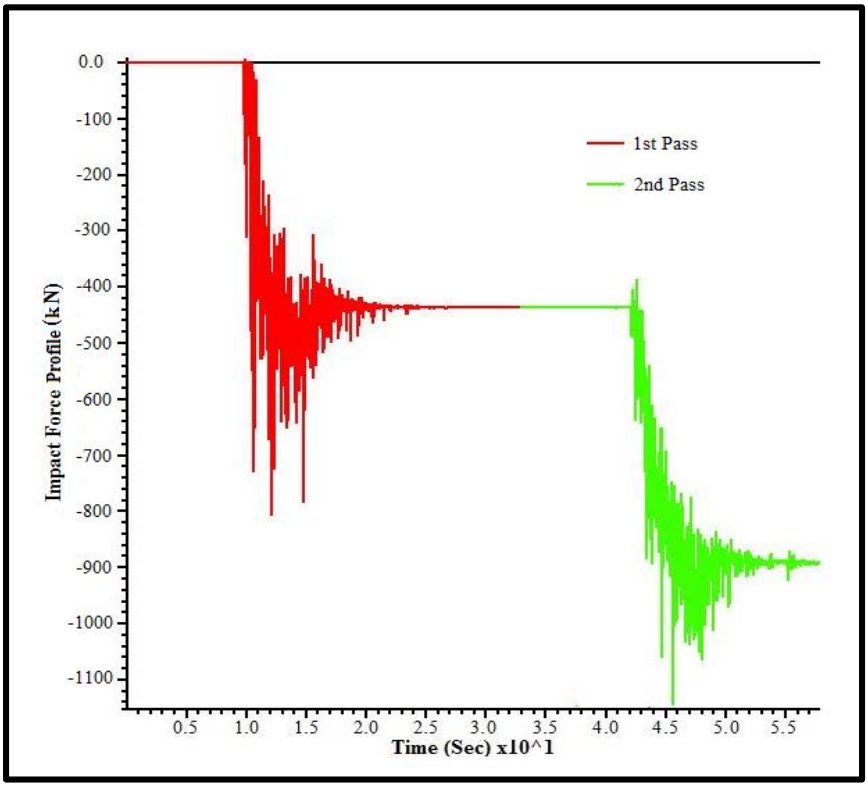

Figure 6.12. DEM Impact Profile on Truck Body due to Shovel Dumping at H_t = 6.33 m

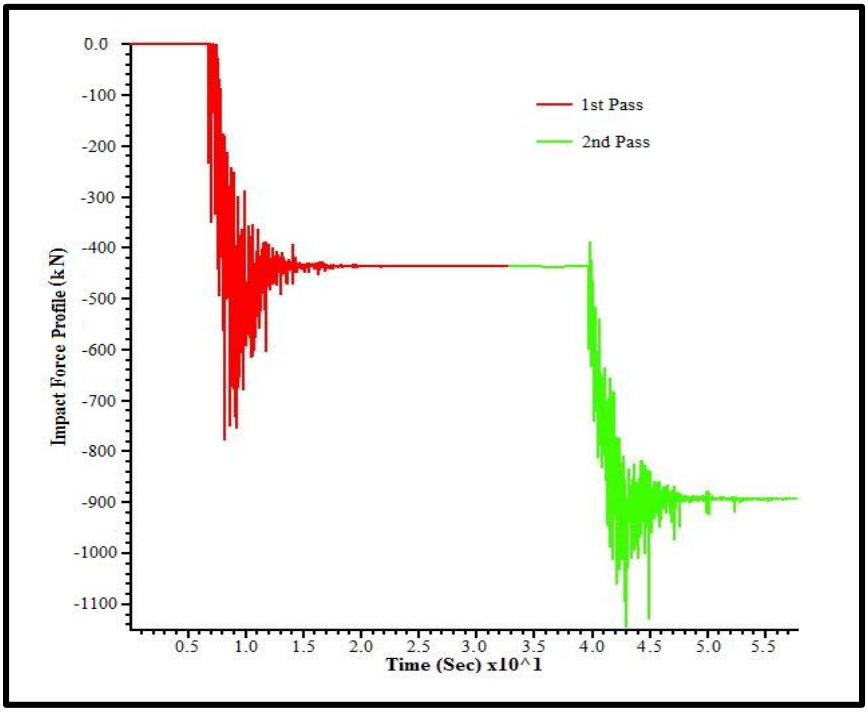

Figure 6.13. DEM Impact Profile on Truck Body due to Shovel Dumping at H_t = 6.00 m

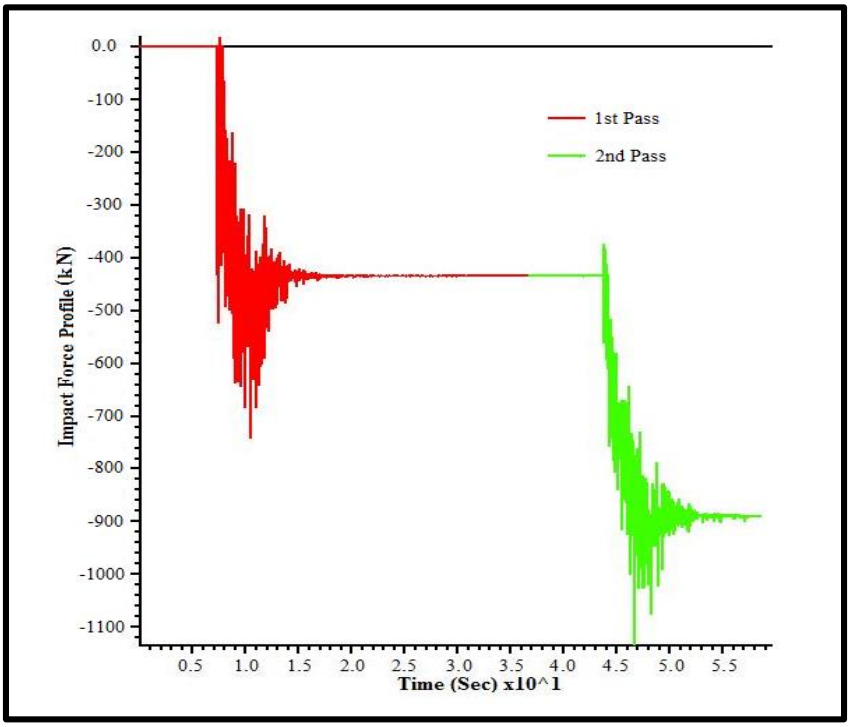

Figure 6.14. DEM Impact Profile on Truck Body due to Shovel Dumping at H_t = 5.50 m

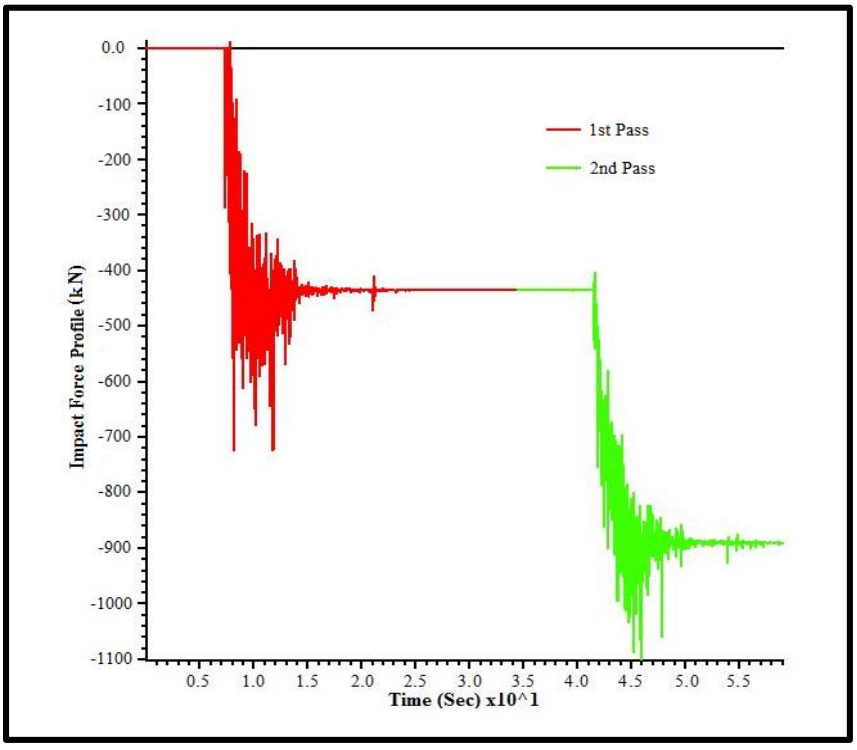

Figure 6.15. DEM Impact Profile on Truck Body due to Shovel Dumping at H_t = 5.33 m

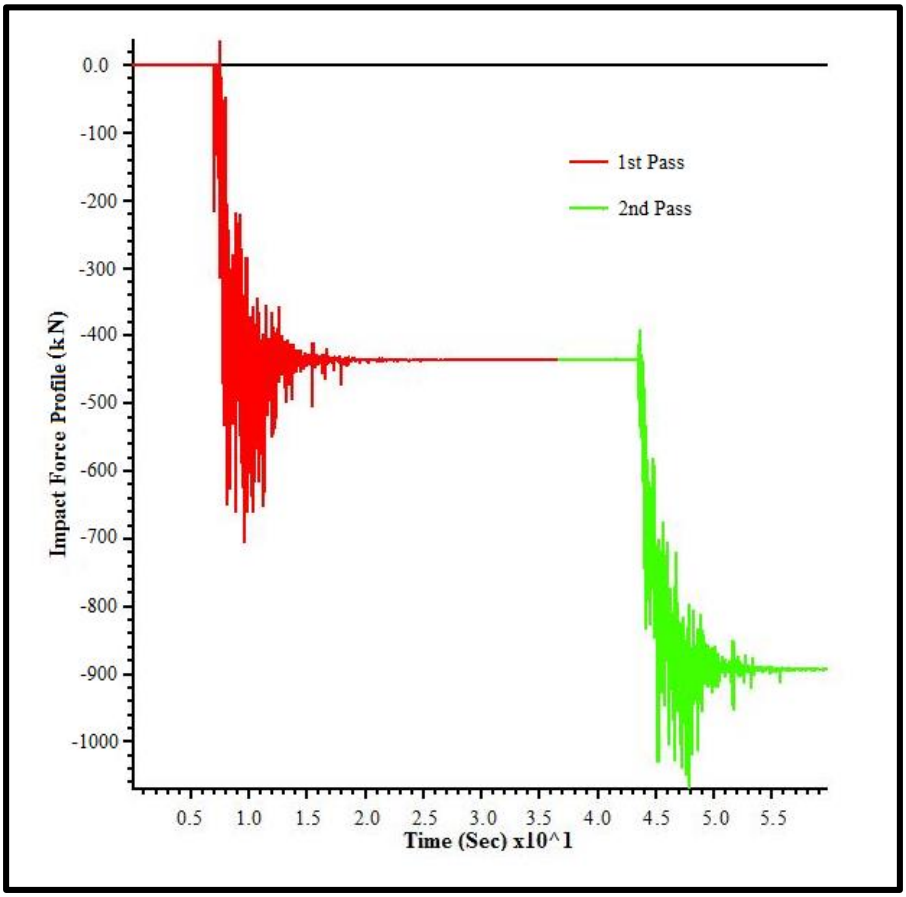

Figure 6.16. DEM Impact Profile on Truck Body due to Shovel Dumping at H_t = 5.00 m

After the first pass, the shovel swings back in 30 seconds, loads 100 tons of material and swings back to complete the second pass. The second pass material makes contact with the truck at 43.6 seconds. The maximum impact force of 631 kN occurs at 47.9 seconds during the second pass. The impact force from the second pass is less than that of first pass due to the cushioning effect. The particles comes to rest at 56 seconds and the impact force again is constant and it includes the total gravitational force of the material from two passes in the truck. Comparing Figure 6.16 with previous five cases, it can be observed that the maximum impact forces from both passes are reduced because of reductions in shovel dumping height.

Figure 6.17 shows the impact force on the truck due to gravity dumping of the dipper payload with a dumping height of 4.90 m. This is the minimum height with appropriate clearance for efficient and effective dumping process. The material makes

contact with the truck at 7.3 seconds during the first pass. The maximum impact force of 692 kN occurs at 9.2 seconds during the first pass. The shovel completes the first pass a 10.4 seconds and returns to repeat the process. The particles completely settle at 18 seconds. After completing the first pass and the particles settle, the total gravitational force of the material in the truck still exists and is similar to the previous cases. After the first pass, the shovel swings back in 30 seconds, loads 100 tons of material and then swings back to complete the second pass. The second pass material makes contact with the truck at 40.5 seconds. The maximum impact force of 621 kN occurs at 44 seconds during the second pass. The impact force from the second pass is less than of the first pass due to the cushioning effect. The particles settle at 54 seconds and the impact force again is constant and it includes the total gravitational force of the material from the two shovel passes in the truck. Comparing Figure 6.17 with the previous cases, it can be observed that the maximum impact forces in both shovel passes are reduced due to reductions in dumping height.

Tables 6.4 and 6.5 contain the maximum impact forces for the first and second passes, respectively. The maximum impact force decreases with decreasing shovel dumping height. The minimum dumping height of 4.90 m is the optimum height that ensures appropriate clearance between the dipper door and the truck edges to avoid jolting during the dumping process. Table 6.6 illustrates the cushioning effect by showing the percent difference in the maximum impact forces between the first and second shovel passes for each dumping height. The results clearly show that for any reduction in dumping height, there is a corresponding reduction in the maximum impact force. The results also show that the maximum impact force for the second pass is less than that of the first pass. This is due to the fact that the material from the first pass in the truck acts as a cushion to reduce impact. The reduction range for the maximum impact force is between 8.2 and 10.5 % as a result of this cushioning effect.

Table 6.7 shows the percent reductions in the maximum impact force for the first shovel pass with respect to the maximum height of 7.33 m. Reductions of 4.88%, 7.42%, 11.45%, 12.01%, 15.08% and 17.34% are achieved by reducing the height from 7.33 m to 6.33, 6.00, 5.50, 5.33, 5.00 and 4.9 m, respectively. Table 6.8 describes the percent increase in the maximum impact force for the first shovel pass with respect to the very last

case with a minimum optimum dumping height of 4.90 m. Percent increases of 1.77%, 4.01%, 7.14%, 14.03%, 15.89% and 20.99% are incurred by increasing the dumping height from 4.90 m to 5.00 m, 5.33 m, 5.50 m, 6.00 m, 6.33 m, and 7.33 m, respectively.

Figure 6.18 is the graphical illustration of the data compiled in Table 6.3 and Table 6.4. And Figures 6.19 and 6.20 are just the graphical illustration of the data compiled in Table 6.6 and Table 6.7 respectively.

6.3. MSC ADAMS SIMULATION RESULTS AND DISCUSSION

Table 6.8 shows the operator's seat RMS acceleration results in y – direction (up – down motion) for all the various dumping distances using the 3 – D virtual simulator for CAT 793D in MSC ADAMS. RMS accelerations of 3.189, 3.008, 3.007, 3.000, 2.947, 2.889 and 2.862 m/s^2 were recorded for dumping heights of 7.33 m, 6.33 m, 6.00 m, 5.50 m, 5.33 m, 5.00 m and 4.9 m, respectively. The results show as the dumping height is reduced, the load is dumped at lower height, resulting in reduced impact force and hence corresponding reduction in RMS acceleration at operator's seat reduces. The results also show that for a dumping distance of 6.33 m, 6.00 m and 5.50 m, the resulting impact force generated by the material dumping is reduced but the RMS acceleration at the operator's seat doesn't change much, This phenomenon, may be due to the fact that for that range of impact force magnitudes, the excitation at the seat is within the resonance envelope of the seat, resulting in almost the same RMS acceleration with changing impact forces. This phenomenon disappears above or below this range. The RMS acceleration changes considerably with changes in impact force for dumping heights outside this range.

The operator's seat RMS acceleration value in y – direction (up – down motion), as reported by Aouad and Frimpong (2013) was 3.56 m/s^2. Table 6.9 shows the percent reduction in RMS acceleration for operator's seat in y – direction in comparison with the reported RMS acceleration value of 3.56 m/s^2. It can clearly be observed that the percent reduction is increased with decreasing dumping height. A percent reduction of 19.61% can be achieved in operator's seat RMS acceleration if the material from the shovel is dumped at an optimum height of 4.9 m, previously determined through the DEM virtual simulation.

Figures 6.21 and 6.22 are just the graphical illustration of the data compiled in Table 6.8 and Table 6.9 respectively.

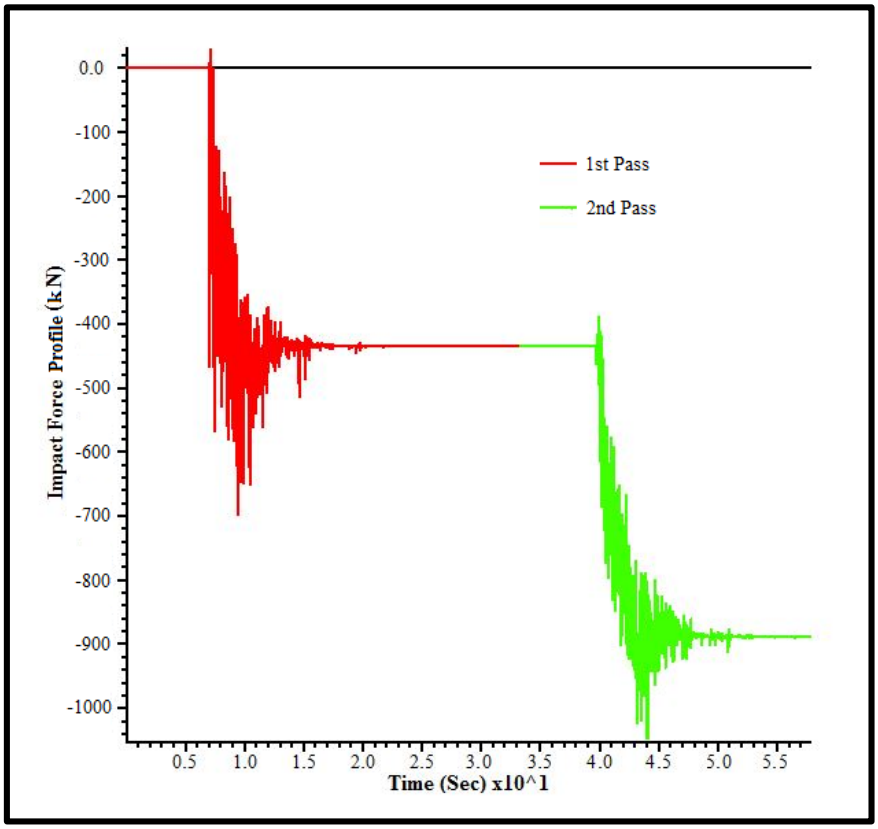

Figure 6.17. DEM Impact Profile on Truck Body due to Shovel Dumping at H_t = 4.90 m

Table 6.3. Maximum Impact Force Magnitude for the 1st Shovel Pass

Dumping Distance (H_t)	Maximum Impact Force Magnitude
(m)	(kN)
7.33	838
6.33	800
6.00	775
5.50	742
5.33	720
5.00	705
4.90	692

Table 6.4. Maximum Impact Force Magnitude for the 2nd Shovel Pass

Dumping Distance (H_t)	Combined Impact Force Maximum Magnitude	Static Gravitational Load of the Rock/Soil Material	Maximum Impact Force Magnitude for the 2nd pass only
(m)	(kN)	(kN)	(kN)
7.33	1,195	438	757
6.33	1,161	438	723
6.00	1,146	438	708
5.50	1,118	438	680
5.33	1,099	438	661
5.00	1,069	438	631
4.90	1,059	438	621

Table 6.5. Percent Difference in Maximum Impact Force Magnitude b/w 1st and 2nd Shovel Pass

Dumping Distance (H_t)	Maximum Impact Force Magnitude for 1st Pass	Maximum Impact Force Magnitude for the 2nd pass	Percent Difference
(m)	(kN)	(kN)	(%)
7.33	838	757	9.64
6.33	797	723	9.24
6.00	775	708	8.66
5.50	742	680	8.38
5.33	720	661	8.19
5.00	705	631	10.52
4.90	692	621	10.25

Table 6.6. Percent Reduction in Maximum Impact Force Magnitude for 1st Shovel Pass w.r.t H_t = 7.33 m (Maximum Dumping Distance)

Dumping Distance (H_t)	Percent Reduction in Maximum Impact Force Magnitude
(m)	(%)
7.33	0
6.33	4.88
6.00	7.42
5.50	11.45
5.33	14.03
5.00	15.89
4.90	17.35

Table 6.7. Percent Increase in Maximum Impact Force Magnitude for 1st Shovel Pass w.r.t H_t = 4.90 m (Minimum Dumping Distance Feasible)

Dumping Distance (H_t)	Percent Increase in Maximum Impact Force Magnitude
(m)	(%)
7.33	20.99
6.33	15.08
6.00	12.01
5.50	7.14
5.33	4.01
5.00	1.77
4.90	0

Table 6.8. Vertical RMS Accelerations for Operator's Seat

Dumping Distance (H_t)	Maximum Impact Force Magnitude for 1st Pass	RMS Acceleration of the Operator' Seat in y – Direction
(m)	(kN)	(m/s^2)
7.33	838	3.189
6.33	800	3.008
6.00	775	3.007
5.50	742	3.000
5.33	720	2.947
5.00	705	2.889
4.90	692	2.862

Table 6.9. Percent Reduction in RMS Acceleration of the Operator' Seat in y – Direction

Dumping Height, H_t (m)	RMS Acceleration (m/s^2)		% Difference
	Aouad and Frimpong (2013	Virtual Model	
7.33	3.560	3.189	10.42
6.33	3.560	3.008	15.51
6.00	3.560	3.007	15.53
5.50	3.560	3.000	15.73
5.33	3.560	2.947	17.22
5.00	3.560	2.889	18.85
4.90	3.560	2.862	19.61

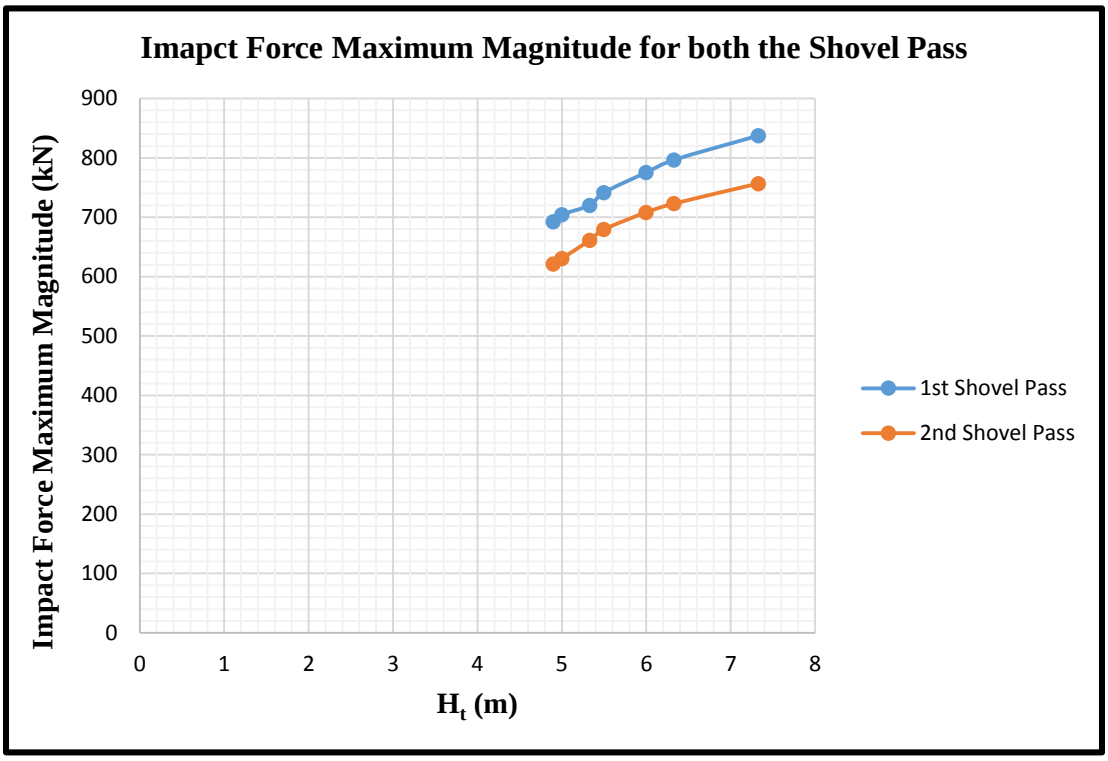

Figure 6.18. Maximum Impact Force from DEM

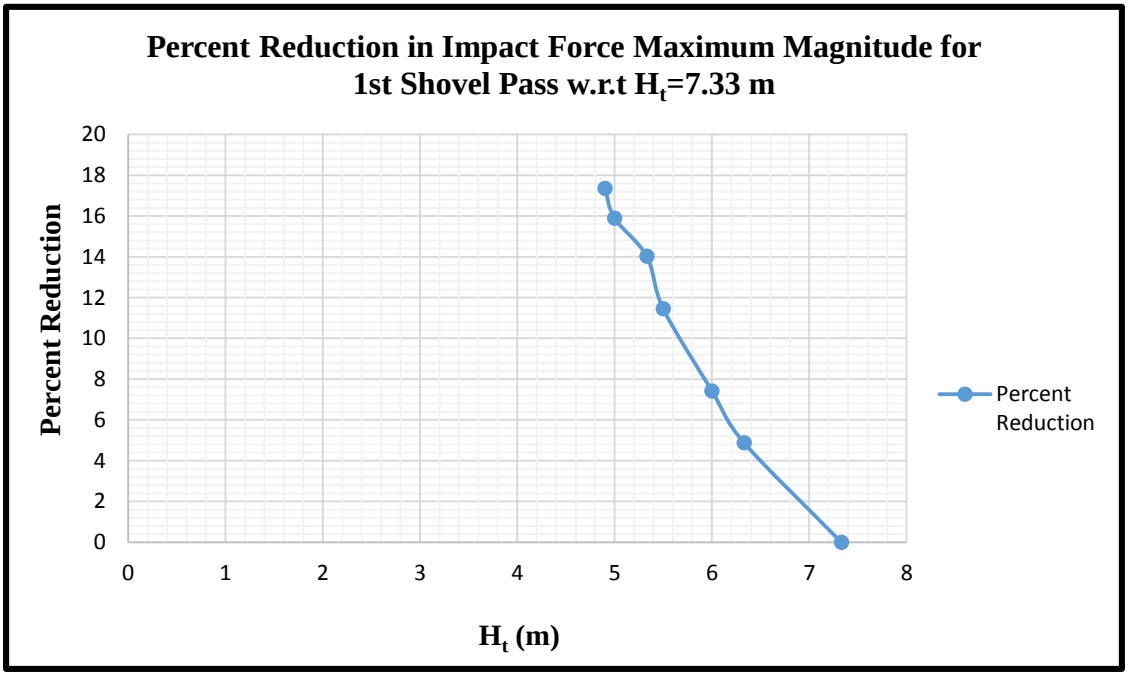

Figure 6.19. Percent Reduction in Maximum Impact Force for 1st Shovel Pass w.r.t H_t = 7.33 m

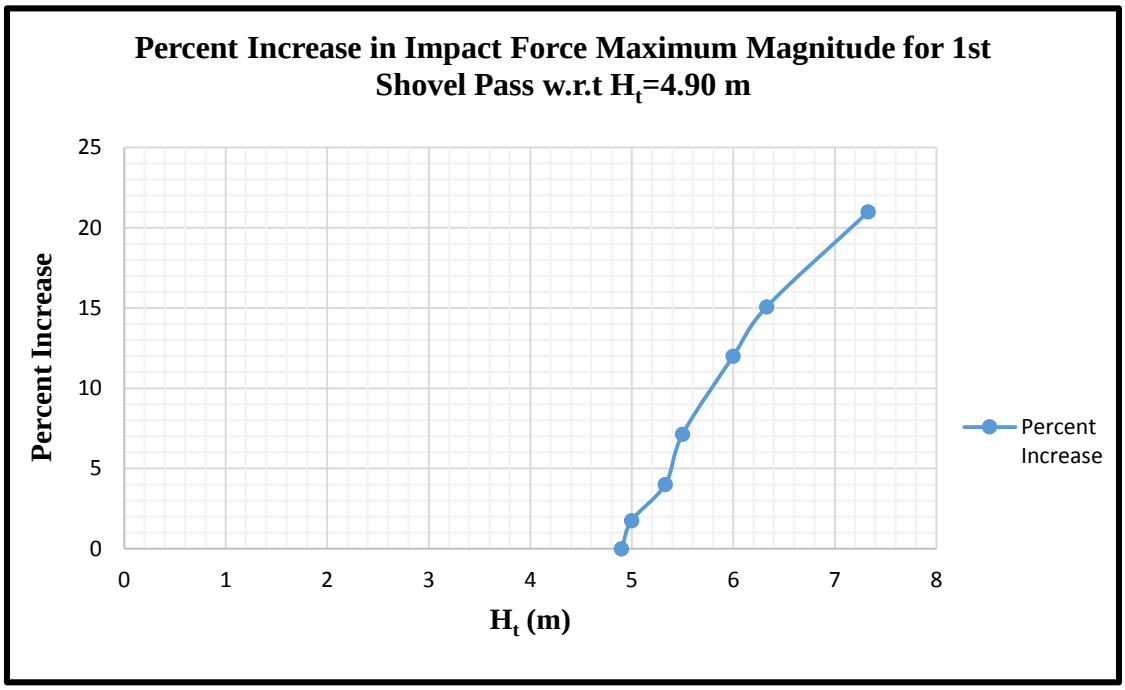

Figure 6.20. Percent Increase in Maximum Impact Force for 1st Shovel Pass w.r.t H_t = 4.90 m

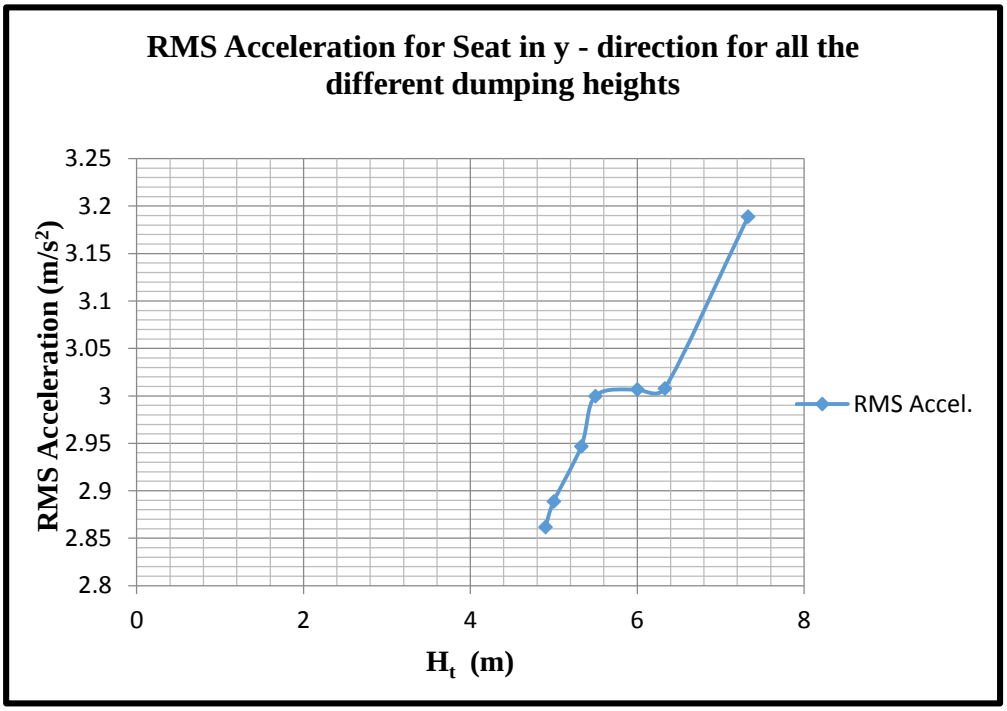

Figure 6.21. RMS Accelerations of Operator's Seat in y - Direction obtained through MSC ADAMS Simulation

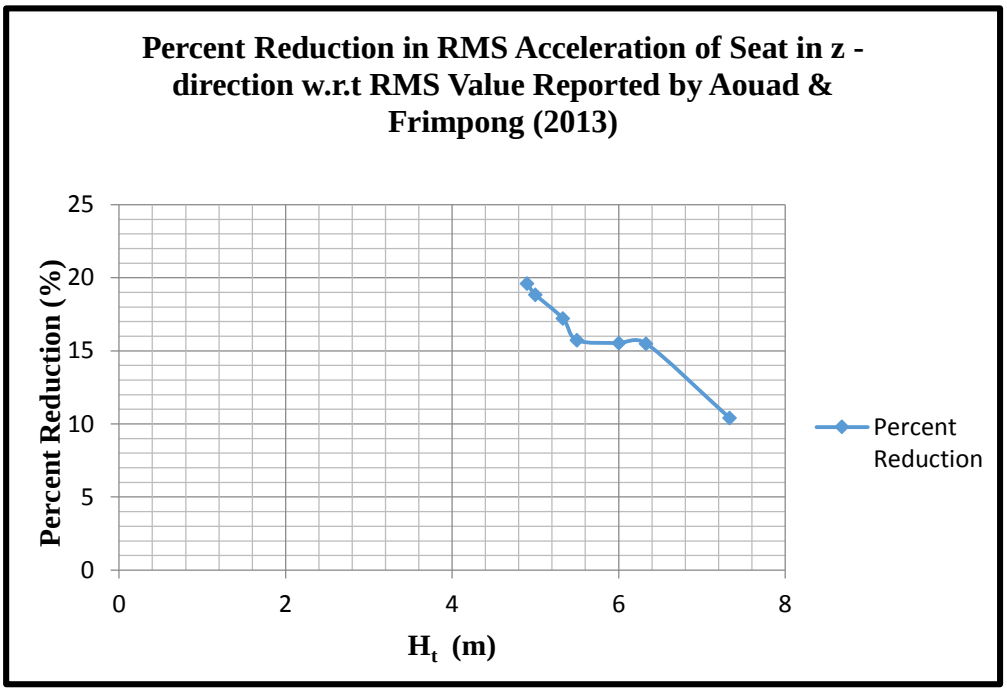

Figure 6.22. Percent Reduction in RMS Acceleration of Operators' Seat in y - Direction w.r.t RMS Value Reported by Aouad & Frimpong (2013)

6.4. SUMMARY

The numerical experiments are conducted to analyze the effectiveness of the mathematical model for predicting the dynamic impulse force for the shovel dumping process. The virtual prototype simulators of the shovel dumping process and truck vibration are simulated successfully in PFC3D and MSC ADAMS respectively. The virtual simulators are build based on the P&H 4100XPC shovel dumping materials into the CAT 793D truck, due to their wide application in surface mining operations. However the study can extended and the models can be used to obtain the optimum dumping height for any large truck being loaded by a corresponding large shovel. It can be observed from the results that the impact force reduces considerable as the dumping height is reduced. A percent reductions of 17.34 % are achieved in impact force magnitude by reducing the dumping height from 7.33 m to 4.9 m. Consequently, a percent reduction of 19.61% can be achieved in the operator's seat vertical RMS acceleration for a dumping height of 4.9 m. Also, a percent reduction between 8.2% and 10.5% can be achieved in the maximum impact force magnitude as a result of this cushioning effect. This reduction in WBV levels

reduces the dangerous impact on human operators for dump trucks and improves the workplace safety and operator's health and safety in surface mining operations.

7. SUMMARY, CONCLUSIONS AND RECOMMENDATIONS

This section summaries the whole research work that has been carried out in this study. It also enlists the conclusions that can be drawn from this research work along with the scientific and industrial contributions of this research work to the body of existing knowledge. This section also presents the recommendation to improve this work.

7.1. SUMMARY

As a result of advancement in technologies, the shovel-truck mining system has become a more flexible, economic and productive method for surface mining operations over the years. One can easily achieve higher economic advantages by matching the larger shovels with larger dump trucks. When these large capacity shovels load large capacity dump trucks with over 100-ton passes under gravity, large impact forces are generated resulting in high frequency shock waves. The shockwaves generated, under high impact shovel loading operations (HISLO), propagate through the truck body, chassis and to the operator's cabin and the seat. The truck operators are, thus, exposed to high levels of whole body vibration (WBV). These WBV levels, under certain HISLO conditions, may exceed the recommended ISO limits for extremely uncomfortable zones. These conditions can have a severe impact on the health and safety of the operators with long-term lower-back problems and other health issues.

Previous research on machine and whole body vibrations exposure and their impact have been limited to relatively small equipment in industries, such as agriculture, military, aerospace, commercial transport and automotive. This research provides a pioneering effort in developing solutions to the problem of high impact forces under HISLO conditions. Detailed mathematical models have been formulated to predict the impact force generated under HISLO conditions. Furthermore, a 3D virtual model of the shovel loading process has been built and simulated in PFC3D. The virtual simulator provides a powerful tool for predicting the impact force generated on the truck body under HISLO conditions. The resulting impact forces from the PFC3D simulation have been used to examine the vibration levels at the operator's seat and the corresponding reductions in the RMS

acceleration levels with decreasing dumping height. The mathematical and the 3D virtual models provide a frontier research study into WBV reductions under the HISLO conditions. Below is a summary of the detailed procedures for achieving the objectives of the research study.

1. The introduction provides the details of the HILSO problems in large scale surface mining operations, as well as, the objectives and scope of the research study. It also outlines the importance of this research and its wide contributions.
2. An in-depth literature survey was carried out to examine the contributions and limitations of the previous and the current body of knowledge on machine vibration, whole body vibration (WBV), impact force modelling, material dynamic simulation and discrete element analysis. From a critical review of the literature, the only fundamental research by Aouad and Frimpong (2013) does not provide a rigorous mathematical model for capturing the impact forces under HISLO conditions. Thus, this research was designed to solve this limitation and to provide solutions to the WBV exposures arising from HISLO conditions in large-scale surface mining operations.
3. A detailed mathematical model has been successfully developed for the dynamic impulse force under HISLO conditions. The formulated mathematical model can be used to determine the impact force generated at the truck body due to the gravity dumping of the material during the shovel dumping process.
4. Numerical experiments have been conducted to analyze the effectiveness of the mathematical model for predicting a more realistic dynamic impulse force for the shovel dumping process. A series of optimal dumping heights have been generated for the HISLO scenarios for analyzing the shovel dumping process.
5. The virtual prototype simulator of the shovel dumping process, consisting of the P&H 4100XPC shovel dumping materials into the CAT 793D truck, has been developed in PFC3D. This 3D model captures the impact force generated at the truck body without the need to conduct physical experiments. Virtual simulation results from the model by Aouad and Frimpong (2013) have been used to validate the results from this study.

6. Using the impact force results for different dumping heights from PFC3D simulation in this study, the virtual model in Aouad and Frimpong (2013) has been used to carry out the vibration analysis in MSC ADAMS. The virtual simulation has been carried out using the P&H 4100XPC shovel to load the CAT 793D and to generate the vertical RMS acceleration at the operator's seat.

7.2. CONCLUSIONS

From the literature surveys, the following conclusions can be drawn.

1. No previous research has been carried out to develop a comprehensive mathematical model for the shovel dumping process under HISLO conditions. In addition, no 3D virtual simulation has been carried out to examine the shovel dumping process under HISLO conditions using a comprehensive mathematical model of the impact force. This is a pioneering fundamental research study for modeling and simulating the shovel dumping process using the continuous material flow process for reducing shockwaves under HISLO conditions. This research has created a frontier in whole body vibration control by modelling the impact force generation at the truck bed and developing method to mitigate those forces.
2. This research endeavor provides contributions and understanding into the body of knowledge of truck vibration mitigation. The reductions in impact forces will definitely affect operator's safety and health under HISLO conditions.

From the mathematical modelling and experimental analysis under HISLO conditions, the following conclusions are drawn.

1. The research study has developed the mathematical model for the dynamic impact force at the truck body due to the gravity dumping of material during the shovel dumping operation.
2. The mathematical model can be used to determine the dynamic impact force at the truck body during the shovel dumping process.

3. Numerical experiments have been conducted for the HISLO case where P&H 4100XPC shovel is used to dump 100 tons of material into CAT 793D dump truck in a single pass.
4. The results of these experiments have been used to analyze the effectiveness of the mathematical model for predicting a more realistic dynamic impulse force.

From the results of experiments and shovel dumping operation simulation in PFC3D and truck vibration simulation in MSC ADAMS, the following conclusions can be drawn.

1. Two shovel passes are simulated virtually in PFC3D. An optimum dumping height of 4.90 m is generated to achieve the required minimum clearance between the dipper door and truck edges.
2. The results from the virtual simulation shows that percent reductions of 4.88%, 7.42%, 11.45%, 12.0%, 15.08% and 17.34 % are achieved by reducing the dumping height from 7.33 m to 6.33 m, 6.00 m, 5.50 m, 5.33 m, 5.00 m and 4.9 m, respectively.
3. These reductions correspond to percent increases of 1.77%, 4.01%, 7.14%, 14.03%, 15.89% and 20.99% for dumping heights increases from 4.90 m to 5.00 m, 5.33 m, 5.50 m, 6.00 m, 6.33 m, and 7.33 m, respectively.
4. A cushioning effect is clearly observed during the second shovel pass due to the material already present in the truck body from the first shovel pass. The reduction in the maximum impact force magnitude ranges between 8.2% and 10.5% as a result of this cushioning effect.
5. The mathematical model of the impulse force function is validated using the published RMS acceleration results from Aouad and Frimpong (2013) under the same constraints and environment. The percent difference between the two results ranged between 0.56% and 7.02% which shows a good agreement.
6. A comparison between the results from the mathematical model and the 3D virtual simulation experiments for the maximum dynamic impact force showed a strong agreement between the two results as well. The percent difference between the two results ranged between 0.03% and 1.48%.

7. Using the impact force results obtained from PFC3D virtual simulation, truck vibration simulation was carried out in MSC ADAMS. A 38-DOF virtual prototype model for the CAT 793D dump truck developed by Aouad and Frimpong (2013) is used to obtain the vertical RMS acceleration for the operator's seat.
8. The RMS acceleration values obtained through this simulation were compared with the value of 3.56 m/s^2 reported by Aouad and Frimpong (2013) for the operator's seat. The results show that a percent reduction of 19.61% can be achieved in the operator's seat vertical RMS acceleration for a dumping height of 4.9 m.
9. The dumping height of 4.90 m is the optimum dumping height for this shovel dumping process. This optimum height is the dumping height with a safe clearance between the lowest edge of the dipper and the upper edges of the truck body that prevents jolting during the dumping process.

7.3. CONTRIBUTIONS OF RESEARCH

This research study provides a much better understanding of the dynamics of the impact force with varying dumping heights. It also illustrates systematic procedures for the magnitudes of the dynamic impact force and the resulting WBV levels. In particular, the research provides the following scientific and industrial contributions to the body of existing knowledge and advances the research frontiers in shovel dumping process.

1. The research results can be effectively utilized to study in detail and reduce WBV levels from any HISLO condition in surface mining operations.
2. The study can also be used to generate the optimum dumping height for any shovel dumping process mathematically or from a 3-D virtual simulation technique.
3. The research can also be used to examine the cushioning effect in the shovel dumping process. This cushioning effect is a measure of the reductions in impulse force resulting from the materials already present in the truck body.
4. The research study provides a novel technology for examining the impact of shovel dumping height on WBV levels for any HISLO operation. This reduction in WBV levels also reduces the dangerous impact on human operators for dump trucks in

these HISLO operations. It improves the workplace safety and operator's health and safety in surface mining operations.

7.4. RECOMMENDATIONS

This research has produced a platform for examining the reductions in WBV exposures for varying dumping heights in any HISLO operation. Further studies are required to enhance the work carried out in this study, as discussed below.

1. As indicated during the development of mathematical model, the truck body parameters were excluded to simplify the model. Further work could be done by including the truck body parameters for determining the impact force on the truck body.
2. These truck components include the chassis, suspension system, operator's seat, tires and the truck body. These components can be added to the virtual simulation model in PFC3D to investigate the effect of the shovel dumping process on the impulse force and the WBV levels especially at the operator's seat.
3. Other methods can be developed to reduce the dump truck vibration. These methods include: (i) design changes for the dump truck to isolate the operator from the truck vibrations; (ii) designing better suspension systems by determining the weakest suspension – chassis links and adding proper isolation links at those junctions; (iii) modifying operator's seat by adding proper support and increased cushioning to minimize the transmitted vibrations to the operator lower back, neck, arms and shoulder; and (iv) compacting bench formation to attenuate the impact force under HSILO conditions.

8. REFERENCES

Albaba, A., Lambert, S., Nicot, F. and Chareye, B. (2014), "DEM simulation of dry granular flow impacting a rigid wall," Computer Methods and Recent Advances in Geomechanics – Oka, Murakami, Uzuoka & Kimoto (Eds.) 2015, Taylor & Francis Group, London, pp. 1869–1874, ISBN: 978-1-138-00148-0, DOI: 10.1201/b17435-331.

Aldinger, J. A., Kenny, J. M. and Keran, C. M. (1995), "Mobile Equipment Accidents in Surface Coal Mines," U.S. Bureau of Mines, Information Circular 9428, pp 51.

Aouad, N. and Frimpong, S. (2013). "Virtual Prototype Simulation of Truck Vibrations in High Impact Shovel Loading Operations," J Powder Metall Min S1:004. doi:10.4172/2168-9806.S1-004.

Aouad, N. and Frimpong, S. (2014). "Lagrangian Formulation and Numerical Solutions to Dump Truck Vibrations under HISLO Conditions," *ASME Journal of Vibration and Acoustics, Vol. 136 / 021020-1.*

Basu, D. and Rao, N. S. V. K. (2012). "Analytical solutions for Euler-Bernoulli beam on visco-elastic foundation subjected to moving load," *Int. J. Numer. Anal. Methods Geomech. ,* 37 (8), 945–960.

Bobaru, F., Rattanadit, K., Promratana, K. and Turner, J.A. (2009) "Force Chains and Resonant Behavior in Bending of a Granular Layer on an Elastic Support," *Faculty Publications from the Department of Engineering Mechanics, Published in Mechanics of Materials* 41:6, pp. 691–706; doi 10.1016/j.mechmat.2009.01.023.

Chang, M. K., Li, Y. F. and Huang, H. W. (2011), "Hazard of Vibration and Health Risk Assessment for Domestic Dump Truck Driver in Taiwan," *Journal of Applied Mechanics and Materials, Vol. 52 – 54,* pp. 186 – 191.

Cundall, P. A. (1971). "A Computer Model for Simulating Progressive Large Scale Movements in Blocky Rock Systems," in Proceedings of the Symposium of the International Society of Rock Mechanics (Nancy, France, 1971), Vol. 1, Paper No. II-8.

Cundall, P. A. (1988). "Formulation of a Three-Dimensional Distinct Element Model - Part I. A Scheme to Detect and Represent Contacts in a System Composed of Many Polyhedral Blocks," Int. J. Rock Mech., Min. Sci. & Geomech. Abstr., 25(3), 107-116.

Cundall, P. A., and O. D. L. Strack. (1979). "A Discrete Numerical Model for Granular Assemblies," Geotechnique, 29(1), 47-65.

Cundall, P. A., and R. Hart. (1992). "Numerical Modeling of Discontinua," J. Engr. Comp., 9, 101-113.

Doktan, M. (2001). "Impact of Blast Fragmentation on Truck Shovel Fleet Performance," *17th International Mining Congress and Exhibition of Turkey,* Antalya, 2001. pp. 375–379.

Eger, T., Smets, M., Grenier, S., and Vibration Research Group (2005), "Whole-Body-Vibration Exposure Experienced During the Operation of Small and Large Load-Haul-Dump Vehicles," *Proc. Of 5th Canadian Rural Health Research Society Conference and the Fourth International Rural Nurses Congress*, Sudbury, ON.

Friedmann, P.P. (1997). "A Fundamental Study of Active Vibration Control in Rotorcraft using the ACSR Approach," *US Army Research Office, Engineering and Environmental Science Division*, Research Triangle Park, NC 27709-2211.

Frimpong, S. (2006). Course Notes on MIN Eng. 4933, "Surface Mining Methods and Equipment," Missouri University of Science & Technology, Rolla MO, USA.

Frimpong, S., Galecki, G. and Chang, Z. (2011), "Dump truck operator vibration control in high-impact shovel loading operations," *International Journal of Mining, Reclamation and Environment, Vol. 25, No. 3,* pp. 213–225.

Harnischfeger Corporation. (2003). "Peak Performance Practices – Excavator Selection," *P&H Mine Pro Services*, Wisconsin, USA.

Hart, R., Cundall, P. A. and Lemos, J. (1988). "Formulation of a Three-Dimensional Distinct Element Model - Part II. Mechanical Calculations for Motion and Interaction of a System Composed of Many Polyhedral Blocks," *Int. J. Rock Mech.*, Min. Sci. & Geomech. Abstract, 25(3), 117-125.

Hosseininia, E. S. (2012), "Discrete element modelling of inherently anisotropic granular assemblies with polygonal particles," Particuology, Vol. 10, Issue 5, Pages 542 – 552.

Hoy, J., Mubarak, N., Nelson, S., Sweerts de Landas, M., Magnusson, M., Okunribido, O. and Pope, M. (2005), "Whole Body Vibration and Posture as Risk Factors for Low Back Pain among Forklift Truck Drivers," *Journal of Sound and Vibration, Vol. 284*, pp. 933 – 946.

ISO 2631 – 1 (1997). "Mechanical Vibration and Shock – Evaluation of Human Exposure to Whole Body Vibration – Part 1: General Requirements," *International Organization for Standardization,* Switzerland.

ISO 2631 – 2 (2003). "Mechanical Vibration and Shock – Evaluation of Human Exposure to Whole Body Vibration – Part 2: Vibrations in buildings (1 Hz to 80 Hz)," *International Organization for Standardization,* Switzerland.

ISO 2631 – 4 (2001). "Mechanical Vibration and Shock – Evaluation of Human Exposure to Whole Body Vibration – Part 4: Guidelines for the evaluation of the effects of Vibration and Rotational Motion on Passenger and Crew Comfort in Fixed guide way Transport Systems," *International Organization for Standardization,* Switzerland.

ISO 2631 – 5 (2004). "Mechanical Vibration and Shock – Evaluation of Human Exposure to Whole Body Vibration – Part 5: Method for Evaluation of Vibration containing Multiple Shocks," *International Organization for Standardization,* Switzerland.

Iverson, S., Jung, S.J. & Biswas, K. (2003). "Comparison of Ore Pass Computer Simulations for Designs Against Dynamic Load," *Annual meeting of the Society for Mining, Metallurgical, and Exploration, Inc.,* Cincinnati, OH, USA, February 26-28, 2003.

Kim, W., Lee, J-W., Kim, H-K. and Doo, M-S., (2001), "Handling Analysis of Active Height Control System using ADAMS," *Proc. of the North American MDI Users' Conference*, Novi, Michigan, USA, 18 – 20 June, 2001.

Kittusamy, N. K. (2002), "Ergonomic Risk Factors – A study of Heavy Earthmoving Machinery Operators," *ASSE Foundation Research*, Oct. 2002, pp. 38 – 45.

Kittusamy, N. K. (2003), "A Checklist for Evaluating Cab Design of Construction Equipment," *Applied Occupational and Environmental Hygiene, Vol. 18,* pp. 721 – 723.

Kittusamy, N. K. (2003), "Self-Reported Musculoskeletal Symptoms among Operators of Heavy Construction Equipment," *XVth Triennial Congress, International Ergonomics Association,* Seoul, Korea, August 24 – 29, 2003.

Kittusamy, N. K. (2003), "A checklist for evaluating cab design of construction equipment," *Applied Occupational and Environmental Hygiene, Vol. 18(10),* pp. 721– 723.

Kittusamy, N. K., Mayton A. G., Jobes, C. C. and Ambrose, D. H. (2003), "N361 A Systematic Comparison of Different Seats on Shuttle Cars Used in Underground Coal Mines," *The 32nd International Congress and Exposition on Noise Control Engineering,* Seogwipo, Korea, August 25 – 28, 2003.

Kittusamy, N. K. and Miller, R. E. (2003), "Comparison of Jolting and Jarring in a Newer and Older Dozer at a Highway Construction Site," *XVth Triennial Congress, International Ergonomics Association,* Seoul, Korea.

Kittusamy, N. K., Viswanathan, M. and Jorgensen, M. J. (2005), "Field Study to Evaluate the Effectiveness of a Continuous Passive Lumbar Motion System," *XIX Annual International Occupational Ergonomics and Safety Conference,* Las Vegas, Nevada, USA.

Law, R.P.H., Lam, A.Y.T. and Choi, K.Y. (2013). "A Numerical Study of Granular Surge Flow through a Row of Baffles," *Proceedings of the 18th International Conference on Soil Mechanics and Geotechnical Engineering*, Paris 2013.

Leonardi, A., Wittel, F. K., Mendoza, M., Vetter, R. and Herrmann, J. (2014), "Particle-fluid-structure interaction for debris flow impact on flexible barriers," Institute for Building Materials, ETH Zurich Computational Physics for Engineering Materials Stefano-Franscini-Platz 3, CH-8093 Zurich, Switzerland**,** arXiv preprint arXiv:1409.8034.

Metz, R. (2007). "Impact and drop testing with ICP® force sensors," *Journal of Sound & Vibrations, Vol. 41, No. 2,* pp. 18-20.

Miller, R. E., Boman, P., Walden, J., Rhoades, s. and Gibbs, R. (2000), "Acceleration and GPS Data Monitor Truck-Haulage Jolts," *Mining Engineering 2000, Vol. 58, No. 2*, pp. 20-22.

Moriguchi, S., Borja, R. I., Yashima, A. and Sawada, K. (2009), "Estimating the impact force generated by granular flow on a rigid obstruction," Acta Geotech, 4(1): 57−71.

Moses, R.W. (1997). "Vertical-Tail-Buffeting Alleviation using Piezoelectric Actuators: Some results of the Actively Controlled Response of Buffet-Affected Tails (ACROBAT) program," *Proc. SPIE, Vol. 3044*, pp. 87 – 98.

PFC (Particle Flow Code) Version 5.0. Documentation. (2014), "Itasca Consulting Group Inc," Minneapolis, MN, USA.

Ruff, T. (2002). "Hazard Detection and Warning Devices: Safety Enhancement for Off-Highway Dump Trucks," *A Compendium of NIOSH Mining Research*. Washington DC.

Ruff, T., Coleman, L. and Martini, L. (2011). "Machine-related injuries in the US mining industry and priorities for safety research," International Journal of Injury Control and Safety Promotion, 18 (1) (2011), pp. 11–20.

Soedel, W. (2005). *"Vibrations of Shells and Plates,"* 3rd edn., Marcel Dekker, New York, USA.

Symposium on *"Habitability of Combat and Transport Vehicles: Noise, Vibration and Motion,"* Prague, Czech Republic, 4 – 7 Oct., 2004, Published in RTO-MP-AVT-110.

Teufelsbauer, H., Wnag, Y., Pudasaini, S. P., Borja, R.I. and Wu, W. (2011), "DEM simulation of impact force exerted by granular flow on rigid structures," Acta Geotechnica (6), 119 – 133 DOI 10.1007/s11440-011-0140-9.

UDEC (Universal Distinct Element Code), Version 5.0. (2011). "Itasca Consulting Group Inc.," Minneapolis, MN, USA.

Wenzhang, Z., Yi, L., Guobiao, S. and Ligong, W. (2000), "Study on Non-Linear Dynamic Characteristic of Vehicle Suspension Rubber Component," *Proc. of the 2000 North American ADAMS User Conference*, Orlando, FL, USA, 19 – 21 June, 2000.

Wickramasinghe, V., Zimcik, D. and Chen Y. (2004). "A Novel Adaptive Structural Impedance Control Approach to Suppress Aircraft Vibration and Noise," *Paper presented at the RTO AVT*.

Yan-hua, S., Min, X., Chun, J., Yu, G. and Fu-Li, W. (2015). "Operator Health Risk Evaluation of Off-Highway Dump Truck under Shovel Loading Condition," *J. Cent. South Univ.*, 22: 2655 – 2664, DOI: 10.1007/s11771-015-2796-z.

VITA

Danish Ali was born on March 7, 1991. He obtained his Bachelor of Science in Mining Engineering from University of Engineering and Technology (UET), Lahore, Pakistan from 2010 to 2014. After his bachelors, he worked as graduate trainee engineer in an open pit surface coal mine for three months. In August 2014, he joined the Master's program in Mining Engineering at Missouri University of Science & Technology (MS&T) in Rolla, MO, formerly known as University of Missouri Rolla (UMR). During his Masters, he worked as a research assistant on an impulse force reduction technology as part of the Heavy Mining Machinery Research Group under the guidance of Dr. Samuel Frimpong. He received his M.S. degree in Mining Engineering in May2016.